



REALIZATION OF A STRIPED SUPERFLUID WITH ULTRACOLD DIPOLAR BOSONS: PHASE COMPETITION, SYMMETRY ENHANCEMENT AND VORTEX SOFTENING

by

Jonathan Michael Fellows

A thesis submitted to
The University of Birmingham
for the degree of
DOCTOR OF PHILOSOPHY

Theory of Condensed Matter Group
School of Physics and Astronomy
College of Engineering and Physical Sciences
The University of Birmingham

May 2013

UNIVERSITY OF
BIRMINGHAM

University of Birmingham Research Archive

e-theses repository

This unpublished thesis/dissertation is copyright of the author and/or third parties. The intellectual property rights of the author or third parties in respect of this work are as defined by The Copyright Designs and Patents Act 1988 or as modified by any successor legislation.

Any use made of information contained in this thesis/dissertation must be in accordance with that legislation and must be properly acknowledged. Further distribution or reproduction in any format is prohibited without the permission of the copyright holder.

Abstract

In this thesis we develop a model of ultracold dipolar bosons in a highly anisotropic quasi-one dimensional optical lattice. We will see that the model is identical to one describing quasi-one-dimensional superconductivity in condensed matter systems giving rise to the possibility of using this ultracold atoms system as an analogue simulator of interesting electronic systems.

In investigating the properties of this model we find a rich phase diagram containing density wave, superfluid, and possibly supersolid phases, accessible by tuning the optical lattice parameters and the alignment of the dipole moments.

An important property of this model turns out to be the existence of an enhanced symmetry at the self dual point where the density wave and superfluid orders are maximally competing. At this point the Berezinskii-Kosterlitz-Thouless transition temperature of either phase must necessarily vanish to zero due to the Hohenberg-Mermin-Wagner theorem.

Inspired by this model we go on to study a more general system in two dimensions with $O(M) \times O(2)$ symmetry which has an enhanced symmetry point of $O(M + 2)$ symmetry. The BKT transition in the $O(2)$ sector is mediated by vortex excitations, but these must somehow disappear as the high symmetry point is approached. Using both a variational argument adapting the standard BKT argument, and a more rigorous RG analysis we show that the size of the vortex cores in such a system must diverge as $1/\sqrt{\Delta}$, where Δ measures the distance from the high symmetry point, and further that the BKT transition temperature must vanish as $1/\ln(1/\Delta)$.

Dedicated, much like myself, to Georgina.

ACKNOWLEDGEMENTS

I would like to take this opportunity to thank the people who made this work possible:

My supervisor, Rob Smith, for teaching me how to do physics;

My housemates, Tim and Dave, for all the tech support;

My collaborators, Chris, Jörg, and especially Sam, for giving me interesting things to think about and always being patient when I say stupid things;

Everyone at KIT and NAG for their hospitality while I was writing this thesis;

My family – Angela, Mum, Dad, Joy, Frank, Sue and Francis – for support of all kinds;

And, most of all, my partner Georgina, for always being there.

PUBLICATIONS

1. JM. Fellows, ST. Carr, CA. Hooley and J. Schmalian,
Unbinding of giant vortices in states of competing order
Phys. Rev. Lett. **109**:15 (2012)[1]

We consider a two-dimensional system with two order parameters, one with $O(2)$ symmetry and one with $O(M)$, near a point in parameter space where they couple to become a single $O(2 + M)$ order. While the $O(2)$ sector supports vortex excitations, these vortices must somehow disappear as the high symmetry point is approached. We develop a variational argument which shows that the size of the vortex cores diverges as $1/\sqrt{\Delta}$ and the Berezinskii-Kosterlitz-Thouless transition temperature of the $O(2)$ order vanishes as $1/\ln(1/\Delta)$, where Δ denotes the distance from the high-symmetry point. Our physical picture is confirmed by a renormalization group analysis which gives further logarithmic corrections, and demonstrates full symmetry restoration within the cores.

2. JM. Fellows and ST. Carr,
Superfluid, solid, and supersolid phases of dipolar bosons in a quasi-one-dimensional optical lattice
Phys. Rev. A. **84**:051602(R) (2011)[2]

We discuss a model of dipolar bosons trapped in a weakly coupled planar array of one-dimensional tubes. We consider the situation where the dipolar moments are aligned by an external field, and we find a rich phase diagram as a function of the angle of this field exhibiting quantum phase transitions between solid, superfluid, and supersolid phases. In the low energy limit, the model turns out to be identical to one describing quasi-one-dimensional superconductivity in condensed matter systems. This opens the possibility of using bosons as a quantum analog simulator of electronic systems, a scenario arising from the intricate relation between statistics and interactions in quasi-one-dimensional systems.

3. JM. Fellows and RA. Smith,
A new two-parameter family of potentials with a tunable ground state
J. Phys. A: Math. Theor. **44**:335302 (2011)[3]

In a previous paper we solved a countably infinite family of one-dimensional Schrödinger equations by showing that they were supersymmetric partner potentials of the standard quantum harmonic oscillator. In this work we extend these results to find the complete set of real partner potentials of the harmonic oscillator, showing that these depend upon two continuous parameters. Their spectra are identical to that of the harmonic oscillator, except that the ground state energy becomes a tunable parameter. We finally use these potentials to analyse the physical problem of Bose-Einstein condensation in an atomic gas trapped in a dimple potential.

4. JM. Fellows and RA. Smith,
Factorization solution of a family of quantum nonlinear oscillators
J. Phys. A: Math. Theor. **42**:335303 (2009)[4]

In a recent paper, Cariñena J F, Perelomov A M, Raiñada M F and Santander M (2008 *J. Phys. A: Math. Theor.* **41** 085301) analyzed a non-polynomial one-dimensional quantum potential representing an oscillator which they argued was intermediate between the harmonic and isotonic oscillators. In particular they proved that it is Schrödinger soluble, and explicitly obtained the wavefunctions and energies of the bound states. In this paper we show that these results can be obtained much more simply by noting that this potential is a supersymmetric partner potential of the harmonic oscillator. We then use this observation to generate an infinite set of potentials which can exactly be solved in a similar manner.

CONTENTS

1	Introduction and Motivation	1
1.1	Motivation	1
1.1.1	Background	1
1.1.2	The Stripe Order	4
1.1.3	Analogue Simulation with Cold Atoms	6
1.1.4	Systems with Competing Order	7
1.2	Thesis Overview	8
2	Bosonization and One Dimensional Systems	11
2.1	Bosonization	11
2.1.1	Bosonization Overview	11
2.1.2	The Luttinger Gas	13
2.1.3	The Luttinger Liquid	16
2.1.4	Bosonizing a Simple Model	21
2.2	Correlation Functions	24
2.3	The Sine-Gordon Model	28
2.3.1	Sine-Gordon Overview	28
2.3.2	Renormalization Group Analysis	30
2.3.3	Exact Properties	38
3	The BKT Transition and Two Dimensional Systems	39
3.1	Hohenberg-Mermin-Wagner Theorem	39

3.1.1	Spontaneous Symmetry Breaking and Goldstone Modes	39
3.1.2	The Bogoliubov Inequality	43
3.1.3	An Example System: The XY Model	45
3.2	The 2D XY Model	47
3.2.1	XY Model Overview	47
3.2.2	2D XY Model at High Temperatures	48
3.2.3	2D XY Model at High Temperatures (again)	51
3.2.4	2D XY Model at Low Temperatures	52
3.3	The Beresinskii-Kosterlitz-Thouless Transition	54
3.3.1	Vortices	54
3.3.2	Topological Terms in the Action	59
3.3.3	BKT in Summary	61
3.4	The Vortex Plasma	62
3.4.1	Renormalization Group Analysis	62
3.4.2	Flow of the Coupling Constants	65
3.4.3	The 2D XY Universality Class	67
4	The Stripe Model	70
4.1	Experimental Setup	70
4.2	Bosonizing a Single Stripe	75
4.3	Weakly Coupling the Stripes	80
4.4	Equivalence to the Original Stripe System	81
4.5	Mean Field Model	82
4.5.1	Mean Field Structure	82
4.5.2	Mean Field Solution	84
4.6	Effective Theory at Close Coupling	89
4.6.1	Coupling the Fields into a Single SU(2) Field	89

4.6.2	A Ginzburg-Landau Treatment of the High Symmetry Point	94
4.6.3	The supersolid state	99
5	The $O(N)$ Nonlinear Sigma Model	101
5.1	Background	101
5.2	The Classical $O(N)$ Nonlinear Sigma Model	103
5.3	The Easy Plane $O(N)$ Nonlinear Sigma Model	108
5.4	The Quantum Easy Plane Nonlinear Sigma Model	113
6	Depletion of Order Due to Enhanced Symmetry	119
6.1	Motivation	119
6.2	Modified Berezinskii-Kosterlitz-Thouless Analysis	120
6.2.1	A Variational Ansatz	120
6.2.2	Another Look at the BKT Argument	122
6.3	Spin Wave Renormalization Analysis	128
6.4	Conclusions	133
7	Conclusions	135
	List of References	I

LIST OF FIGURES

1.1	Cartoon phase diagram of Lanthanum Cuprate	2
2.1	Labelling of particles in 1D	17
2.2	The RG flow of the Sine Gordon model	37
3.1	A cartoon example of spontaneous symmetry breaking	40
3.2	Set-up of the 2D XY Mode	48
3.3	Diagrammatic rules for the 2D XY model at high temperatures	49
3.4	The first non-zero diagram for the 2D XY model at high temperatures	50
3.5	Diagrammatic evaluation of the correlation function for the 2D XY model at high temperatures	51
3.6	A vortex configuration in the XY model	56
3.7	A vortex-anti-vortex pair	58
3.8	The integral contour avoiding each vortex core	60
3.9	Rescaling of the vortex core radius	63
4.1	Cartoon of dipoles on a line	70
4.2	Proposed experimental setup	71
4.3	Schematic distinction between “checkerboard” and “striped” density wave orders.	72
4.4	Cartoon of interacting dipoles	73
4.5	Solvable limits of the Luttinger parameter for Bosons with dipole-dipole interactions	78

4.6	Numerical evaluation of the Luttinger parameter for Bosons with dipole-dipole interactions	79
4.7	Plots of constant Luttinger parameter in the density-angle plane	79
4.8	Mean field phase diagram of the interaction dominated regime	87
4.9	Mean field phase diagram of the hopping dominated regime	88
4.10	Mean field phase diagram including both channels of coupling	89
4.11	Correction to the mean field phase diagram	95
4.12	Bicritical and tetracritical points	98
4.13	Adaptation to the mean field phase diagram	99
6.1	Softened vortex near a high symmetry point	121
6.2	Increase in the vortex core size as the high symmetry point is approached . .	132
6.3	Schematic phase diagram in the vicinity of the enhanced symmetry point . .	133

LIST OF TABLES

4.1	Fitting constants for the Luttinger parameter in a gas of dipoles	78
5.1	Dimension dependent coefficients for the RG flow for the $O(N)$ nonlinear sigma model	108

CHAPTER 1

INTRODUCTION AND MOTIVATION

1.1 Motivation

1.1.1 Background

Low dimensional models describe some of the most interesting strongly correlated systems in nature. One dimensional systems confuse the role of interactions and particle statistics, but present us with a myriad of techniques with which to construct exact solutions. Two dimensions is the lower critical dimension for systems with continuous broken symmetries and yet two dimensional systems possess a special kind of phase transition driven by topological defects.

Of particular interest are the **quasi-one dimensional** systems which consist of a number of effectively one-dimensional systems that weakly couple to one another. The structural anisotropy giving rise to the quasi-one dimensional nature of a condensed matter material may be due to its underlying crystal structure, as is the case in tetrathiafulvalene-tetracyanoquinodimethane (TTF-TCNQ)[5, 6], and in the telephone number compound $\text{Sr}_{14}\text{Cu}_{24}\text{O}_{41}$ [7]. It may instead be an emergent phase of the bulk electronic system, as is seen in the striped phase of the high T_c Cuprate compounds. Recent developments in optical lattice experiments on ultracold gases have led to a number of suggestions for making artificial quasi-one dimensional systems[8, 9, 10, 11, 12].

With so many different quasi-one dimensional condensed matter systems at hand, it would take more than one review to go through them all. Let us then instead discuss only

one motivational example, which is well studied and not a little controversial.

An interesting and topical example of a quasi-one dimensional system is the high T_c cuprate compounds, the story of which begins in 1986 when Bednorz and Müller [13] took some Lanthanum Cuprate and doped it with Barium – thereby discovering the first high temperature superconductor. The parent compound La_2CuO_4 is antiferromagnetic and Mott-insulating at low temperatures. The hole-doped compound $\text{La}_{2-x}\text{Ba}_x\text{CuO}_4$ loses antiferromagnetic order as the dopant concentration is increased and eventually becomes a superconductor which develops a remarkably high T_c (up to about 30K).

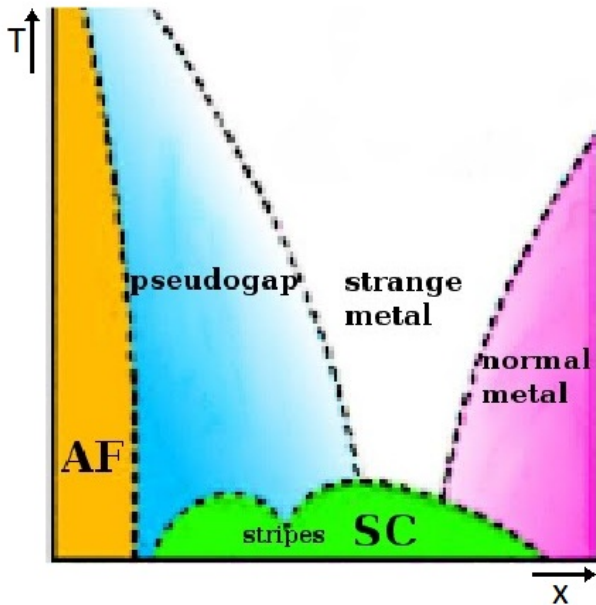


Figure 1.1: Cartoon phase diagram of the Lanthanum Cuprate with stripe order indicated at $1/8$ doping.

In this and in similar compounds, embedded within the superconducting order around $1/8$ doping and seemingly dragging down the transition temperature, there exists a *stripe order* [14], in which domains of antiferromagnetism push the electron-holes into narrow charge carrying channels. These materials are structurally quasi-two dimensional, but in the low temperature stripe ordered phase an emergent quasi-one dimensional behaviour is established.

Whether stripe ordering in high T_c superconductors is a coincidental and antipathetic phase to the superconductivity or a crucial part or a crucial ancillary phase to the onset of high T_c has been a matter of some debate[15, 16, 17, 18, 19, 20, 21].

In this thesis we will make absolutely no attempt to resolve this conflict.

We will focus our attention upon the striped system itself and the interesting physics therein. In order to extricate ourselves from the messy condensed matter background of the system in question, we propose a new experimental realization of the stripe model made up of ultracold dipolar bosons in a fine-tuned optical lattice.

Ultracold atom experiments offer us a powerful new probe of strongly condensed matter correlated systems[22]. The use of optical fields to construct custom trapping potentials offers the experimentalist an unprecedented degree of control over the geometry and energetics of an experimental system[23].

We will construct a cold atom system with the same underlying low energy effective Hamiltonian as one would expect to see within a striped system. Experiments upon such a setup should then be able to give us insights into the behaviour of the striped system. Moreover, a key feature present in these systems, as we shall see later, is the competition between density-wave and superfluid phase. Our proposed cold atom experiment will thus turn out to be a system with which we could study phase competition with a wide range of parameters and a great deal of control.

As a matter of semantics, from this point on we will often refer to all quasi-one dimensional systems simply as **striped systems**, be they striped in the cuprate sense or structurally anisotropic. This is more or less just because the term rolls off the tongue better and takes less time to type (although by that logic perhaps Q1D might have been a better choice). This naming convention is not intended as any sort of comment on the striped phase of cuprates.

Once we have developed our model we will notice that an important aspect is the competition between superconducting and charge density wave orders in two dimensions and an

enhanced symmetry when these orders are in maximal competition. This symmetry enhancement raises an interesting topological question as we will see that it must somehow destroy the natural topological excitations of the system – vortices. We will then be led to investigate the fate of vortices and the special transition they mediate in this and more general systems containing phase competition and symmetry enhancement.

1.1.2 The Stripe Order

Neutron scattering experiments on Cuprate compounds such as $\text{La}_{2-x-y}\text{Nd}_x\text{Sr}_y\text{CuO}_4$ [14] show peaks consistent with the existence of striped domains of charge and spin which can be thought of as effectively one-dimensional structures

Even in their normal state, the high temperature superconductors themselves are not well described within the framework of Fermi liquid theory and so it has been suggested[24] that a better starting point for theoretical investigation of such systems is to use as a basis the quasi-one dimensional nature of the stripe ordered phase. This approach has the added advantage that the one-dimensional electron gas is well understood, and it is known[25] that superconducting long-ranged order can be induced by inter-stripe coupling increasing the dimensionality of the system in what is referred to as *dimensional crossover*. The dimensional crossover from one- to two-dimensional charge transport in high Tc cuprates has been observed as doping is increased past the 1/8 point[26] and the crossover from two- to three-dimensional transport is seen upon exiting the superconducting state[27].

The picture coming from experimental data is that in the region of parameter space we are interested in – the superconducting region – these systems behave like one dimensional electron gases that are coupled into a two-dimensional array; the third dimension would appear to be weakly involved if at all.

The natural strategy then is to treat each stripe as a 1D system and couple these stripes together. The leading relevant inter-stripe couplings are via Josephson and charge-density

wave interactions[28, 29, 30], and so the Hamiltonian proposed for dealing with such a system takes the form $H = H_{\text{intra}} + H_{\text{inter}}$

$$H_{\text{intra}} = \sum_i \int dx \frac{v}{2} \left\{ K(\partial_x \theta_i)^2 + \frac{1}{K}(\partial_x \phi_i)^2 \right\} \quad (1.1a)$$

$$H_{\text{inter}} = \sum_{\langle ij \rangle} \int dx \left\{ J_{\text{SC}} \cos[\sqrt{2\pi}(\theta_i - \theta_j)] + J_{\text{CDW}} \cos[\sqrt{2\pi}(\phi_i - \phi_j)] \right\} \quad (1.1b)$$

The precise meaning of these terms isn't particularly important for now, but the reader might recognize this Hamiltonian as representing an array of Luttinger liquids with interactions which induce superconducting and charge-density wave order.

This Hamiltonian is generic to layered, quasi-one dimensional (striped) systems and would equally well treat a structurally anisotropic material such as $\text{Sr}_{14}\text{Cu}_{24}\text{O}_{41}$. It has been well studied in connection with condensed matter systems through various approaches, but the problem with comparing to experimental condensed matter systems will always be noise and disorder, for this reason we wish to develop an ultracold atomic experiment described by this Hamiltonian where these issues are under control.

Other materials which might be treated by a similar Hamiltonian include the **ladder compounds** such as SrCu_2O_3 which are structurally anisotropic quasi-one dimensional materials which take their name from their ionic structure. An n -leg ladder consists of n ionic chains running parallel to one another with inter-chain coupling of comparable strength to intra-chain coupling. The name for these compounds comes from the 2-leg case, a schematic of which resembles a ladder. These systems are reviewed in [31, 32].

An important feature of the Hamiltonian Eqn.[1.1], which was studied by Carr and Tsvetlik[29], is the competition between charge density wave and superfluid orders. This competition will be a major theme in what follows.

In this thesis we will propose an ultracold atomic experiment for which the low energy effective theory is described by this same Hamiltonian. This system can be thought of as an

analogue quantum simulator of the striped condensed matter systems we have discussed, but with a very high degree of control over the parameters.

1.1.3 Analogue Simulation with Cold Atoms

In his 1981 popular article “Simulating Physics with Computers” [33], Richard Feynman pointed out that any (bosonic) quantum system ought to be able to be simulated exactly by another system in which every site has precisely two basis states, thus giving rise to the concept of the quantum computer. Feynman’s proposal was for a universal quantum computer which would be able to simulate any quantum system in analogy to a classical Turing machine. A universal quantum computer is probably still many years away but recent developments mean that we can now seriously start thinking about simulating specific quantum systems with analogue quantum simulators.

The discoveries that have brought us to this point can be traced back to the creation in 1995 of the first Bose-Einstein condensates of alkali atoms [34, 35]. These early experiments involved a combination of laser and evaporative cooling of heavy alkali atoms confined within a magneto-optical trap.

Although the original work towards BEC formation in atomic gases was done for the sake of studying the condensate itself, it was soon realized that by transferring the degenerate gas from its magnetic trap into an optical lattice, one would have a system that could be employed as an analogue quantum simulator of a condensed matter system [36].

Early forays into using optically confined Bose gases as analogue simulators were focussed chiefly on simulating the behaviour of the Bose-Hubbard model [37, 22], which is defined by the Hamiltonian

$$H = \sum_i \varepsilon_i n_i - J \sum_{\langle ij \rangle} b_i^\dagger b_j + \frac{U}{2} \sum_i n_i (n_i - 1), \quad (1.2)$$

where b_i^\dagger is the bosonic creation operator on the i^{th} site and $n_i = b_i^\dagger b_i$ is the number operator for that site. The nearest-neighbour structure in the simulation is determined entirely by the optical “crystal” set up by the experimentalist and the hopping and site energies, U and ε , can be set by the depth of the optical potential. These experiments proved to be a great success as in 2002 the predicted transition from superfluid to Mott insulator was observed within an optical lattice experiment[38].

The great advantage that analogue simulation with ultracold atoms has over almost any other experiment in condensed matter is the control the experimentalist has over the internal parameters, from lattice spacing to interaction strength (which may be tuned via Feshbach resonances), and the cleanness of the system. If anything optical lattice experiments are too clean and experimentalists are forced to come up with ingenious ways to introduce disorder into their experiments[39].

1.1.4 Systems with Competing Order

The physical feature of the striped materials and our ultracold atomic analogue which we will be most interested in studying is the competition between two kinds of order – superfluidity and density wave – and that fact that this is happening in two dimensions which will lead to questions regarding the nature of the Berezinskii-Kosterlitz-Thouless transition in this system.

This situation – two types of order competing in a two-dimensional system – is certainly not specific to the model in question, and in fact is common to a great number of strongly correlated systems. Consider, for example, the quasi-two dimensional layered organic superconductors such as those based on bisethylenedithiotetrathiofulvalene; the phase diagram of such materials with changing pressure displays a competition between antiferromagnetism and (unconventional) superconductivity[40, 41]. Similarly, the heavy fermion compound CeIn_3 can be tuned to be two-dimensional[42], and demonstrates a competition

between superconductivity and antiferromagnetism[43].

Following the general ideas of Ginzburg-Landau theory, we would like to study such systems with competing order by introducing an order parameter of the correct symmetry group for each broken symmetry, and constructing a free energy functional or action in powers of these order parameters. Formally we could treat the two order parameters as two sectors of a single order parameter, as is common in $SO(5)$ treatments of systems with interacting antiferromagnetic and superconducting phases[44, 45]. In such a treatment there will exist symmetry breaking terms which act to separate out the two sectors of the unified field.

One might now imagine a situation – which will turn out to be the case for our striped model – in which there is a particular fine-tuned point in parameter space where the two phases are in maximal competition such that the symmetry breaking terms vanish and we are left with a single order parameter with a higher symmetry than the two constituent phases combined.

This symmetry enhancement and the effect that the high symmetry point has on the rest of the phase diagram is the feature of the stripe model which we will be most interested in and the conclusions we draw will be applicable to other models with competing order. The peculiarities of ordering in two dimensions *viz* the Hohenberg-Mermin-Wagner theorem and the Berezinskii-Kosterlitz-Thouless transition will greatly inform our considerations of such systems.

1.2 Thesis Overview

In the following two chapters we will introduce some of the basic concepts and methods we will use in developing the stripe model. These two chapters don't include anything new at all, but they do offer us the opportunity to set out all of the mathematics and ideas that will be referred back to. The reader who just wants to get to the meat of this thesis may want

to skip these chapters.

In `BOSONIZATION AND ONE DIMENSIONAL SYSTEMS` we will develop the machinery of bosonization, which is a scheme with which to deal with one-dimensional systems. After a historical and a more schematic introduction to bosonization we will solve a simple example system with the methods we have discussed. While on the subject of one-dimensional systems, we will discuss the Sine-Gordon model and talk about how to treat this model through a momentum-space renormalization group procedure.

In `THE BKT TRANSITION AND TWO DIMENSIONAL SYSTEMS` we discuss the Beresinskii-Kosterlitz-Thouless transition. We will motivate this discussion first by considering the Hohenberg-Mermin-Wagner theorem, and then by solving the 2D-XY model in its high and low temperature limits. In discussing the BKT transition we will see the importance of topological excitations – vortices – in the 2D-XY model, which will motivate us to study the vortex plasma description of this model. We will treat the vortex plasma through a real-space renormalization group procedure.

Having got some of the background concepts out of the way, we will be ready to move on to the first section of original research in this thesis.

In `THE STRIPE MODEL` we will propose an experimental setup involving ultracold dipolar bosons in an anisotropic optical lattice that resembles a two-dimensional array of one-dimensional stripes. We will use the methods we introduced in our discussion of one-dimensional systems to bosonize each stripe and then discuss how the inter-stripe interactions can be included to weakly couple the stripes. The model we develop will turn out to be equivalent to the model already used to treat striped condensed matter systems, but with a wide range of parameters to play with. We will then proceed to work out and solve a mean-field treatment of this system when either density-wave or superfluid behaviour is clearly dominant. When neither phase is dominant over the other, we will find that the system can be treated by an effective non-linear sigma model with a quadratic symmetry

breaking. A Ginzburg-Landau treatment of the zero temperature behaviour of this model will suggest the existence of a regime where density wave and superfluid orders coexist. This regime might be thought of as a supersolid and we will discuss what this means.

We then take a short break from the original content as we pause to discuss THE $O(N)$ NONLINEAR SIGMA MODEL. We develop the renormalization group treatment of this model in D and $D + 1$ dimensions with and without quadratic symmetry breaking.

Finally we will return to original content as we move on to discuss DEPLETION OF ORDER DUE TO ENHANCED SYMMETRY. In this chapter we study the effect of symmetry enhancement on a model with vortex mediated quasi-long ranged order through both a modified BKT argument, and by using the renormalization group flow of a nonlinear sigma model with quadratically broken symmetry that we developed in the previous chapter.

CHAPTER 2

BOSONIZATION AND ONE DIMENSIONAL SYSTEMS

2.1 Bosonization

2.1.1 Bosonization Overview

The physics of one dimensional systems is special for a number of reasons, the most important being that indistinguishable particles on the line are enumerable, and that fermions in one dimension have a Fermi surface consisting of only two points. These properties allow us to perform a procedure known as *bosonization* in which the physics of a full, interacting system is approximated by a non-interacting treatment of the sound waves in the system.

A brief history of the bosonization method is as follows. In 1950 Tomonaga[46] (inspired by a previous comment by Bloch) realised that the low energy physics of a weakly interacting Fermi gas could be approximated by the behaviour of the underlying *bosonic* sound wave excitations. His construction relied upon noticing that one can construct an operator with bosonic commutation relations out of pairs of fermionic operators and required linearising the spectrum about the Fermi surface. Tomonaga's work suffered from being rather complicated and from not offering a full solution scheme.

Over a decade later, in 1963, a very similar model to that arrived at by Tomonaga was considered by Luttinger[47]. This was essentially the same model but now included antiparticles which made it solvable. Luttinger diagonalized the model and constructed the exact solution. Two years later, in 1965, Mattis and Lieb demonstrated that Luttinger's

solution was actually flawed and presented the correct solution; nevertheless this model is now referred to as the (Tomonaga-)Luttinger model. Calculation of expectation values in this model was made simpler in 1974 when Luther and Peschel[48] and simultaneously Mattis[49] demonstrated how to construct the original fermionic operators out of bosonic operators.

Arguably the birth of what would now be called bosonization comes from the 1981 work of Haldane in which he brought together the previous work, filling in the gaps of various proofs to show how the weakly interacting Fermi gas can be exactly solved by constructing a bosonic representation when the spectrum is approximated as linear. In this paper Haldane calculated the excitation spectrum and correlation functions. He also comments in this paper that one ought to be able to construct a bosonic representation of a fermionic one dimensional system even without a linear spectrum. The completion of this work came in the same year when Haldane demonstrated that not only interacting fermions but also interacting bosons in one dimension could be approximated by a non-interacting *harmonic fluid*. From this harmonic fluid construction Haldane was able to calculate exact low energy properties of a one dimensional system regardless of the underlying statistics. He called the universality class of such one dimensional systems the *Luttinger liquid*.

In the following two sections we will derive the bosonized form of an interacting system *twice*. Our first approach will be a pre-eighties style derivation for the weakly interacting Fermi gas in which we linearise the spectrum around the Fermi surface. In analogy to the Fermi gas, we call this approach the The Luttinger Gas; this method is physically illuminating but does not extend well to bosonic systems. To get access to bosonic systems we follow Haldane's harmonic fluid construction to derive the properties of the The Luttinger Liquid. Using the Luttinger liquid approach we will then go on to bosonize a simple model to get a feeling for how the method works and where comparison to physical properties comes in.

2.1.2 The Luttinger Gas

Linearising the spectrum of a weakly interacting Fermi gas around the Fermi momentum, k_F , we have a system with positive and negative linear dispersion $\varepsilon_k = \pm v_F |k|$. We could equivalently think of this as a system consisting of left and right moving electrons with dispersion $\varepsilon_k = \sigma v_F k$, where $\sigma = +1$ for right-movers and $\sigma = -1$ for left-movers.

Quite generally we have the Hamiltonian

$$H = v_F \sum_{\sigma k} \sigma k c_{\sigma k}^\dagger c_{\sigma k} + \frac{1}{2L} \sum_{\sigma k} (V_1(k) \rho_{\sigma k} \rho_{\sigma(-k)} + V_2(k) \rho_{\sigma k} \rho_{-\sigma(-k)}) \quad (2.1)$$

where c, c^\dagger are fermionic operators ($[c, c^\dagger]_+ = 1, [c^{(\dagger)}, c^{(\dagger)}]_+ = 0$)¹, and ρ is the density operator $\rho_k = \sum_q c_{q+k}^\dagger c_q$. The allowed momenta in a system of length L are $k \in \frac{2\pi}{L} \mathbb{Z}$. We find it convenient to flit between the momentum representation and a position representation $\psi(x) = L^{-1/2} \sum_k e^{-ikx} c_k$.

Now the important thing that Tomonaga noticed, and which was shown quite rigorously by Haldane, is that the density operators are more-or-less bosonic operators. This is not immediately clear, but look at the commutator

$$\begin{aligned} [\rho_{\sigma k}, \rho_{\sigma'(-k')}] &= \sum_{qq'} \left[c_{\sigma(q+k)}^\dagger c_{\sigma q}, c_{\sigma'(q'+k')}^\dagger c_{\sigma'(q'+k')} \right] \\ &= \sum_{qq'} c_{\sigma(q+k)}^\dagger \left[c_{\sigma q}, c_{\sigma'(q'+k')}^\dagger c_{\sigma'(q'+k')} \right]_+ - \left[c_{\sigma(q+k)}^\dagger, c_{\sigma'(q'+k')}^\dagger c_{\sigma'(q'+k')} \right]_+ c_{\sigma q} \\ &= \delta_{\sigma\sigma'} \delta_{kk'} \sum_q \left(c_{\sigma(q+k)}^\dagger c_{\sigma(q+k)} - c_{\sigma q}^\dagger c_{\sigma q} \right). \end{aligned}$$

This looks like we should be able to shift the sum and get zero, but that would entail taking one divergent quantity away from another which is a bit dangerous². To be properly normal ordered we need to subtract out the averages $\langle c_{\sigma k}^\dagger c_{\sigma k} \rangle = \Theta(k_f - \sigma k)$; doing so leaves us with

¹We write the commutator and anti-commutator of two objects a and b as $[a, b]_\pm = ab \pm ba$ and usually simplify the notation for the commutator to $[a, b]_- \equiv [a, b]$.

²This anomaly is actually the mistake made by Luttinger that was corrected by Mattis and Lieb.

$$\begin{aligned}
[\rho_{\sigma k}, \rho_{\sigma'(-k')}] &= \delta_{\sigma\sigma'} \delta_{kk'} \sum_q \left(\langle c_{\sigma(q+k)}^\dagger c_{\sigma(q+k)} \rangle - \langle c_{\sigma q}^\dagger c_{\sigma q} \rangle \right) \\
&= \delta_{\sigma\sigma'} \delta_{kk'} \sum_k \left(\Theta(k_f - \sigma(k+q)) - \Theta(k_f - \sigma q) \right) = -\sigma \frac{Lk}{2\pi} \delta_{\sigma\sigma'} \delta_{kk'}.
\end{aligned}$$

We can now easily construct bosonic operators via

$$a_k^\dagger = \sum_\sigma \Theta(\sigma k) \sqrt{\frac{2\pi}{|k|L}} \rho_{\sigma k}, \quad (2.2)$$

where we notice that $\rho_{\sigma k}^\dagger = \rho_{\sigma(-k)}$. This construction fails when $k = 0$, at which point we have $\rho_{\sigma 0} = N_\sigma$. With this in mind, we see that the density operators may be represented as

$$\rho_{\sigma k} = N_\sigma \delta_{0k} + \sqrt{\frac{|k|L}{2\pi}} \left(\Theta(\sigma k) a_k^\dagger + \Theta(-\sigma k) a_{-k} \right). \quad (2.3)$$

This lets us represent the interaction part of the operator in terms of bosonic operators but what should do with the kinetic part? This is where the linear spectrum comes in. We calculate the commutator between the kinetic energy $H_0 = v_f \sum_{\sigma k} \sigma k c_{\sigma k}^\dagger c_{\sigma k}$ and the bosonic annihilation operator a_k^\dagger by considering the commutator of H_0 and $\rho_{\sigma k}$

$$\begin{aligned}
[\rho_{\sigma k}, H_0] &= \sum_{qq'\sigma'} v_f \sigma' q' \left[c_{\sigma(k+q)}^\dagger c_{\sigma q}, c_{\sigma'q'}^\dagger c_{\sigma'q'} \right] \\
&= \sum_{qq'\sigma'} v_f \sigma' q' \left(c_{\sigma(q+k)}^\dagger \left[c_{\sigma q}, c_{\sigma'q'}^\dagger c_{\sigma'q'} \right]_+ - \left[c_{\sigma(q+k)}^\dagger, c_{\sigma'q'}^\dagger c_{\sigma'q'} \right]_+ c_{\sigma q} \right) \\
&= \sum_{qq'\sigma'} v_f \sigma' q' \left(c_{\sigma(q+k)}^\dagger \delta_{\sigma\sigma'} \delta_{q,q'} c_{\sigma'q'} - c_{\sigma'q'}^\dagger \delta_{\sigma\sigma'} \delta_{q+k,q'} c_{\sigma q} \right) \\
&= -v_f \sigma k \sum_q c_{\sigma(q+k)}^\dagger c_{\sigma q} = -v_f \sigma k \rho_{\sigma k}.
\end{aligned}$$

This gives us that

$$\left[a_k^\dagger, H_0 \right] = -v_f |k| a_k^\dagger \quad (2.4)$$

which in turn implies that

$$H_0 = v_F \sum_k |k| a_k^\dagger a_k. \quad (2.5)$$

That the kinetic part of the Hamiltonian is quadratic in the bosonic representation is an important and highly counter-intuitive statement. We will actually prove this more rigorously in a moment, but let us pause to discuss the result further before we do so.

By linearising around the Fermi surface and representing the Hamiltonian in terms of a bosonic combination of fermionic operators we see that the Hamiltonian can be approximated (up to irrelevant constants) by the quadratic form

$$H = \frac{1}{2} \sum_k |k| \begin{pmatrix} a_k^\dagger & a_{-k} \end{pmatrix} \begin{pmatrix} v_F + \frac{V_1(q)}{2\pi} & \frac{V_2(q)}{2\pi} \\ \frac{V_2(q)}{2\pi} & v_F + \frac{V_1(q)}{2\pi} \end{pmatrix} \begin{pmatrix} a_k \\ a_{-k}^\dagger \end{pmatrix} \quad (2.6)$$

This Hamiltonian could now be diagonalized exactly using a Bogoliubov transformation if we so desired but there is no real point as we will be solving a bosonized system in the following section. What is important here is just that the Hamiltonian turns out to be quadratic.

Now in order to see how the fermionic operators we started with can be constructed out of the bosonic operators we are working with, we consider the commutator

$$\begin{aligned} [\rho_{\sigma k}, \psi_{\sigma'}^\dagger(x)] &= L^{-1/2} \sum_{q'} [c_{\sigma(q+k)}^\dagger c_{\sigma q}, c_{\sigma' q'}^\dagger] e^{iq'x} = L^{-1/2} \sum_{q'} c_{\sigma(q+k)}^\dagger \delta_{\sigma\sigma'} \delta_{qq'} e^{iq'x} \\ &= \delta_{\sigma\sigma'} e^{-ikx} \psi_{\sigma'}^\dagger(x) \end{aligned}$$

$$[a_k^\dagger, \psi_\sigma^\dagger(x)] = \Theta(\sigma k) \sqrt{\frac{2\pi}{|k|L}} e^{-ikx} \psi_\sigma^\dagger(x) \quad (2.7)$$

$$[a_k, \psi_\sigma^\dagger(x)] = \Theta(\sigma k) \sqrt{\frac{2\pi}{|k|L}} e^{ikx} \psi_\sigma^\dagger(x) \quad (2.8)$$

From Eqn.[2.7] we want to say $\psi_\sigma^\dagger(x) \propto \exp[-\Theta(\sigma k)(2\pi/kL)^{1/2} e^{-ikx} a_k]$ and from Eqn.[2.8] we want to say $\psi_\sigma^\dagger(x) \propto \exp[\Theta(\sigma k)(2\pi/kL)^{1/2} e^{-ikx} a_k^\dagger]$. With this in mind, we define a new

field

$$\phi_\sigma(x) = \sigma \frac{\pi x}{L} N_\sigma + i \sum_{k \neq 0} \Theta(\sigma k) \sqrt{\frac{2\pi}{|k|L}} e^{-ikx} a_k. \quad (2.9)$$

Notice that the first term is just the $k \rightarrow 0$ limit that we haven't included in the sum, which we leave outside the sum rather than leave the evaluation implicit. In terms of this we can see that the fermionic operators must be expressible as

$$\psi_\sigma^\dagger(x) = L^{-1/2} e^{i\phi_\sigma^\dagger(x)} U_\sigma e^{i\phi_\sigma(x)} \quad (2.10)$$

where U_σ is some unitary operator. Given that we are linearising about the Fermi surface we should have $\psi_\sigma^\dagger(x) \sim e^{i\sigma k_f x}$. We need to do something to ensure that $\psi_\sigma^\dagger(x)$ obeys Fermi statistics. We can do this by setting

$$U_\sigma = e^{i\sigma k_F x} F_\sigma \quad (2.11)$$

where F_σ is an anti-commuting operator which can be interpreted as increasing the number of Fermions in the σ -branch by one, this operator is referred to in the literature as a Klein factor[50].

This completes the Bose-Fermi mapping that comprises a traditional pre-Haldane picture of bosonization. As was discussed in the introduction to this chapter, Haldane extended these ideas in such a way that interacting bosonic systems can be treated within the same bosonization framework as fermions, but the approach he took was very different to the historical approach we have just taken.

2.1.3 The Luttinger Liquid

The direction taken by Haldane in extending the bosonization of the weakly interacting Fermi gas, into what we called the Luttinger gas, to more general interacting systems, which we

are calling the Luttinger liquid method, is based on the realization that indistinguishable particles on the line can nevertheless be labelled according to their relative position from left to right. We will see that this simple fact actually has some very significant consequences for calculating the low energy behaviour of one-dimensional systems.

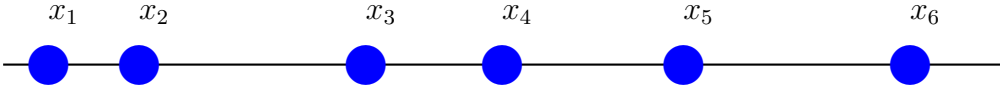


Figure 2.1: In 1D identical particles can be labelled, by taking their order from left to right. As this requires no reference to the origin, this scheme preserves translational invariance.

Let's say we have N identical particles on the line. Our labelling scheme – calling the position of the l^{th} particle along from the left x_l – lets us write the density for this system as

$$\rho(x) = \sum_{l=1}^N \delta(x - x_l). \tag{2.12}$$

We recall that the dimensionality of the system means that (at a fixed point in time) the *ordered* set of coordinates $\{x_l\}$ unambiguously defines the positions of the particles in this system. It is however more convenient to abandon this cumbersome set in favour of a single function $\ell : \mathbb{R} \mapsto \mathbb{R}$ which we allow to vary continuously subject to the following constraints

1. $\ell(x)$ must be monotonic in x (with no loss in generality we can say monotonically increasing).
2. $\ell(x_l) \equiv l$.

Recalling the transformation rule for the Dirac Delta function,

$$\delta(f(x)) = \sum_{y|f(y)=0} \frac{1}{|\partial_y f(y)|} \delta(x - y),$$

we realise that we can write the density of this system in terms of the labelling function $\ell(x)$ via

$$\rho(x) = \partial_x \ell(x) \sum_l \delta(\ell(x) - l).$$

Now by employing one of the multitude representations of the delta function (in this case we use the Poisson summation formula) this becomes

$$\rho(x) = \partial_x \ell(x) \sum_m e^{2\pi i m \ell(x)}.$$

Now let's imagine that these N particles live on a line of length L . If everything were homogeneous then the density on the line would be $\rho_0 = N/L$ and so a sane and sensible labelling function would be $\ell_0(x) = \rho_0 x$. We are well advised to consider fluctuations around this homogeneous limit so we express our labelling function as

$$\ell(x) = \ell_0(x) - \frac{1}{\pi} \varphi(x).$$

The monotonicity of $\ell(x)$ requires that the fluctuation amplitude, $\varphi(x)$, should be thought of as some low amplitude oscillatory function with period $\sim \rho_0$.

In terms of the fluctuation field, the density field is thus given by

$$\rho(x) = (\rho_0 - \partial_x \varphi(x)) \sum_m e^{2im[\pi\rho_0 x - \varphi(x)]}. \quad (2.13)$$

If one were to average this density over distances large compared to the inter-particle separation ($\sim 1/\rho_0$) the fluctuations in this exponent would act to cancel themselves out leaving only the constant term in the exponential. Hence from far away we would expect to see the *smearred density*

$$\tilde{\rho}(x) = \rho_0 - \frac{1}{\pi} \partial_x \varphi(x). \quad (2.14)$$

Up to this point we have made no reference to the statistics of the particles in question. An astounding feature of one dimensional physics is that it actually makes very little difference!

For the sake of definiteness we will continue down this line of thought assuming that the particles we have are identical bosons; we will later come back and see what would have happened if we were assuming the particles to be fermions.

Having written the density of the system in terms of an oscillatory fluctuation field, we might desire to express the creation and annihilation operators in a similar manner. To this end let us write the creation operator as

$$\psi^\dagger(x) = \sqrt{\rho(x)}e^{-i\theta(x)}. \quad (2.15)$$

We now need to fix the commutator of θ and φ so that the bosonic commutation relation

$$[\psi(x), \psi^\dagger(x')] = \delta(x - x') \quad (2.16)$$

is satisfied. Assuming (quite reasonably) that θ commutes with itself at all points we require that

$$[\rho(x), e^{-i\theta(x')}] = \delta(x - x')e^{-i\theta(x')}. \quad (2.17)$$

Simply by inspection we find that this last commutation relationship is satisfied (for the smeared density at least) if we put

$$\left[\frac{1}{\pi} \partial_x \varphi(x), \theta(x') \right] = -i\delta(x - x') \quad \text{or equivalently} \quad \left[\varphi(x), \frac{1}{\pi} \partial_{x'} \theta(x') \right] = i\delta(x - x'). \quad (2.18)$$

This shows us that $\varphi(x)$ possesses a canonically conjugate “momentum” field

$$\Pi(x) = (\hbar/\pi)\partial_x \theta(x). \quad (2.19)$$

With this commutation relation in place, to the level of approximation of the smeared density, we can write the creation operator as

$$\psi^\dagger(x) = \sqrt{\rho_0 - \frac{1}{\pi} \partial_x \varphi(x)} e^{-i\theta(x)}. \quad (2.20a)$$

To improve upon this smeared creation operator (which, when considering global properties of the system, isn't strictly necessary) we would have to include the higher harmonics within the density. To do so requires us to take the square root of a delta function, the problem with which is that the root of a delta function is not well defined. Recall that the delta function is not truly a function but is a measure and that multiplication among such, as opposed to convolution, is not a defined operation. Nevertheless, if we consider a nascent representation of the delta function, such as the zero width limit of a Gaussian, we can see that this will maintain its shape upon squaring so that we can loosely say that, up to some limiting procedure specific constant, the square root of a delta function is another delta function and hence

$$\psi^\dagger(x) \propto \sqrt{\rho_0 - \frac{1}{\pi} \partial_x \varphi(x)} \sum_{m \text{ even}} e^{i[\pi m \rho_0 x - m \varphi(x)]} e^{-i\theta(x)} \quad (2.20b)$$

$$= \sqrt{\rho_0 - \frac{1}{\pi} \partial_x \varphi(x)} \left(1 + 2 \sum_m \cos 2m [\pi \rho_0 x - \varphi(x)] \right) e^{-i\theta(x)}. \quad (2.20c)$$

As promised, let us now consider how our considerations so far would differ were the particles in question fermions, in which case the commutation relation Eqn.[2.16] would become an *anti*-commutation

$$[\psi(x), \psi^\dagger(x')]_+ = \delta(x - x'). \quad (2.21)$$

We can arrange this, without altering the commutator of φ and θ by taking two things into account. Firstly we know the commutator of these fields is $[\varphi(x), \theta(x')] = \frac{\pi}{2} i \operatorname{sgn}(x - x')$ and secondly $e^{i[\pi m \rho_0 x - m \varphi(x)]}$ changes sign as it passes through each particle. Thus an anti-commuting field can be constructed by inserting this phase into each term of the sum in Eqn.[2.20b] with the effect that it picks up a minus sign under particle exchange due to the $\operatorname{sgn}(x - x')$ term. Hence the fermionic creation operator may be written as

$$\psi^\dagger(x) \propto \sqrt{\rho_0 - \frac{1}{\pi} \partial_x \varphi(x)} \sum_{m \text{ odd}} e^{i[\pi m \rho_0 x - m \varphi(x)]} e^{-i\theta(x)} \quad (2.22a)$$

$$\approx \sqrt{\rho_0 - \frac{1}{\pi} \partial_x \varphi(x)} e^{i\pi \rho_0 x - i\varphi(x)} e^{-i\theta(x)}. \quad (2.22b)$$

2.1.4 Bosonizing a Simple Model

So how does this all help? We work with bosons (although the fermionic case is next to identical) and consider the archetypal Hamiltonian for interacting particles on the line

$$H = \frac{\hbar^2}{2m} \int_0^L dx \partial_x \psi^\dagger(x) \partial_x \psi(x) + \frac{1}{2} \int_0^L dx dx' V(x-x') \rho(x) \rho(x'). \quad (2.23)$$

We plug in the dual fields φ and θ , and linearise by dropping highly oscillatory terms, so that up to a smeared level of approximation the fields are

$$\left. \begin{array}{l} \rho(x) \\ \psi^\dagger(x) \end{array} \right\} \Rightarrow \left\{ \begin{array}{l} \rho_0 - \partial_x \varphi(x) \\ \sqrt{\rho_0} e^{-i\theta(x)} \end{array} \right. \quad (2.24)$$

Upon dropping irrelevant constants, Eqn.[2.23] becomes

$$H = \frac{\hbar^2 \rho_0}{2m} \int_0^L dx (\partial_x \theta(x))^2 + \frac{1}{2\pi^2} \int_0^L dx dx' V(x-x') \partial_x \varphi(x) \partial_{x'} \varphi(x'). \quad (2.25)$$

Assuming now that the interaction is sufficiently close ranged, we can introduce velocity scales

$$v_J = \frac{\pi \hbar \rho_0}{m} \quad (2.26a)$$

$$v_N \sim \frac{V(0)}{\pi \hbar}, \quad (2.26b)$$

which represent the phase stiffness and density stiffness respectively, and the Hamiltonian

takes the simple quadratic form

$$H = \frac{\hbar}{2\pi} \int_0^L dx v_J (\partial_x \theta(x))^2 + v_N (\partial_x \varphi(x))^2. \quad (2.27)$$

The identical form is given when we consider fermions instead. This Hamiltonian is referred to as the (Tomonaga-)Luttinger liquid. We have seen that the effective low energy (long wavelength) physics of a system comprising of *either* fermions or bosons with short ranged interactions in one dimension can be reduced to a harmonic model of field variables with canonical commutation relations *i.e.* a model with *bosonic* degrees of freedom.

The procedure we have just undergone is an interpretation of the construction given by Haldane[51] and is now known as *bosonization* (although Haldane called it the harmonic fluid description). Good reviews of the bosonization approach to one-dimensional systems are given in [52] [53]. The bosonization procedure shows us that many models in one dimension can be described within a single framework and hence these models belong to the same *universality class*. This universality class, the so called *Luttinger liquid* class, blurs the line between Bose-Einstein and Fermi-Dirac statistics, and hence suffers from its inability to describe model-specific features. An alternative derivation totally within the functional integral is possible[54].

The harmonic model we have derived is exactly soluble and we shall consider the solution later on. There are, however, a few small details to the construction that we have brushed under the carpet that we ought to look into now. There are, it turns out, topological considerations that need to be taken into account.

We started out with particles roaming around on the real line, and then restricted this down to the region $[0, L]$. Such a restriction is appropriate when considering, for example, cold atoms in a (quasi-)one-dimensional optical trap, which is bound to have finite extent. We may also want to explicitly consider what happens if particles are set in a ring formation as is possible in optical lattice experiments. Let us then consider the same system but with

periodic boundary conditions so that $\psi^\dagger(x+L) = \psi^\dagger(x)$. Looking to Eqn.[2.20] and Eqn.[2.22] we see that

$$\varphi(x+L) = \varphi(x) + \pi N \quad (2.28a)$$

$$\theta(x+L) = \theta(x) + \pi J, \quad (2.28b)$$

where N is the number of particles and J is some integer; J can be seen to obey the following selection rules depending upon the particle statistics:

$$\text{Bosons:} \quad (-1)^J = 1 \quad (2.28c)$$

$$\text{Fermions:} \quad (-1)^{J+N} = 1. \quad (2.28d)$$

Now to actually solve this harmonic model, as in many cases, the easiest approach is within the functional integral. However this is not so informative, so we hang on to the non-commuting operators and expand into Fourier space. To satisfy their correct commutation relations, the dual fields are expanded as

$$\varphi(x) = \varphi_0 + \pi x \frac{N}{L} + \left(\frac{v_J}{v_N} \right)^{\frac{1}{4}} \sqrt{\frac{\pi}{2L}} \sum_q \frac{1}{\sqrt{q}} \left[e^{-iqx} b(q) + e^{iqx} b^\dagger(-q) \right] \quad (2.29a)$$

$$\theta(x) = \theta_0 + \pi x \frac{J}{L} + \left(\frac{v_N}{v_J} \right)^{\frac{1}{4}} \sqrt{\frac{\pi}{2L}} \sum_q \frac{\text{sgn}(q)}{\sqrt{q}} \left[e^{iqx} b^\dagger(q) + e^{-iqx} b(-q) \right], \quad (2.29b)$$

where the field $b^\dagger(q)$ creates a long wavelength density fluctuation with momentum q , and the following commutators are set (unless otherwise stated, all other terms commute)

$$[b(q), b^\dagger(q')] = \delta_{q,q'} \quad (2.29c)$$

$$[N, e^{-i\theta_0}] = e^{-i\theta_0} \quad (2.29d)$$

$$[J, e^{-i\varphi_0}] = e^{-i\varphi_0} \quad (2.29e)$$

Given that a change in φ_0 represents a global shift of the particles, we see that the mean current operator is $\frac{1}{\pi}\partial_x\varphi$. Substituting the Fourier transformed fields into the Hamiltonian Eqn.[2.27] we arrive at the following expression

$$H = \hbar v_s \sum_q |q| b_q^\dagger b_q + \frac{\pi}{2} \hbar v_s \frac{(N - N_0)^2}{KL} + \frac{\pi}{2} \hbar v_s \frac{KJ^2}{L}, \quad (2.30)$$

where $N_0 = \rho_0 L$ and we have introduced the constants

$$K = \sqrt{\frac{v_J}{v_N}} \quad (2.31a)$$

$$v_s = \sqrt{v_J v_N} \quad (2.31b)$$

The form the Hamiltonian is now in gives us a clear physical picture of what the bosonization procedure is doing: we have represented the low energy excitations of a one-dimensional system as *phonons* with sound speed v_s . This form also allows us to see a physical meaning for the so called *Luttinger parameter* K , by looking at the adiabatic compressibility κ of the fluid at zero temperature. For the Hamiltonian above we have

$$\frac{1}{\kappa} = \rho_0^2 \left(\frac{\partial \mu}{\partial \rho} \right)_{\rho=\rho_0} = \rho_0 N \left(\frac{\partial^2 E_0(N)}{\partial N^2} \right)_{N=N_0} = \pi \rho_0^2 \frac{\hbar v_s}{K}, \quad (2.32)$$

so the Luttinger parameter is proportional to the compressibility of the fluid of phonons.

2.2 Correlation Functions

Finally, in our considerations of bosonization and the Luttinger liquid, let us actually solve for the correlation functions in this system.

In the immortal words of Victor Popov: “It turns out that we can associate with any Bose system a functional integral over the space of complex functions” [55]. For further

information on functional integrals in condensed matter field theory I would recommend the larger of Popov's books[56] or Altland and Simons' textbook on the matter[57]; other good sources are [53] and [58]. Assuming we are all happy with finding correlation functions within the functional integral, let us plough on.

We have a partition function and action functional

$$\mathcal{Z} = \int \mathcal{D}[\varphi, \Pi] e^{-S[\varphi, \Pi]/\hbar} \quad (2.33a)$$

$$S[\varphi, \Pi] = \int_0^{\beta\hbar} d\tau \int_0^L dx \left\{ \frac{\pi K v_s}{2\hbar} \Pi(\tau, x)^2 + \frac{\hbar v_s}{2\pi K} (\partial_x \varphi(\tau, x))^2 - i\Pi(\tau, x) \partial_\tau \varphi(\tau, x) \right\}. \quad (2.33b)$$

If we just want correlation functions in the fluctuation field φ we can decouple the momentum using

$$\Pi(\tau, x) \Rightarrow \Pi(\tau, x) + i \frac{\hbar}{\pi K v_s} \partial_\tau \varphi(\tau, x),$$

under which the action becomes

$$S = \frac{\hbar}{2\pi K} \int_0^{\beta\hbar} d\tau \int_0^L dx \left\{ \frac{1}{v_s} (\partial_\tau \varphi(\tau, x))^2 + v_s (\partial_x \varphi(\tau, x))^2 \right\} + \frac{\pi K v_s}{2\hbar} \int_0^{\beta\hbar} d\tau \int_0^L dx \Pi(\tau, x)^2.$$

Now letting $r = (r_0, r_1) = (v_s \tau, x)$, we get the correlation function

$$\begin{aligned} \langle \varphi(r) \varphi(r') \rangle &= \frac{\int \mathcal{D}[\varphi] \varphi(r) \varphi(r') e^{-\frac{1}{2\pi K} \int d^2 r (\nabla_r \varphi(r))^2}}{\int \mathcal{D}[\varphi] e^{-\frac{1}{2\pi K} \int d^2 r (\nabla_r \varphi(r))^2}} \\ &= \frac{K}{2} \ln |r - r'| = \frac{K}{4} \ln \left(\frac{(x - x')^2 + v_s^2 (\tau - \tau' + \varepsilon)^2}{\varepsilon^2} \right), \end{aligned}$$

where the ultraviolet cut-off ε is introduced to force time ordering. Due to the symmetry under the duality transformation $S[\varphi, \theta; K] = S[\theta, \varphi; 1/K]$, we also see that $\langle \theta(r) \theta(r') \rangle = \frac{1}{2K} \ln |r - r'|$. From this we see that the correlations in this system scale as

$$\langle \psi(r) \psi^\dagger(r') \rangle = \rho_0 \left\langle e^{i[\theta(r) - \theta(r')]} \right\rangle = \rho_0 e^{-\frac{1}{2} \langle [\theta(r) - \theta(r')]^2 \rangle} \sim \rho_0 |r - r'|^{-\frac{1}{2K}}.$$

Hence we see that for free fermions $K \rightarrow 1$ and for free bosons $K \rightarrow \infty$. In the above we have used the fact that for any action quadratic in ϕ ,

$$\langle \cos \phi \rangle = \langle e^{i\phi} \rangle = e^{-\frac{1}{2}\langle \phi^2 \rangle}, \quad (2.34)$$

to prove this we simply requires us to complete the square within the functional integral. This equation crops up rather a lot in our future considerations.

For sake of completeness we ought to consider the skew correlations $\langle \varphi \theta \rangle$, to which end it is easiest to move into momentum space. Our convention for the Fourier transform in d spatial dimensions, which we shall adopt throughout, is

$$f(\tau, \mathbf{x}) = \sum_{\mathbf{k} \in \left(\frac{2\pi}{L}\right)^d \mathbb{Z}^d} \sum_{\substack{\omega \in \frac{\pi}{\beta\hbar} 2\mathbb{Z} \text{ (bosons)} \\ \omega \in \frac{\pi}{\beta\hbar} (2\mathbb{Z}+1) \text{ (fermions)}}} \frac{e^{i\mathbf{k}\cdot\mathbf{x}} e^{-i\omega\tau}}{L^d \beta\hbar} f(\omega, \mathbf{k}) \quad (2.35a)$$

$$\xrightarrow{L \rightarrow \infty} \int \frac{d^d k}{(2\pi)^d} \sum_{\omega} \frac{e^{i(\mathbf{k}\cdot\mathbf{x} - \omega\tau)}}{\beta\hbar} f(\omega, \mathbf{k}), \quad (2.35b)$$

the inverse of which is

$$f(\omega, \mathbf{k}) = \int_0^L dx \int_0^{\beta\hbar} d\tau e^{-i(\omega\tau - \mathbf{k}\cdot\mathbf{x})} f(\tau, \mathbf{x}). \quad (2.35c)$$

If we let $p = (p_0, p_1) = (v_s^{-1}\omega, k)$, then in momentum space the action Eqn.[2.33b] becomes

$$\begin{aligned} S &= \frac{\hbar}{L\beta\hbar} \sum_p \left\{ i \frac{k\omega}{\pi} \theta(p) \varphi^*(p) + \frac{v_s K}{2\pi} k^2 |\theta(p)|^2 + \frac{v_2}{2\pi K} k^2 |\varphi(p)|^2 \right\} \\ &= \frac{\hbar}{2} \frac{1}{L\beta\hbar} \sum_p \begin{pmatrix} \theta^*(p) & \varphi^*(p) \end{pmatrix} \left\{ \frac{k}{\pi} \begin{pmatrix} kv_s K & i\omega \\ i\omega & kv_s/K \end{pmatrix} \right\} \begin{pmatrix} \theta(p) \\ \varphi(p) \end{pmatrix} \\ &= \frac{\hbar}{2} \frac{1}{L\beta\hbar} \sum_{p,p'} \begin{pmatrix} \theta^*(p) & \varphi^*(p) \end{pmatrix} \left\{ \frac{\delta_{p,p'} \pi}{\omega^2 + v_s k^2} \begin{pmatrix} v_s/K & -i\omega/k \\ -i\omega/k & v_s K \end{pmatrix} \right\}^{-1} \begin{pmatrix} \theta(p') \\ \varphi(p') \end{pmatrix}. \end{aligned}$$

So we have found a matrix Green's function (the thing that is being inverted) in Fourier

space which we simply need to convert to real space to find that

$$G(r) = \begin{pmatrix} \langle \theta(r)\theta(0) \rangle & \langle \theta(r)\varphi(0) \rangle \\ \langle \varphi(r)\theta(0) \rangle & \langle \varphi(r)\varphi(0) \rangle \end{pmatrix} = \begin{pmatrix} \frac{1}{4K} \ln \left(\frac{x^2 + v_s^2(\tau + \varepsilon)^2}{\varepsilon^2} \right) & -i \arg \{v_s \tau + \varepsilon + ix\} \\ -i \arg \{v_s \tau + \varepsilon + ix\} & \frac{K}{4} \ln \left(\frac{x^2 + v_s^2(\tau + \varepsilon)^2}{\varepsilon^2} \right) \end{pmatrix}. \quad (2.36)$$

Here we have completely solved the quadratic model in 1+1 dimensions. The structure of this model was basically that of the archetypal gaussian model in euclidean $d+1$ dimensions which underpins all of what will follow:

$$\mathcal{Z} = \int \mathcal{D}[\phi] e^{-S[\phi]} \quad S[\phi] = \frac{1}{2g} \int_0^{\beta\hbar} d\tau \int d^d x \left\{ \frac{1}{v^2} (\partial_\tau \phi)^2 + (\nabla_x \phi)^2 \right\}. \quad (2.37a)$$

Before we proceed, now seems a good time to mention various limits that we will take in our future dealings with models of this type.

At very low temperatures $\beta\hbar \gg L/v$, so in the thermodynamic limit ($L \rightarrow \infty$) it is prudent to draw the space and time degrees of freedom together as $r = (v\tau, x)$ and we see that the model with d spatial dimensions and 1 temporal dimension is equivalent to a model with $d+1$ spatial dimensions and no temporal dimensions,

$$S[\phi] = \frac{1}{2g} \int_{\mathbb{R}^{d+1}} d^{d+1}r (\nabla_r \phi)^2. \quad (2.37b)$$

On the other hand, at high temperatures $\beta\hbar \ll L/v$, we might expand the field as in Fourier modes as $\phi(\tau, x) = \phi(x) + \phi_1(x) \cos(\tau\pi/\beta\hbar) + \dots$ and then we may as well throw away the time dependence as high order harmonics which will vanish in a stationary phase approximation. In such a thermally static approximation the model becomes one with d spatial dimensions and no temporal dimensions,

$$S[\phi] = \frac{\beta\hbar}{2g} \int_{\mathbb{R}^d} d^d r (\nabla_r \phi)^2. \quad (2.37c)$$

In any case, the Green's function for this unperturbed model is readily available. This kind of system however forms a foundation for future, more complicated, scenarios.

2.3 The Sine-Gordon Model

2.3.1 Sine-Gordon Overview

We will top off this discussion of one dimensional systems by considering a particularly interesting 1D system, the sine-Gordon model. This system is something that will be of special interest to us later, because not only will we see it appear explicitly when we develop a mean field description of a striped system, but also because we will see that this model is part of the same universality class as another system we will draw from, the XY model.

After a broad introduction to the sine-Gordon model we will embark upon an analysis via a renormalization group treatment. This will afford us the opportunity to familiarize ourselves with renormalization techniques which make up a large part of the later original content of this thesis.

The sine-Gordon model (in two Euclidean dimensions) is described by the action

$$\mathcal{Z}_{\text{SG}} = \int \mathcal{D}[\phi] e^{-S_{\text{SG}}[\phi]} \quad S_{\text{SG}} = \int d^2r \left\{ \frac{1}{8\pi d} (\nabla_r \phi)^2 + 2\mu \cos \phi \right\}. \quad (2.38)$$

The name “sine-Gordon” is a poor pun on “Klein-Gordon”, to which this model is superficially similar. No really.

The sine-Gordon model crops up naturally in the context of bosonization when we try to incorporate lattice effects. In particular, if there is a finite lattice spacing, a , momentum is only conserved modulo $2\pi/a$, and so the particles are allowed to loan and borrow momentum from the lattice. Such a process is referred to as an umklapp (from the German *umklappen* – to turn over) and corresponds physically to the scattering of a pair from one side of the Fermi surface to the other. To see how this gives us an interaction of the sine-Gordon form we look to Eqn.[2.13]. In the presence of a lattice and at full filling the term in the exponent $\rho_0 x$ is an integer and so $e^{2im\pi\rho_0 x}$ no longer oscillates quickly acting to smear out the density,

but is just equal to 1. Then when looking at density-density interactions we need to include terms coming from $e^{2im\pi\varphi(x)}$, the lowest order of which gives us a term $\rho_0^2 \cos[2\varphi(x)]$ which gives us precisely the form of the SG model.

The sine-Gordon model also finds a home throughout physics; for example the classical sine-Gordon equation in Minkowski $d + 1$ ¹ dimensions

$$\left(\nabla_x^2 - \frac{1}{v^2}\partial_t^2\right)\phi(x, t) = \sin\phi(x, t) \quad (2.39)$$

may be used to describe the phase slip in a $2D$ Josephson tunnel junction[59] and also appears as the continuum limit of the Frenkel-Kontorova model of propagation of crystal dislocations[60].

In light cone coordinates, $p = \frac{1}{2}(x + vt)$, $q = \frac{1}{2}(x - vt)$ the classical sine-Gordon equation in $1 + 1$ Minkowski dimensions adopts the form

$$\partial_p \partial_q \phi(p, q) = \sin\phi(p, q), \quad (2.40)$$

for which form, Ablowitz *et al*[61] have formulated the inverse scattering problem and hence solved the initial value problem. In particular the classical sine-Gordon equation in $1 + 1$ dimensions admits soliton solutions such as

$$\phi_u(x, t) = 4 \arctan \exp \left\{ \frac{x - ut}{\sqrt{1 - (u/v)^2}} \right\},$$

which are referred to as *kinks*.

As with many similar integrable systems, there exists a *Backlund transformation* between solutions of the classical sine-Gordon equation. We notice that if ϕ is a solution of Eqn.[2.40], then another solution ψ can be found due to the construction

¹The d here is the actual dimension of space where as the d in the action Eqn.[2.38] is the scaling dimension of the sine-Gordon model. Apologies for reusing a letter.

$$\begin{aligned}\partial_p \psi &= \partial_p \phi + 2a \sin\left(\frac{\psi + \phi}{2}\right) \\ \partial_q \psi &= -\partial_q \phi + \frac{2}{a} \sin\left(\frac{\psi + \phi}{2}\right)\end{aligned}$$

Coleman[62] has shown that the sine-Gordon model Eqn.[2.38] can be mapped directly onto the massive Thirring model, which is exactly diagonalizable by Bethe ansatz [63].

By quantizing the kink solutions of the sine-Gordon model, Zamolodchikov[64] has calculated the exact S-matrix of the sine-Gordon model which is in agreement with that calculated for the massive Thirring model by Korepin[65].

Lukyanov and Zamolodchikov [66] have found many exact expectation values of local fields in the sine Gordon model which we will refer to later¹.

For the time being, in order to get a feel for what is going on in the sine-Gordon model, we will inspect this model from a renormalization group perspective.

2.3.2 Renormalization Group Analysis

The concept of renormalization group (for a review of which see [67]), which we will encounter throughout this thesis, was developed in its modern form by Kenneth Wilson [68, 69], for which he was awarded the 1982 Nobel prize.

The fundamental idea sitting beneath the renormalization group is startlingly simple. We imagine that it is possible to declare for a given system a fundamental length scale a separating high and low energy fluctuations; this could be an ultraviolet cutoff, as in the example we will pursue, or the size of a block of spins, as in Kadanoff's analysis of the Ising model (of which a particularly fine explanation is given in [70]). Consider now a rescaling of

¹Our choice of parametrisation for the sine-Gordon model corresponds directly to that of Lukyanov and Zamolodchikov (this being why it is written as it is, for ease of comparison). Their parameter β corresponds to our scaling dimension via $d = 2\beta^2$.

a , $a \rightarrow \tilde{a} > a$, it may so happen that the effective action at length scales $> a$ is invariant under such a transformation except for a redefinition of the system's coupling parameters $\{J_i\} \rightarrow \{\tilde{J}_i\}$; in which case we will call the system renormalizable. Then imagine repeating the same rescaling procedure; every time we rescale we are left with the same model but with different coupling constants, so we can come up with *running* coupling parameters $\{J_i(a)\}$ that *flow* with the fundamental scale a . The nature of this flow can tell us a great deal about a model because it tells us how the system operates as we move toward macroscopic length scales. Of particular interest are the *fixed points* at which the coupling constants are unchanged by variations in a , because these divide the flow of couplings into regimes of qualitatively different behaviour.

Without an example before us this description of the renormalization group (RG) approach is not so clear, so we will proceed to work out the renormalization flow within the Sine Gordon model.

Pressing on, our first goal in our quest to find the RG flow of the SG model is to find an effective theory of the low energy excitations in terms of an ultraviolet momentum cutoff Λ . Having then *coarse-grained* the system, we will inspect how the system responds to variation of the UV scale.

With an intrinsic momentum cutoff, Λ , the Fourier expansion of the field ϕ in Eqn.[2.38] adopts the form (from now on we won't bother to put vectors in bold face unless there is a risk of ambiguity)

$$\phi(r) = \int_{0 < |p| < \Lambda} \frac{d^2 p}{(2\pi)^2} e^{ip \cdot r} \phi(p). \quad (2.41a)$$

In order to coarse grain this system we want to extract out a shell of high momentum *fast modes*. To this end we shall define fast and slow modes with respect to a granularity parameter λ ,

$$\phi_\lambda(r) = \int_{0 < |p| < \frac{\Lambda}{\lambda}} \frac{d^2 p}{(2\pi)^2} e^{ip \cdot r} \phi(p) \quad (\text{Slow}) \quad (2.41b)$$

$$\phi_+(r) = \int_{\frac{\Lambda}{\lambda} < |p| < \Lambda} \frac{d^2 p}{(2\pi)^2} e^{ip \cdot r} \phi(p) \quad (\text{Fast}) \quad (2.41c)$$

We can think of the SG action as a perturbation atop the action of a free field:

$$S_{\text{SG}}[\phi] = S_0[\phi] + 2\mu \int d^2 r \cos \phi(r) \quad S_0[\phi] = \frac{1}{2} \int d^2 r \frac{1}{4\pi d} (\nabla_r \phi(r))^2, \quad (2.42)$$

Given that the fast field, ϕ_+ , and slow field, ϕ_λ , are automatically orthogonal to one another, we can divide the partition function into an integral over the two sectors

$$\mathcal{Z} = \int \mathcal{D}[\phi_\lambda] e^{-S_0^\lambda} \int \mathcal{D}[\phi_+] e^{-S_0^+ - 2\mu \int d^2 r \cos \phi(r)},$$

where S_0^+ and S_0^λ are the free action restricted to the fast and slow sectors respectively.

The coarse graining of the system is accomplished by integrating over the fast modes. To this end we denote by \mathcal{Z}_0^+ and $\langle \dots \rangle_0^+$ the partition function and thermal average with respect to the fast action S_0^+ . We will also employ the *fast propagator*

$$G_0^+(r_1 - r_2) = \langle \phi_+(r_1) \phi_+(r_2) \rangle_0^+ = \int_{\frac{\Lambda}{\lambda} < |p| < \Lambda} \frac{d^2 p}{(2\pi)^2} e^{ip \cdot (r_1 - r_2)} \frac{4\pi d}{p^2}. \quad (2.43)$$

Upon integrating out the fast field the partition functions becomes

$$\mathcal{Z}_{\text{SG}} = \mathcal{Z}_0^+ \int \mathcal{D}[\phi_\lambda] e^{-S_0^\lambda} \left\langle e^{-2\mu \int d^2 r \cos(\phi_\lambda(r) + \phi_+(r))} \right\rangle_0^+.$$

Now treating μ as a small parameter, we may expand the exponential and then re-exponentiate to find

$$\begin{aligned}
\mathcal{Z}_{\text{SG}} &= \mathcal{Z}_0^+ \int \mathcal{D}[\phi_\lambda] e^{-S_0^\lambda} \left\langle 1 - 2\mu \int \mathbb{d}^2 r \cos(\phi_\lambda(r) + \phi_+(r)) \right. \\
&\quad \left. + 2\mu^2 \int \mathbb{d}^2 r_1 \mathbb{d}^2 r_2 \cos(\phi_\lambda(r_1) + \phi_+(r_1)) \cos(\phi_\lambda(r_2) + \phi_+(r_2)) \right\rangle_0^+ + \mathcal{O}(\mu^3) \\
&= \mathcal{Z}_0^+ \int \mathcal{D}[\phi_\lambda] e^{-S_0^\lambda} e^{-2\mu \int \mathbb{d}^2 r \langle \cos(\phi_\lambda(r) + \phi_+(r)) \rangle_0^+} \\
&\quad \times e^{-2\mu^2 \int \mathbb{d}^2 r_1 \mathbb{d}^2 r_2 \langle \cos(\phi_\lambda(r_1) + \phi_+(r_1)) \rangle_0^+ \langle \cos(\phi_\lambda(r_2) + \phi_+(r_2)) \rangle_0^+} \\
&\quad \times e^{-2\mu^2 \int \mathbb{d}^2 r_1 \mathbb{d}^2 r_2 \langle \cos(\phi_\lambda(r_1) + \phi_+(r_1)) \cos(\phi_\lambda(r_2) + \phi_+(r_2)) \rangle_0^+} + \mathcal{O}(\mu^3).
\end{aligned}$$

We can perform the relevant averages to find that

$$\begin{aligned}
\langle \cos(\phi_\lambda(r) + \phi_+(r)) \rangle_0^+ &= \cos \phi_\lambda e^{-\frac{1}{2}G_0^+(0)} \\
\langle \cos(\phi_\lambda(r_1) + \phi_+(r_1)) \cos(\phi_\lambda(r_2) + \phi_+(r_2)) \rangle_0^+ \\
&= \frac{1}{2} e^{-G_0^+(0)} \left\{ e^{G_0^+(r_1-r_2)} \cos(\phi_\lambda(r_1) - \phi_\lambda(r_2)) + e^{-G_0^+(r_1-r_2)} \cos(\phi_\lambda(r_1) - \phi_\lambda(r_2)) \right\},
\end{aligned}$$

which shows us that the partition function can be rewritten as

$$\begin{aligned}
\mathcal{Z}_{\text{SG}} &= \mathcal{Z}_0^+ \int \mathcal{D}[\phi_\lambda] \exp \left\{ -S_0^\lambda - 2\mu e^{-\frac{1}{2}G_0^+(0)} \int \mathbb{d}^2 r \cos \phi_\lambda(r) \right. \\
&\quad \left. + \mu^2 e^{-G_0^+(0)} \int \mathbb{d}^2 r_1 \mathbb{d}^2 r_2 \left(e^{G_0^+(r_1-r_2)} - 1 \right) \cos(\phi_\lambda(r_1) - \phi_\lambda(r_2)) \right. \\
&\quad \left. + \mu^2 e^{-G_0^+(0)} \int \mathbb{d}^2 r_1 \mathbb{d}^2 r_2 \left(e^{-G_0^+(r_1-r_2)} - 1 \right) \cos(\phi_\lambda(r_1) + \phi_\lambda(r_2)) \right\} + \mathcal{O}(\mu^3).
\end{aligned}$$

Now, $G_0^+(r)$ is built up of Fourier modes with momenta within a fine slither $\Lambda/\lambda < |p| < \Lambda$ and hence is dominated by the region $|r| \sim \lambda/\Lambda \ll 1$. Notice that because $G_0^+(r)$ is small for $|r| > 0$, so is $e^{\pm G_0^+(r)} - 1 \sim \pm G_0^+(r)$.

In our coarse graining of the partition function, it hence suffices to expand as a Taylor series in $r_1 - r_2$. Setting

$$\begin{aligned}
u &= \frac{1}{2}(r_1 + r_2) & v &= r_1 - r_2 \\
r_1 &= u + \frac{1}{2}v & r_2 &= u - \frac{1}{2}v,
\end{aligned}$$

the relevant expansions are

$$\begin{aligned}
\phi_\lambda(r_1) + \phi_\lambda(r_2) &\approx 2\phi(u) \\
\phi_\lambda(r_1) - \phi_\lambda(r_2) &\approx v \cdot \nabla_u \phi_\lambda(u) \\
\cos(\phi_\lambda(r_1) - \phi_\lambda(r_2)) &\approx 1 - \frac{1}{2}v^2 |\nabla_u \phi_\lambda(u)|^2.
\end{aligned}$$

Now to leading order the partition function has become

$$\begin{aligned}
\mathcal{Z}_{\text{SG}} &= \mathcal{Z}_0^+ \int \mathcal{D}[\phi_\lambda] \exp \left\{ -\frac{1}{2} \int \mathrm{d}^2 r \frac{1}{4\pi d} (\nabla_r \phi_\lambda(r))^2 - 2\mu e^{-\frac{1}{2}G_0^+(0)} \int \mathrm{d}^2 r \cos \phi_\lambda(r) \right. \\
&\quad \left. + \mu^2 e^{-G_0^+(0)} \int \mathrm{d}^2 u \mathrm{d}^2 v \left(e^{G_0^+(v)} - 1 \right) \left(1 - \frac{1}{2}v^2 |\nabla_u \phi_\lambda(u)|^2 \right) \right. \\
&\quad \left. + \mu^2 e^{-G_0^+(0)} \int \mathrm{d}^2 u \mathrm{d}^2 v \left(e^{-G_0^+(v)} - 1 \right) \cos(2\phi_\lambda(u)) \right\} + \mathcal{O}(\mu^3).
\end{aligned}$$

We can drop the constant term as this will just rescale the free energy density, which we won't be looking at. The $\cos 2\phi_\lambda$ term represents a higher harmonic than anything else at play here so we will neglect it. Then setting

$$A = e^{-G_0^+(0)} \int \mathrm{d}^2 v \left(e^{G_0^+(v)} - 1 \right) v^2,$$

\mathcal{Z} takes the form

$$\mathcal{Z}_{\text{SG}} \approx \mathcal{Z}_0^+ \int \mathcal{D}[\phi_\lambda] \exp \left\{ -\frac{1}{2} \int \mathrm{d}^2 r \left(\frac{1}{4\pi d} + A\mu^2 \right) (\nabla_r \phi_\lambda(r))^2 - 2\mu e^{-\frac{1}{2}G_0^+(0)} \int \mathrm{d}^2 r \cos \phi_\lambda(r) \right\}.$$

This now looks more or less like what we started with, except that the field here is ϕ_λ

rather than ϕ . We can get this in terms of ϕ by rescaling distances and momenta via $r \rightarrow \lambda r$, $p \rightarrow \frac{1}{\lambda}p$, which turns Eqn.[2.41b] into Eqn.[2.41a]. Now the effective partition function for slow modes, as a function of the granularity, is given by

$$\mathcal{Z}_{\text{SG}}(\lambda) \approx \int \mathcal{D}[\phi_\lambda] e^{-\frac{1}{2} \int d^2r \left\{ \frac{1}{4\pi d_\lambda} (\nabla_r \phi(r))^2 + 2\mu_\lambda \cos \phi(r) \right\}}, \quad (2.44)$$

where the running coupling constants are defined by

$$\mu_\lambda = \lambda^2 e^{-\frac{1}{2}G_0^+(0)} \mu \quad (2.45a)$$

$$d_\lambda^{-1} = d^{-1} + 4\pi\mu^2 e^{-G_0^+(0)} \int d^2v \left(e^{G_0^+(v)} - 1 \right) v^2 \quad (2.45b)$$

Quite clearly this model is renormalizable – we have shown that the coarse grained action Eqn.[2.44] does not alter its form under changes in the UV scale with running coupling constants given by Eqn.[2.45]. Now we just need to work out how the running coupling constants flow. To get a handle on this, we make the outer momentum shell as slender as possible by putting $\Lambda/\lambda = \Lambda - d\Lambda$, i.e. $\lambda = 1 + d\Lambda/\Lambda$. This allows us to write the fast propagator as

$$\begin{aligned} G_0^+(r_1 - r_2) &= \int_{\Lambda-d\Lambda < |p| < \Lambda} \frac{d^2p}{(2\pi)^2} e^{ip \cdot (r_1 - r_2)} \frac{4\pi d}{p^2} \\ &= \int_{\Lambda-d\Lambda < |p| < \Lambda} d|p| \frac{d}{\pi|p|} \int_0^{2\pi} d\theta e^{i|p||r| \cos \theta} \\ &= \int_{\Lambda-d\Lambda < |p| < \Lambda} d|p| \frac{d}{\pi|p|} \times 2\pi J_0(|p||r|) \\ &= 2d J_0(\Lambda|r|) \frac{d\Lambda}{\Lambda} \end{aligned}$$

where $J_\alpha(x)$ is the Bessel function of the first kind $J_\alpha(x) = \sum_m \frac{(-1)^m}{m!} \frac{(x/2)^{2m+\alpha}}{(m+\alpha)!}$, so that $J_0(0) = 1$.

The running coupling constants thus become

$$\begin{aligned}\mu_\lambda &= \mu + (2-d)\frac{d\Lambda}{\Lambda}\mu \\ d_\lambda^{-1} &= d^{-1} + 4\pi\mu^2 \int d^2r \, 2dJ_0(\Lambda|r|)\frac{d\Lambda}{\Lambda} = d^{-1} + Bd\mu^2\frac{d\Lambda}{\Lambda^5}\end{aligned}$$

where B is a dimensionless constant coming from the integral. Now by writing $\mu_\lambda = \mu + d\mu$ and $d_\lambda^{-1} = d^{-1} + dd^{-1}$, we have a set of differential equations describing the flow of the running coupling constants

$$\frac{d\mu}{\mu} = (2-d)\frac{d\Lambda}{\Lambda} \tag{2.46a}$$

$$\frac{d(d^{-1})}{(d^{-1})} = Bd\mu^2\frac{d\Lambda}{\Lambda^5}. \tag{2.46b}$$

The all important fixed points for this flow occur when the scaling dimension is exactly two. Homing in on this region, the flow is approximately

$$\begin{aligned}\frac{1}{2}(d-2)d(d) &= \left(\sqrt{B}\frac{\mu}{\Lambda}\right) d\left(\sqrt{B}\frac{\mu}{\Lambda}\right) \\ \Rightarrow (d-2)^2 &= 4B\frac{\mu^2}{\Lambda^2} + \nu.\end{aligned}$$

We hence see that the flow is hyperbolic as illustrated in figure Fig.[2.2].

The implication of this flow is that there is a phase transition between strong and weak coupling limits around the critical scaling dimension $d = 2$. Even in the limit $\mu \rightarrow 0$ this transition persists and tells us that for $d > 2$ the effect of the cosine interaction is negligible whereas for $d < 2$ it will always dominate.

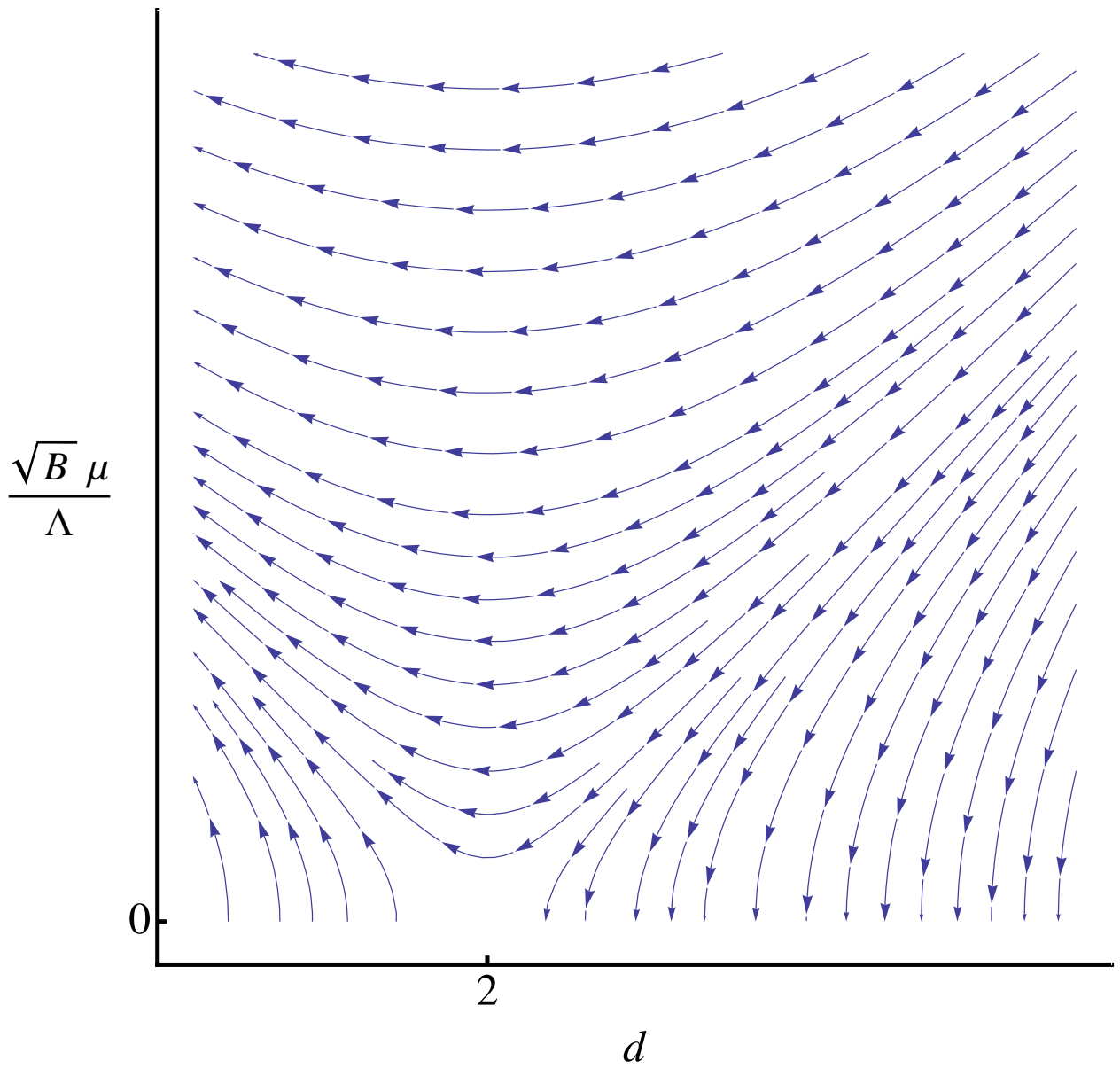


Figure 2.2: The RG flow of the Sine Gordon model: notice that even as $\mu \rightarrow 0$ a transition is present at the critical scaling dimension $d = 2$.

2.3.3 Exact Properties

As for the correlation functions, notice that the scaling dimension is defined such that

$$\langle \cos \phi(r_1) \cos \phi(r_2) \rangle_0 \sim |r - r'|^{-2d};$$

this means that $\cos \phi$ scales as $(\text{length})^{-d}$ and hence μ scales as $(\text{length})^{d-2}$ and hence the transition is at $d = 2$. This is why we call d the scaling dimension of the cosine perturbation.

The transition is also apparent when we look at the expectation values within the SG model calculated by Lukyanov and Zamolodchikov; after a bit of algebra their expression can be written

$$\langle \cos \phi \rangle = \frac{\Gamma(1 - \frac{1}{2-d})}{\Gamma(\frac{1}{2-d})} \frac{\Gamma(-\frac{d}{2})}{\Gamma(\frac{d}{2})} \frac{\Gamma(\frac{1}{2-d} - \frac{1}{2})}{\Gamma(\frac{1}{2} - \frac{1}{2-d})} \left[\frac{\Gamma(1 - \frac{d}{2})}{\Gamma(\frac{d}{2})} \pi \mu \right]^{\frac{d}{2-d}}. \quad (2.47)$$

In this form we can also see that something interesting ought to happen at the $d = 1$ point. That is actually the model you would arrive at upon bosonizing free fermions, so $d = 1$ represents an exactly solvable limit.

As we would expect from the renormalization group analysis, there is a divergence in the correlation function as the critical scaling dimension $d = 2$ is approached.

CHAPTER 3

THE BKT TRANSITION AND TWO DIMENSIONAL SYSTEMS

3.1 Hohenberg-Mermin-Wagner Theorem

3.1.1 Spontaneous Symmetry Breaking and Goldstone Modes

Melvyn Bragg once said that “Spontaneous symmetry breaking” is one of the most beautiful phrases in the English language. Putting aesthetics to one side, it is certainly one of the most important concepts in modern physics. Very generally, a system is said to exhibit spontaneous symmetry breaking if the underlying laws governing it are invariant under some symmetry transformation, whereas the system itself is changed by that transformation. In more physical language we would say that a spontaneously broken symmetry of a Hamiltonian is such that the ground state of the Hamiltonian is not an eigenstate of the generator of the symmetry.

As an everyday picture of spontaneous symmetry breaking, imagine you are at a posh dinner party with a number of people at a circular table. Each place is set and between each place is a wine glass. There is a perfect symmetry to the table with regards to the glasses, and if you were to move any number of places clockwise or anticlockwise you would see a glass in the same place. You don't know the convention for which glass is yours and it appears that none of the other guests do¹, so, trying not to make a *faux pas*, you all wait

¹Bread on the left, drink on the right – **b-d** – a mnemonic for which is to place your hands palm on the table.

to see what someone else does before reaching for a glass – the symmetry remains unbroken. Now your host arrives and proposes a toast, he lifts the glass to his right and you and all of your compatriots follow suit. The symmetry of the table is now broken, moreover this symmetry breaking has been spontaneous.

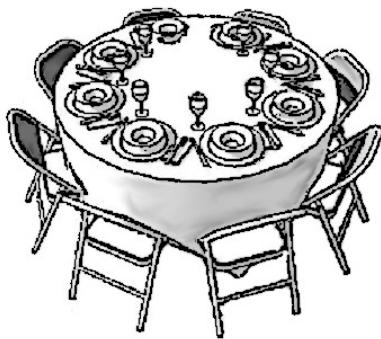


Figure 3.1: A cartoon example of spontaneous symmetry breaking: There is a left-right symmetry in the positioning of the glasses until someone takes a drink at which point the symmetry is spontaneously broken.

As a more physical and less glib example of spontaneous symmetry breaking consider an ordinary iron bar magnet. Any schoolchild could tell you¹ that in a ferromagnet all the spins align along the same axis, but there couldn't be anything in the physics that decides what that axis is, else every bar magnet would have the same orientation and the universe would be a rather different place. So if there is nothing inherent to the physics that decides what axis the spins in a magnet should point along; they must all conspire to align in one direction simultaneously – i.e. the symmetry is broken spontaneously.

To be more definite we construct an action describing classical magnetism using Ginzburg-Landau theory. The action should depend only upon the local magnetization $\mathbf{m} = (m_x, m_y, m_z)$ and its derivatives, so we want the functional form to be

$$S[\mathbf{m}] = \int d^d r \mathcal{L}(\mathbf{m}, \nabla \mathbf{m} \dots).$$

¹A child of five would understand this. Send someone to fetch a child of five.

The action should be translationally and rotationally invariant and in the absence of any external field we ought to be able to rotate between the sectors of \mathbf{m} , so the kind of terms we should expect to see in the action are

$$S[\mathbf{m}] = \int d^d r \left\{ \frac{t}{2} |m|^2 + u |m|^4 + \dots + \frac{K}{2} (\nabla \mathbf{m})^2 + L (\nabla^2 \mathbf{m})^2 + \dots - \mathbf{h} \cdot \mathbf{m} \right\},$$

where $t, u, K, L \dots$ are phenomenological parameters, and \mathbf{h} is an applied external field. For our purposes we can say $L = 0$.

We can just take a saddle point approximation and minimize S over \mathbf{m} . For $K > 0$ the action is minimized by $\mathbf{m}(\mathbf{r}) = m \mathbf{n}$ where the constant m minimises $\frac{t}{2} m^2 + u m^4 - |h| m$ and \mathbf{n} is a unit vector pointing in the direction of the external field \mathbf{h} . In the case where $|h| = 0$ we have $m = \sqrt{-t/4u}$ if $t < 0$ and $m = 0$ otherwise.

When $|h| = 0$ there is nothing in the model that determines the direction of \mathbf{n} . The magnitude of the magnetization is fixed by minimizing the action but the direction is fixed by a classic example of spontaneous symmetry breaking.

There is a degenerate manifold of ground states corresponding to all the possible directions for the magnetization to point along. This implies the existence of excitations made up of gentle rotations through this manifold. Such excitations are called spin waves in this system and Goldstone modes more generally. Goldstone modes are present in any system exhibiting a continuous, spontaneously broken symmetry, and there will be one for each degree of freedom in the ground state manifold. This result is referred to as Goldstone's theorem.

Let us now construct the Goldstone modes themselves. As \mathbf{n} is a unit vector we can parametrize it as $\mathbf{n} = (\pi_1, \pi_2, \sqrt{1 - \pi_1^2 - \pi_2^2})$. These fields π_i are the Goldstone modes. Pulling out the constant minimum, S_0 , of the action, we can re-write in terms of these modes alone as

$$S - S_0 = \frac{Km^2}{2} \int \mathrm{d}^d r (\nabla n)^2 \approx \frac{Km^2}{2} \int \mathrm{d}^d r \{(\nabla \pi_1)^2 + (\nabla \pi_2)^2 + \mathcal{O}(\pi^4)\}.$$

With no loss in generality we can say that the spontaneous magnetization is in the $(0, 0, 1)$ direction, then we could treat the Goldstone modes as small perturbations and drop the $\mathcal{O}(\pi^4)$ terms.

Left now with a quadratic action we can easily calculate the first correction the the magnetization $M = \langle m_z \rangle = m - m \langle \pi_1^2 \rangle - m \langle \pi_2^2 \rangle$. We consider

$$\langle \pi_1^2 \rangle = \frac{1}{Km^2} \int \frac{\mathrm{d}^d k}{(2\pi)^d} \frac{1}{k^2}$$

Now for $d \leq 2$ this integral is divergent. This is simply because the Goldstone modes are massless.

We are led to conclude that the spontaneous magnetization itself is a fallacy, and that for $d \leq 2$ this long range order simply cannot develop. Intuitively we can see why this should be the case as the massless Goldstone modes cost next to nothing and hence shake any order apart.

This is an example of the Hohenberg-Mermin-Wagner theorem which states that there is no possible long range order at finite temperatures in a system with continuous spontaneous symmetry breaking in two or fewer dimensions.

Our informal discussion here was intended to put across the ideas of spontaneous symmetry breaking and the Hohenberg-Mermin-Wagner theorem, but we have by no means proven HMW theorem even for the model at hand. At best we have shown that perturbation theory fails when we try to expand around an ordered state. For a formal proof of HMW it is simplest to turn to the Bogoliubov inequality.

3.1.2 The Bogoliubov Inequality

To prove the Hohenberg-Mermin-Wagner theorem in a rigorous manner, it is useful to consider an inequality due to Bogoliubov. In this section we will state and prove the validity of this inequality.

We consider the thermal expectation of some operator X in a system evolving according to a Hamiltonian H ,

$$\langle X \rangle = \frac{\text{tr} \{ X e^{-\beta H} \}}{\text{tr} \{ e^{-\beta H} \}} \quad (3.1)$$

Bogoliubov's inequality in a very general form states that for any non-zero operators A and C on the same Hilbert space as the Hamiltonian H

$$\frac{1}{2} \langle [A, A^\dagger]_+ \rangle \geq k_B T \frac{\langle [C^\dagger, A] \rangle^2}{\langle [[C, H], C^\dagger] \rangle}. \quad (3.2)$$

To prove this inequality it is expedient to introduce the Bogoliubov inner product¹

$$(A, B)_{\text{BV}} = \sum_{E_m \neq E_n} \langle n | A^\dagger | m \rangle \langle m | B | n \rangle \frac{W_m - W_n}{E_n - E_m}, \quad (3.3)$$

where the sum is taken over eigenstates $\{|n\rangle, E_n\}$ of the Hamiltonian and the weight factors W are given by

$$W = \frac{e^{-\beta E}}{\text{tr} \{ e^{-\beta H} \}}. \quad (3.4)$$

To prove this inequality we first note that if $E_m < E_n$ then $W_m > W_n$, so that the ratio of $W_m - W_n$ and $E_n - E_m$ is always positive. We then manipulate as follows

¹Is this really an inner product? Conjugate symmetry and linearity are clearly satisfied, but it is not *a priori* obvious that $(\cdot, \cdot)_{\text{BV}}$ is positive-definite. Actually this is positive definite because each term in the summation for $(A, A)_{\text{BV}}$ is proportional to $|\langle m | A | n \rangle|^2$, each of these factors is greater than or equal to zero and at least one of these must be non-zero.

$$\begin{aligned}
\frac{W_m - W_n}{E_n - E_m} &= \frac{W_m + W_n}{E_n - E_m} \frac{W_m - W_n}{W_m + W_n} = \frac{W_n + W_m}{E_n - E_m} \frac{e^{-\beta E_m} - e^{-\beta E_n}}{e^{-\beta E_m} + e^{-\beta E_n}} \\
&= \frac{W_n + W_m}{E_n - E_m} \frac{e^{\beta \frac{E_n - E_m}{2}} - e^{-\beta \frac{E_n - E_m}{2}}}{e^{\beta \frac{E_n - E_m}{2}} + e^{-\beta \frac{E_n - E_m}{2}}} \\
&= \frac{W_n + W_m}{E_n - E_m} \tanh \left(\beta \frac{E_n - E_m}{2} \right) \\
&\leq \frac{\beta}{2} (W_n + W_m),
\end{aligned}$$

in which we have used $\tanh x \leq x$ for all $x \geq 0$. From this inequality we see that

$$\begin{aligned}
(A, A)_{\text{BV}} &\leq \frac{\beta}{2} \sum_{E_m \neq E_n} \langle n | A^\dagger | m \rangle \langle m | A | n \rangle (W_m + W_n) \\
&\leq \frac{\beta}{2} \sum_n \langle n | A^\dagger \sum_m | m \rangle \langle m | A W_n | n \rangle + \frac{\beta}{2} \sum_m \langle m | A \sum_n | n \rangle \langle n | A^\dagger W_m | m \rangle \\
&= \frac{\beta}{2} \sum_n \langle n | A^\dagger A \frac{e^{-\beta H}}{\text{tr}\{e^{-\beta H}\}} | n \rangle + \frac{\beta}{2} \sum_m \langle m | A A^\dagger \frac{e^{-\beta H}}{\text{tr}\{e^{-\beta H}\}} | m \rangle \\
&= \frac{\beta}{2} \frac{\text{tr}\{A^\dagger A e^{-\beta H}\}}{\text{tr}\{e^{-\beta H}\}} + \frac{\beta}{2} \frac{\text{tr}\{A A^\dagger e^{-\beta H}\}}{\text{tr}\{e^{-\beta H}\}} \\
&= \frac{\beta}{2} \langle [A, A^\dagger]_+ \rangle
\end{aligned}$$

Applying the Schwartz inequality to the Bogoliubov inner product we then have

$$(A, A)(B, B) \geq |(A, B)|^2 \quad \Rightarrow \quad \frac{\beta}{2} \langle [A, A^\dagger]_+ \rangle (B, B)_{\text{BV}} \geq |(A, B)_{\text{BV}}|^2 \quad (3.5)$$

In particular, choosing $B = [C^\dagger, H]$ we find that

$$\begin{aligned}
(B, B)_{\text{BV}} &= \sum_{E_m \neq E_n} \langle n | [H, C] | m \rangle \langle m | [C^\dagger, H] | n \rangle \frac{W_n - W_m}{E_m - E_n} \\
&= \sum_{E_m \neq E_n} \langle n | [H, C] | m \rangle \langle m | (E_n - E_m) C^\dagger | n \rangle \frac{W_m - W_n}{E_n - E_m} \\
&= \sum_{mn} \langle n | [H, C] | m \rangle \langle m | \frac{e^{-\beta H}}{\text{tr}\{e^{-\beta H}\}} C^\dagger | n \rangle - \sum_{mn} \langle n | [H, C] | m \rangle \langle m | C^\dagger \frac{e^{-\beta H}}{\text{tr}\{e^{-\beta H}\}} | n \rangle \\
&= \frac{\text{tr}\{[H, C] e^{-\beta H} C^\dagger\}}{\text{tr}\{e^{-\beta H}\}} - \frac{\text{tr}\{[H, C] C^\dagger e^{-\beta H}\}}{\text{tr}\{e^{-\beta H}\}} \\
&= \langle [C^\dagger, [H, C]] \rangle.
\end{aligned}$$

Similarly,

$$(A, B)_{\text{BV}} = \langle [C^\dagger, A^\dagger] \rangle.$$

Putting all of these into to Schwartz inequality we immediately arrive at

$$\frac{\beta}{2} \langle [A, A^\dagger]_+ \rangle \langle [C^\dagger, [H, C]] \rangle \leq \langle [C, A] \rangle^2$$

and so the Bogoliubov inequality is proven.

The Bogoliubov inequality places a strict upper bound on the thermal expectation value of any observable. As such, to prove Hohenberg-Mermin-Wagner theorem it is sufficient to simply demonstrate that this upper bound is zero for the order parameter at long distances.

3.1.3 An Example System: The XY Model

The Hohenberg-Mermin-Wagner is very general but the proof is rather difficult for the general case. The Bogoliubov inequality helps us prove it for specific systems. The proof for a given symmetry (XY/ $O(2)$, Heisenberg/ $O(3)$) goes along similar lines so we will focus in this section on a specific system. The case originally studied by Mermin and Wagner[71] was the

Heisenberg model, but for the remainder of this chapter we will be looking into the XY model so this will be the case we prove here. A proper introduction to the XY model is coming up later, for the time being let us just consider the Hamiltonian

$$H = - \sum_{ij} J_{ij} \cos(\phi_i - \phi_j) - h \sum_i \cos \phi_i.$$

We need not be too restrictive about the nature of the exchange interaction, but we will demand that it is of even parity and that it is sufficiently short ranged that $Q = \sum_r |J(r)|r^2$ remains finite.

To exploit the Bogoliubov inequality, we want to pick operators A and C to put into the Bogoliubov inequality Eqn.[3.2] such that the order parameter $m = \langle \sum_i \cos \phi_i / N \rangle$ comes in.

To get this term to come out we can set

$$A = \sum_i e^{-ikr_i} \sin \phi_i \quad C = \sum_i e^{-ikr_i} \frac{\partial}{\partial \phi_i}$$

then we can calculate the appropriate commutators as follows

$$\begin{aligned} \langle [[C, H], C^\dagger] \rangle &= \sum_{ij} e^{ik(r_i - r_j)} \left\langle \frac{\partial^2 H}{\partial \phi_i \partial \phi_i} \right\rangle \\ &= \sum_{ij} 2J_{ij} (1 - e^{ik(r_i - r_j)}) \langle \cos(\phi_i - \phi_j) \rangle + h \sum_i \langle \cos \phi_i \rangle \\ &= 2N \sum_{r_{ij}} |J(r_{ij})| (1 - \cos kr_{ij}) \langle \cos(\phi_i - \phi_j) \rangle + hNm \\ &\leq N \left(k^2 \sum_r |J(r)|r^2 + hm \right) = N(Qk^2 + hm) \end{aligned}$$

$$\begin{aligned} \langle [C, A] \rangle &= \sum_i \langle \cos \phi_i \rangle = Nm \\ \langle [A^\dagger, A]_+ \rangle &= \sum_{ij} 2 \langle \sin \phi_i \sin \phi_j \rangle e^{ik(r_i - r_j)} \end{aligned}$$

Sticking these bits into the Bogoliubov inequality we see that

$$\sum_{ij} \langle \sin \phi_i \sin \phi_j \rangle e^{ik(r_i - r_j)} N(Qk^2 + hm) \geq k_B T N^2 m^2,$$

rearranging and integrating over all momenta we arrive at

$$\frac{k_B T m^2}{Q} \int d^d k \frac{1}{k^2 + \frac{hm}{Q}} \leq \sum_i \frac{\langle \sin^2 \phi_i \rangle}{N} \leq 1.$$

For dimension $d < 3$ this integral has an infrared divergence as $h \rightarrow 0$. The only way for the inequality to hold then is if $m \rightarrow 0$ (or $T \rightarrow 0$ if we allow that limit). We thus see very clearly that the system prohibits spontaneous magnetization at finite temperatures, which is the essence of Hohenberg-Mermin-Wagner theorem.

3.2 The 2D XY Model

3.2.1 XY Model Overview

Let us picture a two dimensional square lattice of classical 2D spins of unit magnitude, spaced an equal distance a apart from one-another. We suppose that these spins interact via a constant nearest neighbour interaction such that a pair gives an energy contribution of $-J$ when they are parallel and $+J$ when they anti-parallel, with a continuum of adjoining values in between these limits. The action we construct, which is the simplest possible action for a phase like variable $e^{i\theta}$ in 2D, must then be

$$S_{XY}[\theta] = -\beta J \sum_{\langle ij \rangle} s_i \cdot s_j = -\beta J \sum_{\langle ij \rangle} \cos(\theta_i - \theta_j), \quad (3.6)$$

where the summation is taken over nearest neighbouring sites and in which we have parametrized our unit spins by $s = (\cos \theta, \sin \theta)$.



Figure 3.2: Set-up of the 2D XY Model

The first thing we should do with this model, as with any model, is to investigate its extremal limits, so let us look into the high and low temperature regimes in some detail.

3.2.2 2D XY Model at High Temperatures

At high temperatures, $\beta J \ll 1$, it seems eminently sensible to attempt to expand the partition function for the 2D XY model as a power series in βJ . So doing, to lowest order we find

$$\begin{aligned}
 \mathcal{Z}_{\text{XY}} &= \int \mathcal{D}[\theta] e^{-S_{\text{XY}}[\theta]} = \int_0^{2\pi} \left(\prod_k \frac{d\theta_k}{2\pi} \right) e^{\beta J \sum_{\langle ij \rangle} \cos(\theta_i - \theta_j)} \\
 &\approx \int_0^{2\pi} \left(\prod_k \frac{d\theta_k}{2\pi} \right) \prod_{\langle ij \rangle} (1 + \beta J \cos(\theta_i - \theta_j)) \\
 &= \int_0^{2\pi} \left(\prod_k \frac{d\theta_k}{2\pi} \right) \left[1 + \beta J \sum_{\langle ij \rangle} \cos(\theta_i - \theta_j) + (\beta J)^2 \sum_{\langle ij \rangle, \langle kl \rangle} \cos(\theta_i - \theta_j) \cos(\theta_k - \theta_l) + \dots \right].
 \end{aligned}$$

To approach this sum we just need the following integrals:

$$\begin{aligned}
 \int_0^{2\pi} \frac{d\theta}{2\pi} (\beta J) \cos(\alpha - \theta) (\beta J) \cos(\theta - \gamma) &= \frac{\beta J}{2} (\beta J) \cos(\alpha - \gamma) \\
 \int_0^{2\pi} \frac{d\theta}{2\pi} (\beta J) \cos(\alpha - \theta) &= \beta J \delta_{\alpha\theta}.
 \end{aligned}$$

We can now set up a kind of proto-diagrammatic expansion; denoting $\beta J \cos(\theta_i - \theta_j)$ by an edge linking the sites i and j , these integrals tell us that linking the edge from i to j to the

edge from j to k gives $\frac{\beta J}{2}$ times an edge from i to k , and that edges that link onto themselves give a contribution to the sum of βJ whilst edges with a free tail give a contribution of zero. These diagrammatic rules are illustrated in Fig.[3.2.2]. The net result is that the only diagrams contributing to the partition function are those that are topologically circular.

We now have that the partition function for the 2D XY model at high temperatures can be thought of as the sum over all *loops* on the lattice, with each loop contributing $2 \left(\frac{\beta J}{2}\right)^\ell$ to the partition function, where ℓ is the length of the loop. The first such contribution is shown in Fig.[3.2.2].

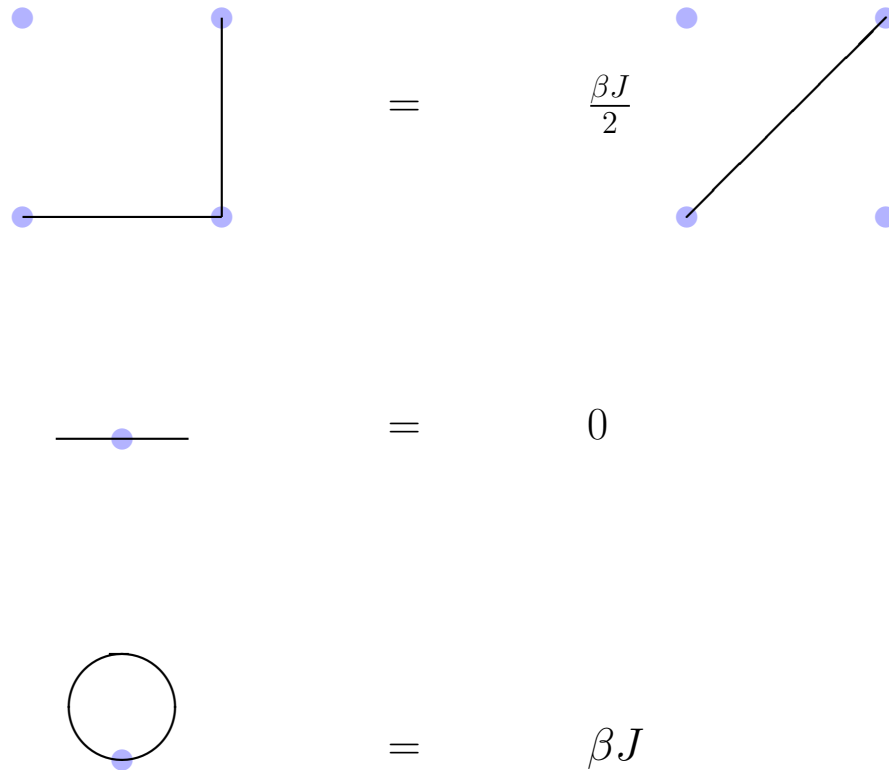
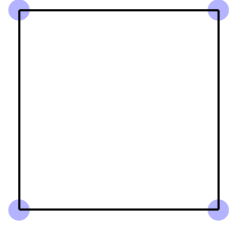


Figure 3.3: Diagrammatic rules for the 2D XY model at high temperatures



$$= \beta J \times \left(\frac{\beta J}{2} \right)^3$$

Figure 3.4: The first non-zero diagram for the 2D XY model at high temperatures

The very same argument can be applied to the site-to-site correlation function

$$\begin{aligned} \langle s_m \cdot s_n \rangle &= \int \mathcal{D}[\theta] \cos(\theta_m - \theta_n) e^{-S_{XY}[\theta]} \\ &\approx \int_0^{2\pi} \left(\prod_k \frac{d\theta_k}{2\pi} \right) \cos(\theta_m - \theta_n) \prod_{\langle ij \rangle} (1 + \beta J \cos(\theta_i - \theta_j)). \end{aligned}$$

The diagrammatic rules are unchanged, the only difference being that we start out with an edge from site m to site n at the outset. Immediately we see that the only contributions to the correlation function come from links that complete a circuit between m and n and the lowest order contribution will come from the shortest route on the lattice from n to m , as illustrated in Fig.[3.2.2].

As such, to leading order the correlation function is simply given by

$$\langle s_m \cdot s_n \rangle \sim \left(\frac{\beta J}{2} \right)^{\|r_m - r_n\|_{\#}} = e^{-\frac{1}{\xi} \|r_m - r_n\|_{\#}},$$

where $\|\cdot\|_{\#}$ is the norm (*i.e.* the distance) on the lattice (which becomes the Euclidean norm in the limit where the lattice vanishes) and, ξ , is the correlation length

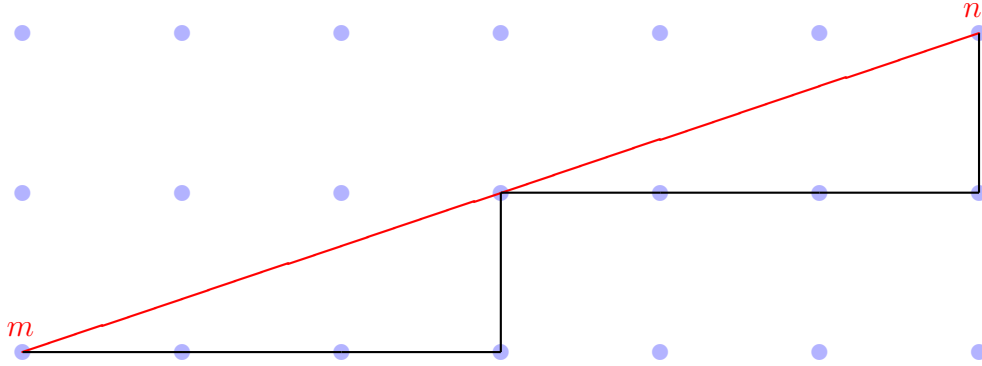


Figure 3.5: Diagrammatic evaluation of the correlation function for the 2D XY model at high temperatures

$$\xi = \frac{a}{\ln 2 - \ln \beta J}.$$

We can now say that in the high temperature phase correlations vanish exponentially with correlation length ξ and hence this represents a disordered phase.

3.2.3 2D XY Model at High Temperatures (again)

One might worry a little about the very first step we made in which we approximated $e^{\beta J \cos(\theta_i - \theta_j)}$ by $1 + \beta J \cos(\theta_i - \theta_j)$, and then proceeded to consider higher orders in βJ . There is clearly some concern regarding consistency.

Actually there is no need to worry because we can avoid this approximation entirely. Consider the expansion of the exponential in terms of the modified Bessel function of the first kind

$$e^{\beta J \cos(\theta_i - \theta_j)} = I_0(\beta J) + 2 \sum_{k=1}^{\infty} I_k(\beta J) \cos k(\theta_i - \theta_j)$$

The relevant integral we require now is

$$\int_0^{2\pi} \frac{d\theta}{2\pi} I_k(\beta J) \cos k(\alpha - \theta) I_l(\beta J) \cos l(\theta - \gamma) = \frac{I_k(\beta J)}{2} I_l(\beta J) \cos l(\alpha - \gamma) \delta_{kl}$$

The Kronecker delta in this integral tells us that the various Fourier modes completely decouple from one another. We could set up a diagrammatic procedure for this problem akin to the prior approximation with different diagrams for each harmonic, but the point is that different harmonics don't join up to one another. For the correlation function we actually want to calculate only the first harmonics that give any contribution, and we still need to count loops so one can see straight off that the lowest order contribution will be

$$\langle s_m \cdot s_n \rangle \sim I_0(\beta J/2)^{R^2 - \|r_m - r_n\|_{\#}} I_1(\beta J/2)^{\|r_m - r_n\|_{\#}}, \quad (3.7)$$

where R is the system size. We haven't yet taken a limit, but it is now perfectly safe to do so. Working with small βJ we can just Taylor expand these Bessel functions to find

$$\langle s_m \cdot s_n \rangle \sim \left(1 + \frac{(\beta J)^2}{16}\right)^{R^2 - \|r_m - r_n\|_{\#}} \left(\frac{\beta J}{4} + \frac{(\beta J)^3}{128}\right)^{\|r_m - r_n\|_{\#}}, \quad (3.8)$$

So we see that our initial estimate wasn't half bad at all.

3.2.4 2D XY Model at Low Temperatures

We should now be confident in saying that at high temperatures the 2D XY model is disordered with exponential decay in correlation functions. Now as for the behaviour in low temperatures, where the correlation length becomes much larger than the lattice spacing and our loop expansion breaks down, we might treat the lattice spacing a as a small parameter and attempt to replace the action with that of a continuum model.

$$\begin{aligned}
S_{\text{XY}} &= -\beta J \sum_{\langle ij \rangle} s(r_i) \cdot s(r_j) \\
&= -\beta J \sum_i \{s(r_i) \cdot s(r_i + ae_x) + s(r_i) \cdot s(r_i + ae_y)\} \\
&= -\beta J \sum_x \sum_y s(x, y) \cdot [s(x + a, y) + s(x, y + a)] \\
&\approx -\beta J \sum_x a \sum_y a \left[\frac{2}{a^2} s(r) \cdot s(r) + \frac{1}{2a} (\partial_x + \partial_y) s(r) \cdot s(r) + \frac{1}{2} s(r) \cdot (\partial_x^2 + \partial_y^2) s(r) \right] \\
&\xrightarrow{a \rightarrow 0} 2\beta J L^2 + \frac{\beta J}{2} \int \mathrm{d}^2 r (\nabla s)^2.
\end{aligned}$$

Remembering that each s should have unit magnitude, we realize that, up to irrelevant constants, the continuum limit of the 2D XY model is the 2D $O(2)$ nonlinear sigma model (we will discuss the nonlinear sigma model in detail later on)

$$\mathcal{Z}_{\text{XY}} \xrightarrow{a \rightarrow 0} \mathcal{Z}_{O(2)} = \int \mathcal{D}[s \in \mathbb{R}^2] \delta(s^2 - 1) e^{-S[s]} \quad S[s] = \frac{\beta J}{2} \int \mathrm{d}^2 r (\nabla s)^2. \quad (3.9)$$

Among all the nonlinear sigma models the $O(2)$ case is particularly interesting because it admits a trivial parametrization,

$$s = \begin{pmatrix} \cos \phi \\ \sin \phi \end{pmatrix} \implies \mathcal{Z} = \int \mathcal{D}[\phi] e^{-\frac{\beta J}{2} \int \mathrm{d}^2 r (\nabla \phi)^2}.$$

A naive calculation of the correlation functions then proceeds as follows

$$\begin{aligned}
\langle s(r) \cdot s(0) \rangle &= \langle \cos(\phi(r) - \phi(0)) \rangle = e^{-\frac{1}{2} \langle [\phi(r) - \phi(0)]^2 \rangle} \sim e^{\langle \phi(r)\phi(0) \rangle} \\
\langle \phi(r)\phi(0) \rangle &= \int^{1/a} \frac{d^2p}{(2\pi)^2} \frac{e^{ip \cdot r}}{\beta J p^2} = \frac{1}{2\pi\beta J} \int^{|r|/a} \frac{dx}{x} \int_0^{2\pi} \frac{d\theta}{2\pi} e^{ix \cos \theta} \\
&\sim -\frac{1}{2\pi\beta J} \ln(|r|/a) \\
\therefore \langle s(r) \cdot s(0) \rangle &\sim \left(\frac{a}{|r|} \right)^{\frac{1}{2\pi\beta J}}
\end{aligned}$$

We then see that, as opposed to the high temperature case where there was exponential decay in correlation functions and hence no long ranged order, at sufficiently low temperatures (this phrase “sufficiently low” being the focus of the rest of this chapter) the correlations will decay **algebraically** and so the system has developed a *quasi-long-ranged-order* (QLRO).

This point is crucial – Hohenberg-Mermin-Wagner theorem tells us that the system cannot order in two dimensions at finite temperature, but there is wiggle room; so long as correlations do decay in the far field HMW is satisfied. A system with algebraic decay still has correlations going to zero at infinity, but the correlation length (in the sense you would apply to exponential decaying correlations) has become infinite.

3.3 The Beresinskii-Kosterlitz-Thouless Transition

3.3.1 Vortices

Having now deduced that the 2D XY model possesses a disordered regime at high temperatures and a QLRO regime at lower temperatures, we are led to ask ourselves by precisely what mechanism the QLRO system acquires disorder, and furthermore at what temperature this transition takes place. The transition at play will turn out to be an example of

the Berezinskii-Kosterlitz-Thouless¹ transition, in which disordering is brought about by the accumulation of topological defects.

The reason that topological considerations must be taken into account can be traced back to the fact that the field ϕ with which we parametrize the spin orientation is defined only up to an integer multiple of 2π . This allows us to consider configurations of spins such that the traversal of a closed path will increase ϕ by $2\pi n$. This integer n defines a kind of *topological charge* enclosed by the path. A simple example of such a topologically non-trivial configuration could be given by $\phi(r, \theta) = \theta$, as illustrated in Fig.[3.3.1].

A topological defect such as this is referred to in this context as a **vortex**.

We will consider other configurations of this type, with azimuthal symmetry radiating out of the vortex core. The magnitude of the topological distortion can be obtained by integrating around a closed path that circles the core; in the above example we have

$$\oint \mathrm{d}\ell \cdot \nabla\phi = \oint (e_r \mathrm{d}r + e_\theta \mathrm{d}\theta) \cdot \left(e_r \partial_r + e_\theta \frac{1}{r} \partial_\theta \right) \theta = \oint \mathrm{d}\theta = 2\pi.$$

¹As a side note; the BKT transition is named for Vadim Berezinskii, John Kosterlitz and David Thouless – these having posited its existence separately and in different contexts, Berezinskii in 1971[72] [73] and Kosterlitz and Thouless in 1973[74] [75]. Now to give Berezinskii his due, his work does predate that of Kosterlitz and Thouless by two years, but as a proud alumnus of the School of Mathematics at the University of Birmingham – from which Kosterlitz and Thouless were operating at the time of their discovery – I feel that I ought to side with my kinsmen and hence would refer to call the ‘BKT’ transition simply the ‘KT’ transition, I include the ‘B’ only so as to avoid offending possible Russian readers. However I digress.

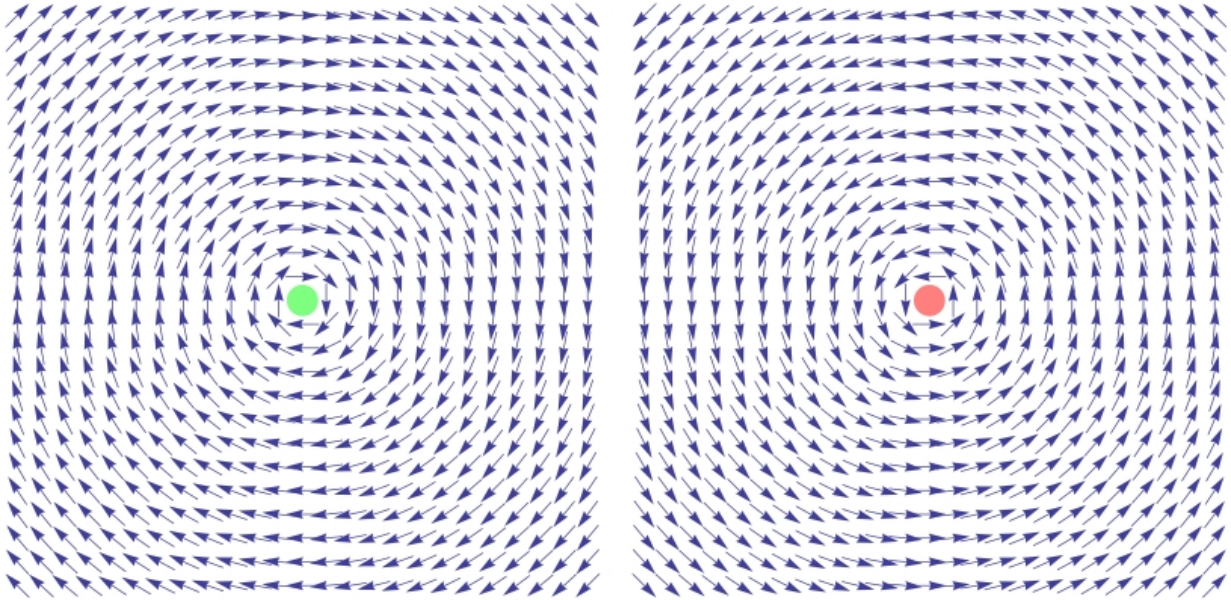


Figure 3.6: The simplest topologically non-trivial configuration in the 2D XY model – a vortex (left) or an anti-vortex (right).

We need to take care that the path does not pass through the core so we have to distinguish between the core region, $|r - r_{\text{core}}| < a$, and the rest of the plane.

Considering a general vortex, with topological charge n , we have

$$\oint \mathrm{d}\ell \cdot \nabla\phi = 2\pi n,$$

which would imply that

$$\nabla\phi = \frac{n}{|r - r_{\text{core}}|} e_{(r-r_{\text{core}})} \times e_z.$$

This allows us to consider the contribution to the action from a single vortex of charge n . If we call the system size R (which we may later take off to infinity), taking care to avoid the core region, we find that

$$S[\phi] = S_{\text{core}} + \frac{\beta J}{2} \int_{|r-r_{\text{core}}|>a} \mathrm{d}^2r \frac{n^2}{|r - r_{\text{core}}|^2} = S_{\text{core}} + \pi\beta J n^2 \ln(R/a).$$

So the contribution to the action has a core part and term which scales logarithmically with system size. The core part may be neglected so long as a UV cut-off is in place, effectively this corresponds to placing to core off the lattice.

Let's imagine now that a single vortex was the only game in town. There would be $(R/a)^2$ places you could put the core so the partition function would be

$$\mathcal{Z} = \left(\frac{R}{a}\right)^2 e^{-S_{\text{core}} - \pi\beta J \ln(R/a)} = e^{-S_{\text{core}}} \left(\frac{R}{a}\right)^{2 - \frac{\pi J}{k_B T}}.$$

In the thermodynamic limit ($R \rightarrow \infty$) this diverges for $k_B T > \frac{\pi}{2} J$ and vanishes for $k_B T < \frac{\pi}{2} J$. Hence we expect a transition. This is the basic idea of the BKT transition – a fight between the configurational entropy $2 \ln(R/a)$ and the energy $\pi J \ln(R/a)$. Now we just need to fill in the details.

When we only allow for single vortices, we see a low temperature regime where the potential energy dominates the free energy and vortices are disallowed, whereas at high temperatures the configurational entropy swamps the potential energy and spontaneous formation of vortices becomes favourable.

It is this spontaneous vortex formation that marks the transition from quasi-long-ranged correlations to disorder in the 2D XY model. This is the Berezinskii-Kosterlitz-Thouless transition.

To get a better handle on the transition temperature, we ought to allow for two or more vortices. As an example we consider a vortex-anti-vortex pair, i.e.

$$\begin{aligned} \phi(r) &= \phi_{\circlearrowleft}(r + s/2) - \phi_{\circlearrowright}(r - s/2) \\ \phi_{\circlearrowleft}(r, \theta) = \theta &\Rightarrow \nabla \phi_{\circlearrowleft} = \frac{1}{|r|} e_{\theta} = \frac{1}{|r|} e_r \times e_z. \end{aligned}$$

When $|r| \gg |s|$ this configuration is approximately

$$\begin{aligned}
\phi(r) &\approx \left(\phi_{\circlearrowleft}(r) + \frac{1}{2} s \cdot \nabla \phi_{\circlearrowleft}(r) + \frac{1}{4} (s \cdot \nabla)^2 \phi_{\circlearrowleft}(r) \right) - \left(\phi_{\circlearrowright}(r) - \frac{1}{2} s \cdot \nabla \phi_{\circlearrowright}(r) + \frac{1}{4} (s \cdot \nabla)^2 \phi_{\circlearrowright}(r) \right) \\
&= s \cdot \nabla \phi_{\circlearrowleft}(r) \\
\Rightarrow \nabla \phi(r) &= s \cdot \nabla \frac{1}{|r|} e_{\theta} = -\frac{1}{|r|^2} (s_{\theta} e_r + s_r e_{\theta}) \\
\Rightarrow (\nabla \phi)^2 &= \frac{|s|^2}{|r|^4},
\end{aligned}$$

and so the integral in the action vanishes as $\frac{1}{r^3}$ so that the action is finite. Indeed the remainder of the action is approximately that of two single vortices screened by an infrared cutoff $\sim |s|$, so we have an action for the vortex-anti-vortex pair that is finite.

Such *vortex dipoles* give a finite contribution to the partition function and, as such, are available at any temperature. We may hence think of the BKT transition as being due to a kind of gas of tightly bound vortex-anti-vortex pairs present in the system which may unbind to form a plasma of solitary vortices at sufficiently high temperatures.

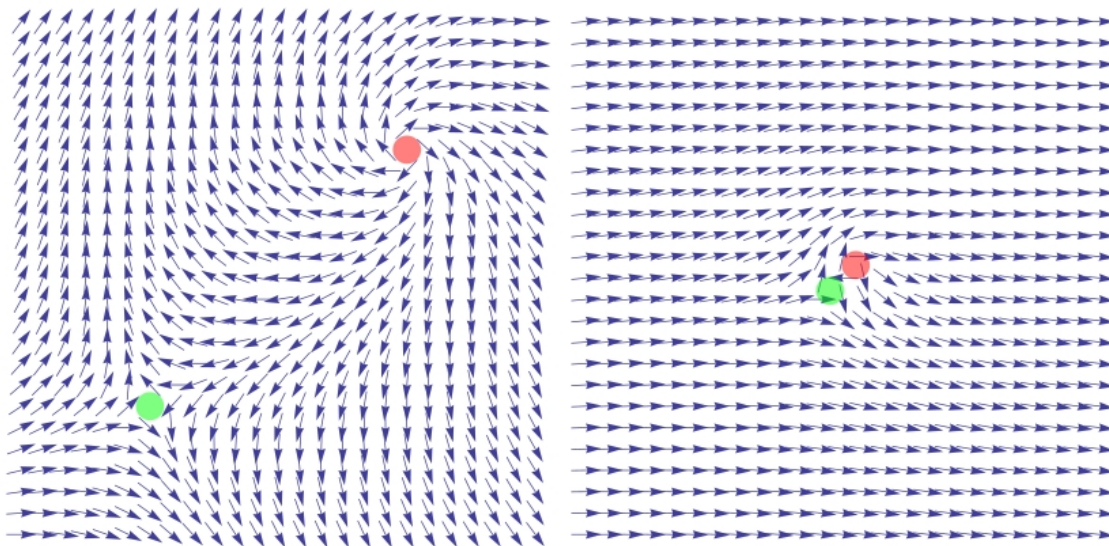


Figure 3.7: A vortex-anti-vortex pair. Left: a close up view showing the form of the distortion, Right: a far-field view showing that a dipolar pair of vortices has zero energy at infinity.

3.3.2 Topological Terms in the Action

Now in order to investigate the competition between the vortices and the non-topological spin-wave behaviour we would expect from finite fluctuations, we need to pull the vortices out of the action.

In terms of the distortion field, $u = \nabla\phi$, the action is

$$S = \frac{\beta J}{2} \int d^2r u^2.$$

The curl of the distortion field is zero (obviously) everywhere except for some isolated points at which are sited the vortices. With Stoke's theorem to hand we can write the topological charge enclosed by some path as

$$\oint d\ell \cdot u = \int d^2r e_z \cdot (\nabla \times u),$$

if we then have a collection of vortices situated at $\{r_i\}$ and with topological charge $\{n_i\}$, in order for the above to hold we must set

$$\nabla \times u = \sum_i 2\pi n_i \delta(r - r_i) e_z.$$

This expression allows us to break the field into a regular part φ and a topologically singular part ψ via

$$u = \nabla\varphi - \nabla \times (e_z\psi).$$

We can then solve to find an explicit form of the singular part via

$$\begin{aligned} \nabla \times u &= e_z \nabla^2 \psi = \sum_i 2\pi n_i \delta(r - r_i) e_z \\ \Rightarrow \psi &= \sum_i n_i \ln \left| \frac{r - r_i}{a} \right|. \end{aligned}$$

This in hand, and employing that the the divergence of a curl is simply zero, we may

express the action as

$$\begin{aligned}
S &= \frac{\beta J}{2} \int d^2r (\nabla\varphi + \nabla \times (e_z\psi))^2 \\
&= \frac{\beta J}{2} \int d^2r (\nabla\varphi)^2 + \frac{\beta J}{2} \int d^2r (\nabla \times (e_z\psi))^2 \\
&= S_{\text{sw}}[\varphi] + \frac{\beta J}{2} \int d^2r (\nabla\psi)^2 \\
&= S_{\text{sw}}[\varphi] + \frac{\beta J}{2} \int_{\Gamma} d^2r \psi (-\nabla^2)\psi + \frac{\beta J}{2} \oint_{\partial\Gamma} d\ell \cdot (\psi \nabla\psi),
\end{aligned}$$

where the final integral is over contours encircling each vortex as illustrated in Fig.[3.3.2], by excluding each core region in this manner we remove non-physical singularities but we must now remember to add the core contributions back in by hand.

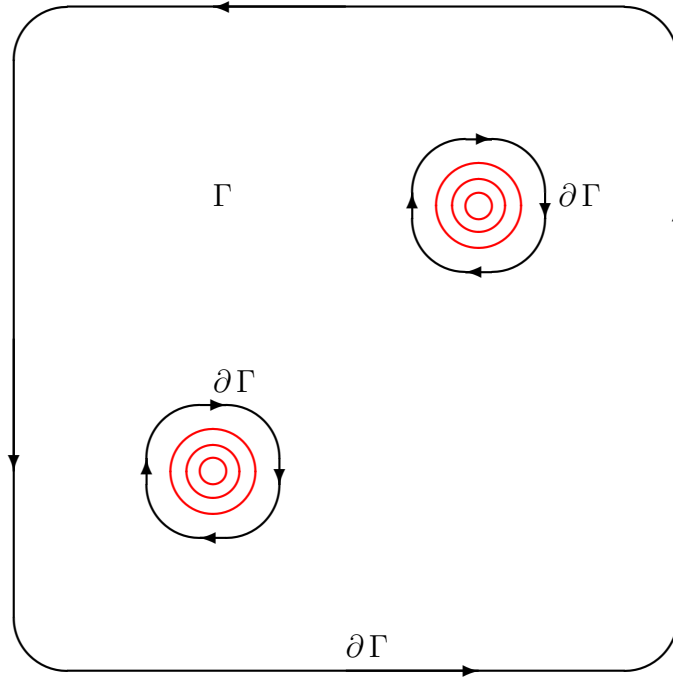


Figure 3.8: The integral contour avoiding each vortex core

The action has broken into two decoupled contributions; a spin wave channel S_{sw} account-

ing for harmonic fluctuations and a topological excitation channel

$$\begin{aligned}
S_{\text{top}} &= \sum_i S_{\text{core}}(n_i) + \frac{\beta J}{2} \int_{\Gamma} d^2 r \left(\sum_i n_i \ln \left| \frac{r - r_i}{a} \right| \right) \left(-2\pi \sum_j n_j \delta(r - r_j) \right) \\
&= \sum_i S_{\text{core}}(n_i) - 2\pi\beta J \sum_{i < j} n_i n_j \ln \left| \frac{r_i - r_j}{a} \right|.
\end{aligned}$$

The separation of the action into two distinct channels allows us to factorize the partition function. Supposing the vortices are only allowed a charge of ± 1 , for neutrality we need the same number of vortices and anti-vortices. We need to sum over every possible number of vortices and account for double counting by dividing each term by the $(N!)^2$ ways of labelling N vortices and N anti-vortices, this gets us

$$\mathcal{Z} = \underbrace{\int \mathcal{D}[\varphi] e^{-S_{\text{sw}}[\varphi]}}_{\mathcal{Z}_{\text{sw}}} \underbrace{\sum_{N=0}^{\infty} e^{-2NS_{\text{core}}} \frac{1}{(N!)^2} \int \left(\prod_{k=1}^{2N} \frac{d^2 r_k}{a^2} \right) e^{4\pi^2 \beta J \sum_{i < j} \sigma_i \sigma_j C\left(\frac{r_i - r_j}{a}\right)}}_{\mathcal{Z}_{\text{top}}} \quad (3.10)$$

in which $C(r) = \frac{1}{2\pi} \ln |r|$, $\sigma_i = \pm 1$ and the appearance of a $1/a^2$ term is an unavoidable artefact of replacing the sum over all possible placements of vortices with an integral.

From this we can see that the thermodynamics of the vortices in the 2D XY model in this limit is equivalent to that of a Coulomb plasma in the grand canonical ensemble with $-2S_{\text{core}}$ taking on the role of the chemical potential.

3.3.3 BKT in Summary

A lot has just happened here so some recapitulation is in order. So far, in order to explain the transition from exponential decay in correlations at high temperatures to algebraic decay at low temperatures in the 2D XY model, we have invoked the BKT transition in which the transition is mediated by unbinding of vortex-anti-vortex pairs.

We have seen that a single vortex contributes as energy $\sim \pi J \ln(R/a)$ and an entropy $\sim 2 \ln(R/a)$ so that the free energy, $F = E - TS = (\pi J - 2k_B T) \ln(R/a)$, changes sign at $k_B T = \frac{\pi}{2} J$. This gives upper estimate for the transition temperature T_{BKT} .

We have drawn an analogy between the low temperature phase and a gas of bound “dipoles” made of a vortex and an anti-vortex, which transits to a plasma at higher temperatures. The analogy with a plasma carries through to the mathematics where we can see that the vortices act like a gas interacting through a 2D Coulomb potential.

3.4 The Vortex Plasma

3.4.1 Renormalization Group Analysis

To top off our discussion of the 2D XY model and the BKT transition, we will follow Kosterlitz [75] in a renormalization study of the critical properties of the vortex plasma.

We have an effective Hamiltonian

$$H_{\text{vortex}}^{(N)} = - \sum_{i < j}^{2N} 4\pi^2 J \sigma_i \sigma_j C \left(\frac{r_i - r_j}{a} \right)$$

with $\sigma_i = \pm 1$ and assuming charge neutrality so that $\sum_i \sigma_i = 0$.

We also have an effective *fugacity density*, z , or equivalently an effective *chemical potential*, μ , defined by

$$z = \frac{1}{a^2} e^{-S_{\text{core}}} = e^{\beta \mu}.$$

In these terms, the partition function of the vortex plasma in the grand canonical ensemble is

$$\mathcal{Z}_{\text{vortex}} = \sum_N \frac{1}{(N!)^2} \int \mathrm{d}^2 r_1 \dots \mathrm{d}^2 r_{2N} e^{-\beta (H_{\text{vortex}}^{(N)} + 2\mu)}.$$

In the following it will prove convenient to symmetrize the sum and to hide the energy scale in the charge, so letting $p_i = \sqrt{\pi J} \sigma_i$ we get

$$\mathcal{Z}_{\text{vortex}} = \sum_N \frac{z^{2N}}{(N!)^2} \int \mathrm{d}^2 r_1 \dots \mathrm{d}^2 r_{2N} e^{\beta \sum_{i \neq j}^{2N} p_i p_j \ln \left| \frac{r_i - r_j}{a} \right|}.$$

As it stands, the integration is taken over $\mathbb{R}^{2 \times 2N}$ excluding the vortex-core balls $|r_i - r_j| < a$.

In order to renormalize this system, we deform the fundamental length scale of the system, the vortex core radius, by $a \rightarrow a + \mathrm{d}a$. This amounts to extracting from the region of integration the infinitesimal annuli $a < |r_i - r_j| < a + \mathrm{d}a$.

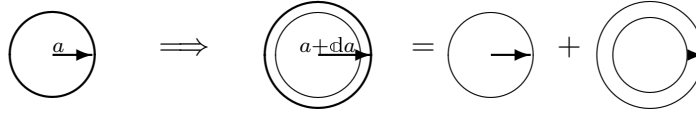


Figure 3.9: Rescaling of the vortex core radius.

Each annulus carries an infinitesimal weight $\mathrm{d}a$ so we need to keep only terms containing up to a single correction. Thus the original integral might be expressed as the rescaled integral plus a sum over all distinct pairs (i, j) of an integral where $r_{k \neq i, j}$ are integrated over their rescaled region, with r_j integrated over the original unscaled region and r_i integrated over the annulus $a < |r_i - r_j| < a + \mathrm{d}a$.

The partition function prefers to bind vortex pairs of opposite charge so we can set $p_i = -p_j$, then pulling out all terms in the Hamiltonian containing an r_i or an r_j we get the annular integral in r_i as

$$\int_{a < |r_i - r_j| < a + \mathrm{d}a} \mathrm{d}^2 r_i e^{\beta \left(2 \sum_k p_i p_k \ln \left| \frac{r_i - r_k}{a} \right| + 2 \sum_k p_k p_j \ln \left| \frac{r_k - r_j}{a} \right| \right)} = \int_{a < |r_i - r_j| < a + \mathrm{d}a} \mathrm{d}^2 r_i \prod_k \left(\frac{|r_i - r_k|}{|r_j - r_k|} \right)^{2\beta p_i p_k}$$

The radial integral, being infinitesimal, is rather trivial. Employing a place-holding vector α of length a , this integral is simply

$$\int_0^{2\pi} \mathrm{d}\theta \prod_k \left(1 + \frac{2\alpha \cdot (r_j - r_k)}{|r_j - r_k|^2} + \frac{a^2}{|r_j - r_k|^2} \right)^{\beta p_i p_k} a \mathrm{d}a,$$

with θ being the angle α makes to the axis.

We can safely assume that three vortices will not come close together, given that two of them will always have equal charge, and so we can expand this integral in $a/|r_j - r_k|$.

Expanding to second order, we first take note that any terms linear in α will self-cancel under integration around a circle, and all other terms will just pick up a 2π . This in mind the integral must be

$$2\pi a \mathrm{d}a \left[1 + \beta^2 p^4 \sum_k \frac{a^2}{|r_j - r_k|^2} + \beta^2 p^2 \sum_{k \neq l} p_k p_l \frac{a^2 (r_j - r_k) \cdot (r_j - r_l)}{|r_j - r_k|^2 |r_j - r_l|^2} \right].$$

In the remaining integral over r_j , remember this is taken over the original unscaled region, we get

$$2\pi a \mathrm{d}a \left[A - 2\pi a^2 \beta^2 p^2 \sum_{k \neq l} p_k p_l \ln \left| \frac{r_k - r_l}{a} \right| \right],$$

in which A is the area of the plane (which, rather disturbingly, becomes unbounded in the thermodynamic limit but fortunately is multiplied by an infinitesimal) and $p^2 = \pi J$.

Now rearranging the sum in the partition function so that the $(N + 1)^{\text{th}}$ correction sits with the N^{th} term (so that the number of integrals aligns), the partition function is now

$$\begin{aligned} \mathcal{Z} &= \sum_N \frac{z^{2N}}{(N!)^2} \int \mathrm{d}^{4N} r \left[1 + \frac{z^2}{(N+1)^2} \sum_{i,j=1}^{N+1} 2\pi a \mathrm{d}a \left(A - 2\pi a^2 \beta^2 p^2 \sum_{k \neq l} p_k p_l \ln \left| \frac{r_k - r_l}{a} \right| \right) \right] \\ &\quad \times \exp \left(\beta \sum_{m \neq n} p_m p_n \ln \left| \frac{r_m - r_n}{a} \right| \right). \end{aligned}$$

Re-exponentiating the infinitesimal terms, we have

$$\begin{aligned} \mathcal{Z} &= \sum_N \frac{z^{2N}}{(N!)^2} \int \mathrm{d}^{4N} r \exp \left\{ z^2 2\pi a \mathrm{d}a \left(A - 2\pi a^2 \beta^2 p^2 \sum_{k \neq l} p_k p_l \ln \left| \frac{r_k - r_l}{a} \right| \right) + \beta \sum_{i \neq j} p_i p_j \ln \left| \frac{r_i - r_j}{a} \right| \right\} \\ &= e^{2\pi z^2 A a \mathrm{d}a} \sum_N \frac{z^{2N}}{(N!)^2} \int \mathrm{d}^2 r_1 \dots \mathrm{d}^2 r_{2N} e^{\beta \left(1 - (2\pi)^2 \beta p^2 (z a^2)^2 \frac{\mathrm{d}a}{a} \right) \sum_{i \neq j} p_i p_j \ln \left| \frac{r_i - r_j}{a} \right|} \end{aligned}$$

This is now very nearly in the same form as the original partition function except that the integral is now over a rescaled domain.

We can now unravel that rescaling with a change of variables $r \rightarrow r(1 + \frac{da}{a})$, taking into account this rescaling, the partition function returns to its original form, up to low order corrections, but with new coupling constants

$$\begin{aligned} z_a &= z \left(1 + 2\frac{da}{a} - \beta p^2 \frac{da}{a} \right) \\ \beta_a &= \beta \left(1 - (2\pi)^2 \beta p^2 (za^2)^2 \frac{da}{a} \right). \end{aligned}$$

The free energy per unit area F , which normalizes the partition function, has also renormalized

$$F_a = 2\pi z^2 a da + F.$$

3.4.2 Flow of the Coupling Constants

In the spirit of the renormalization group we have shown that under variation of the fundamental length scale – the vortex core radius – the partition function of the vortex plasma description of the BKT transition in the 2D XY model retains its form excepting that that fugacity, inverse temperature, and free energy per unit area flow according to the recursion relations

$$(a^2 z_a) = (a^2 z) \left[1 + (2 - \pi\beta J) \frac{da}{a} \right] \tag{3.11a}$$

$$(\pi\beta_a J) = (\pi\beta J) \left[1 - (2\pi)^2 \pi\beta J (a^2 z)^2 \frac{da}{a} \right] \tag{3.11b}$$

$$F_a = 2\pi (a^2 z)^2 \frac{da}{a^3} + F, \tag{3.11c}$$

where we have rearranged terms purely for convenience.

To extract the RG flow of these coupling constants we need to cast the recursion relations

in differential form. Let us set

$$\begin{aligned} a^2 z &= u & a^2 z_a &= u + \mathrm{d}u \\ \pi\beta J &= v & \pi\beta_a J &= v + \mathrm{d}v \\ & & F_a &= F + \mathrm{d}F. \end{aligned}$$

Through which we find a set of differential equations governing the flow

$$\frac{\mathrm{d}u}{u} = (2 - v) \frac{\mathrm{d}a}{a} \quad (3.12a)$$

$$\frac{\mathrm{d}v}{v} = -(2\pi)^2 v u^2 \frac{\mathrm{d}a}{a} \quad (3.12b)$$

$$\mathrm{d}F = 2\pi u^2 \frac{\mathrm{d}a}{a^3}. \quad (3.12c)$$

First of all we notice a fixed point in the fugacity at $v = 2$, $k_B T = \frac{\pi}{2} J$. This was our original hypothesized transition temperature and we can now interpret it in terms of the sign of the chemical potential of the vortices, where the fixed point corresponds to the tipping point between vortices costing energy and paying energy.

To look at the flow around this fixed point we must expand around $v = 2$. In the near vicinity of the fixed point we have

$$\mathrm{d}(u^2) = 2(u^2)(2 - v)\mathrm{d}(\ln a)$$

$$\mathrm{d}(2 - v) = (4\pi)^2 (u^2)\mathrm{d}(\ln a).$$

The solution of these equations gives

$$\begin{aligned} (4\pi u)^2 - (2 - v)^2 &= \text{const.} \\ \Rightarrow (4\pi a^2 z)^2 - \left(2 - \frac{\pi J}{k_B T}\right)^2 &= \text{const.} \end{aligned}$$

Then simply by looking at the direction of the flow we can see that a first correction to

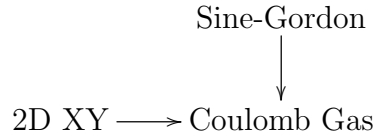
the BKT transition temperature is given by

$$k_B T_{\text{BKT}} = \frac{\pi J}{2 + 4\pi a^2 z} \quad (3.13)$$

3.4.3 The 2D XY Universality Class

The marked similarity between the RG flow form of the Coulomb plasma underlying the vortex unbinding transition in the 2D XY model and that of the Sine Gordon model leads us to raise suspicious eyebrows as to the connections between these seemingly disparate systems.

We will in fact show that there is a direct mapping between the Coulomb gas and the Sine-Gordon model and hence gain some insight into the underlying *universality class*.



To establish the connection between these systems we consider the partition function of a typical 2D Sine-Gordon system

$$\mathcal{Z}_{\text{SG}} = \int \mathcal{D}[\phi] e^{-S_{\text{SG}}[\phi]} \quad S_{\text{SG}} = \int d^2 r \left\{ \frac{1}{8\pi d} (\nabla_r \phi)^2 + 2\eta \cos \phi \right\}.$$

where we have changed notation from Eqn.[2.38] simply to avoid confusing the parameter μ in that form with the chemical potential.

With respect to the average over the free system ($\eta = 0$), we could write

$$\mathcal{Z}_{\text{SG}} = \left\langle e^{-2\eta \int d^2 r \cos \phi} \right\rangle_0,$$

where $\langle \phi(r)\phi(r') \rangle_0 = 2d \ln \left| \frac{r-r'}{a} \right| = 4\pi d C \left(\frac{r-r'}{a} \right)$.

Expanding the exponential we have

$$\mathcal{Z}_{\text{SG}} = \sum_{n=0}^{\infty} \frac{(-2\eta)^n}{n!} \int \mathrm{d}^2 r_1 \dots \mathrm{d}^2 r_n \langle \cos \phi(r_1) \dots \cos \phi(r_n) \rangle_0.$$

We can group together the cosines using

$$\begin{aligned} \cos \phi_1 \cos \phi_2 &= \frac{1}{2} [\cos(\phi_1 - \phi_2) + \cos(\phi_1 + \phi_2)] \\ \cos \phi_1 \cos \phi_2 \cos \phi_3 &= \frac{1}{4} [\cos(\phi_1 - \phi_2 - \phi_3) + \cos(\phi_1 - \phi_2 + \phi_3) + \cos(\phi_1 + \phi_2 - \phi_3) \\ &\quad + \cos(\phi_1 + \phi_2 + \phi_3)] \end{aligned}$$

and so on by induction.

We have frequently – if not explicitly – employed the fact that for a Gaussian model

$$\langle \cos(a_1 \phi(r_1) + a_2 \phi(r_2) + \dots) \rangle = \mathrm{e}^{-\frac{1}{2} \langle (a_1 \phi(r_1) + a_2 \phi(r_2) + \dots)^2 \rangle}, \quad (3.14)$$

the proof of which comes quite simply from completing the square within the functional integral.

We must however note that in the absence of some fancy regularization, $\langle \phi(r_1) \phi(r_2) \rangle$ has a positive divergence at $r_1 = r_2$ and so $\langle \cos(a_1 \phi(r_1) + a_2 \phi(r_2) + \dots) \rangle = 0$ **unless** $\sum_i a_i = 0$, in which case the divergences will cancel out and we'll see a finite contribution.

Looking at the term $\langle \pm \cos(\phi(r_1) \pm \phi(r_2) \pm \dots \pm \phi(r_n)) \rangle$, we see that the average is only non-zero when $n = 2N$ and even then we require there to be the same number of + and – terms, for which there are $\binom{2N}{N}$ possible combinations.

An exact representation of the Sine-Gordon model is hence

$$\mathcal{Z}_{\text{SG}} = \sum_{N=0}^{\infty} \frac{(-2\eta)^{2N}}{(2N)!} \int \mathrm{d}^2 r_1 \dots \mathrm{d}^2 r_{2N} \binom{2N}{N} \frac{1}{2^{2N-1}} \left\langle \cos \left(\sum_{k=1}^{2N} (-1)^k \phi(r_k) \right) \right\rangle_0.$$

Tidying this up a little we have

$$\mathcal{Z}_{\text{SG}} = \sum_{N=0}^{\infty} \frac{\eta^{2N}}{(N!)^2} \int \mathbb{d}^2 r_1 \dots \mathbb{d}^2 r_{2N} \left\langle e^{i \sum_{k=1}^{2N} (-1)^k \phi(r_k)} \right\rangle_0.$$

Computing the averages and extracting self interaction terms gives us then

$$\mathcal{Z}_{\text{SG}} = \sum_{N=0}^{\infty} \frac{\eta^{2N}}{(N!)^2} \int \mathbb{d}^2 r_1 \dots \mathbb{d}^2 r_{2N} e^{\sum_{i \neq j} (\pm) 4\pi d C \left(\frac{r_i - r_j}{a} \right)}.$$

We now see clearly by comparison with Eqn.[3.10] that the Sine-Gordon model is perfectly equivalent to a vortex plasma with fugacity $z = \eta$ and inverse temperature $\pi\beta J = d$.

CHAPTER 4

THE STRIPE MODEL

4.1 Experimental Setup

Now with some mathematics behind us, we are ready for our first encounter with the main protagonist of this thesis, a toy model consisting of dipolar bosons trapped in a weakly coupled planar array of one-dimensional stripes, or in short the *Stripe Model*. We have already discussed during the introduction our motivation for considering this system. Let us now see how it may be constructed.

We imagine a system in which a gas of dipolar bosons is arranged in a two-dimensional array of one-dimensional homogeneous cigar-clouds as illustrated in Fig.[4.2]. Such a configuration might be achieved by applying a strong two dimensional optical lattice such that the confinement in the z -direction completely suppresses motion in that direction, whilst that in the y -direction may allow some weak hopping between stripes. In principal, and if experimentally expedient, a weak lattice could also be present along the x -direction without affecting our future considerations, just as long as the lattice is incommensurate with the density of bosons.

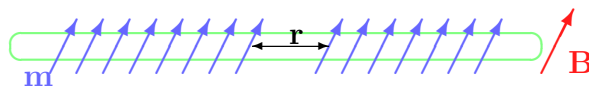


Figure 4.1: Cartoon of dipoles on a line: Notice that the gas is fully polarised by the applied field so that the dipole moment of every atom points in the same direction.

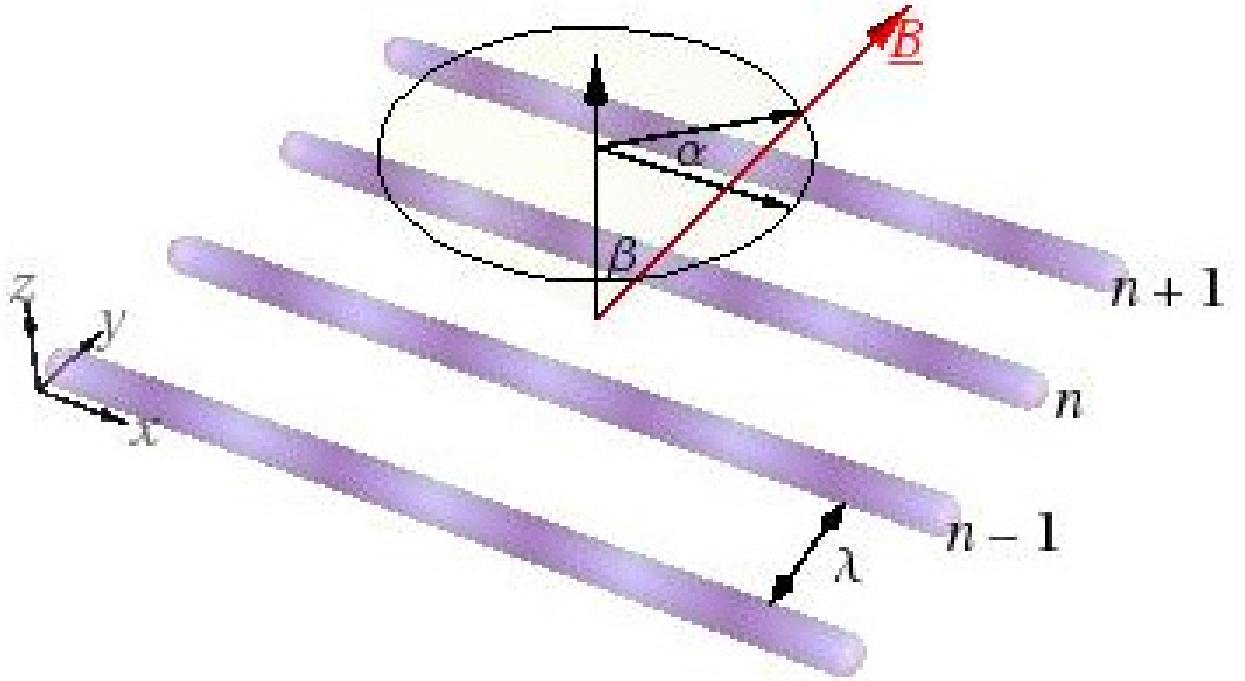


Figure 4.2: Proposed experimental set up: An optical lattice in the y -direction separates the trapped dipolar bosons into weakly coupled stripes. The dipole moments of the bosons are polarized by an external field, B , which may be rotated in three dimensions to change the effective interactions.

We allow for interactions between the stripes through a dipole-dipole interaction which would be tunable via the direction of the dipole moment. A similar experimental setup, but with the possible hopping between stripes neglected, was considered by Kollath, Meyer and Giamarchi[76]. They considered the phase diagram in terms of the dipole orientation with respect to the plane and found that, in addition to the high temperature “sliding Luttinger liquid” phase, in which typical one-dimensional effects such as algebraic decay in correlation functions survive into the quasi-two-dimensional system (the sliding Luttinger liquid phase has not yet, to the best of my knowledge, been experimentally observed), their system allows a phase with superfluid correlations and two distinct density wave orders – one checkerboard and one striped, as illustrated in Fig.[4.3].

Conversely; Ho, Cazalilla and Giamarchi have considered a similar setup where inter-

stripe hopping is allowed, but in the absence of a dipole-dipole interaction coupling neighbouring tubes [77]. Ho *et al* consider the effect of hopping versus an applied axial periodic potential and find a transition from superfluid to Mott insulator.

We allow both forms of inter-stripe coupling to be present and we will pay particular attention to their competition. Due to the anisotropy of the lattice and the freedom of the dipole moment to point anywhere in 3D space, we have a good deal of control over the relative dipole-dipole interaction strength in the longitudinal and transverse directions. As opposed to Kollath *et al*, who considered their phase diagram in terms of the angle made by the dipole moment to the plane, we will fix the angle, β , made to the plane in such a way that the interactions are always repulsive and tune the angle, α , between the horizontal projection and the dipole moment (see Fig.[4.2]).

The dipole-dipole interaction, be it magnetic, electric or whatever, between particle at \mathbf{x}_1 and \mathbf{x}_2 separated by $\mathbf{r} = \mathbf{x}_2 - \mathbf{x}_1$ with respective (unit) dipole moments \mathbf{m}_1 and \mathbf{m}_2 (see Fig.[4.4]) is given by

$$V_{\text{dd}} = \frac{C_{\text{dd}}}{4\pi} \frac{(\mathbf{e}_1 \cdot \mathbf{e}_2) r^2 - 3(\mathbf{e}_1 \cdot \mathbf{r})(\mathbf{r} \cdot \mathbf{e}_2)}{r^5}, \quad (4.1)$$

where C_{dd} is the strength of the dipole-dipole interaction.

If the dipole cloud is polarized by an external field so that the all the dipole moments point in the same direction, we call the angle they make to the horizontal α and the angle made to the plane β , then the moment can be parameterized $\mathbf{m} = \cos \alpha \cos \beta \mathbf{e}_x + \sin \alpha \cos \beta \mathbf{e}_y + \sin \beta \mathbf{e}_z$.

We also parametrize the displacement vector $\mathbf{r} = r \cos \theta \mathbf{e}_x + r \sin \theta \mathbf{e}_y$ so that the dipole-dipole

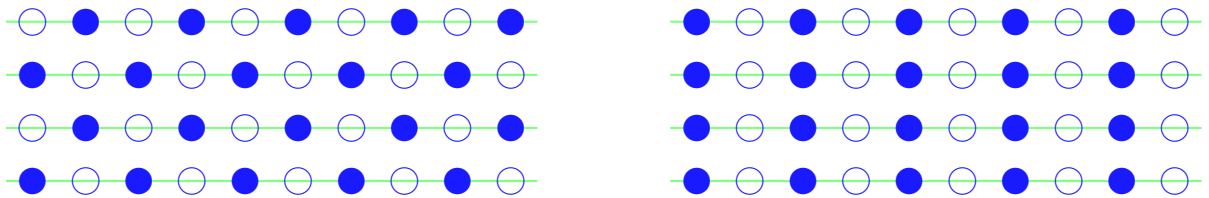


Figure 4.3: Schematic distinction between “checkerboard” (left) and “striped” (right) density wave orders.

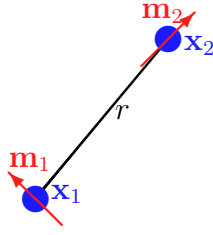


Figure 4.4: Cartoon of dipoles on a line with $r = |\mathbf{x}_1 - \mathbf{x}_2|$.

interaction takes the form

$$V_{\text{dd}} = \frac{C_{\text{dd}}}{4\pi} \frac{1 - 3 \cos^2 \beta \cos^2(\alpha - \theta)}{r^3}.$$

In order to guarantee that all interactions are repulsive but still allow the maximum possible anisotropy between inter- and intra-chain interactions, we fix the angle β made to the plane so that $\cos \beta = 1/\sqrt{3}$, this choice of angle is referred to in the literature as the *magic angle* [10]. This angle locked in, the interaction becomes

$$V_{\text{dd}} = \frac{C_{\text{dd}}}{8\pi} \frac{1 - \cos 2(\alpha - \theta)}{r^3}.$$

In order to account for the dimensional anisotropy we wish to study, we need to break this interaction into a longitudinal part covering intra-stripe interactions, and a transverse part for the inter-stripe interactions, $V_{\text{dd}} = V_{\text{dd}}^{\text{intra}} + V_{\text{dd}}^{\text{inter}}$. For the inter-stripe interactions we will keep only nearest-stripe interactions (noting that including next-nearest and higher terms won't push us out of the universality class we will eventually find ourselves in) and also take a smearing limit¹ so that a particle only notices its direct counterparts in neighbouring stripes.

¹Cards on the table here: this smearing approximation in which we lump all the interactions of $(x, n\lambda)$ with $(x + \delta, (n \pm 1)\lambda)$ where $\delta \in (-\lambda, \lambda)$ into the interaction with $(x, (n \pm 1)\lambda)$ is throwing away a lot of detail, but first of all we need to do this in order to arrive at a model we have any hope of attacking and secondly we are soon going to be bosonizing the stripes, at which point we will be smearing over the inter-particle distance so as long as the spacing between the tubes is of the same order as the spacing between the particles we aren't really changing anything. This said, Quintanilla *et al*[10] have studied a very similar setup using fermions instead of bosons and by calculating the interaction in reciprocal space have argued that the nearest neighbour approximation isn't actually that bad at low densities.

With this approximation in place, the interaction experienced by particles at $(x, y) = (x, n\lambda)$ and $(x', n'\lambda)$, where λ is the inter-stripe separation, becomes

$$V_{\text{dd}}^{\text{intra}} = \frac{C_{\text{dd}}}{4\pi} \frac{\sin^2 \alpha}{|x - x'|^3} \delta_{nn'} \quad (4.2a)$$

$$V_{\text{dd}}^{\text{inter}} = \frac{C_{\text{dd}}}{4\pi} \frac{\cos^2 \alpha}{\lambda^3} \delta(x - x') \delta_{nn'} \quad (4.2b)$$

We are now in a position to be able to write the Hamiltonian for this system. Each stripe will have its own contribution $H_{\text{stripe}}^{(n)}$ which contains the kinetic energy of its constituent particles and an intra-stripe interaction term, and a contribution due to its coupling with its neighbours $H_{\text{couple}}^{(n)}$. The latter will contain a hopping term, to which we assign an energy cost J_{\perp} , and an inter-stripe interaction term that will be proportional to $V_{\text{dd}}^{\text{inter}}$ (although not necessarily equal because we ought to integrate over the Wannier functions in adjacent chains). The complete Hamiltonian is thus $H = \sum_n H_{\text{stripe}}^{(n)} + H_{\text{couple}}^{(n)}$, where

$$H_{\text{stripe}}^{(n)} = \int \mathrm{d}x \psi_n^{\dagger}(x) \left(-\frac{\hbar}{2m} \partial_x^2 \right) \psi_n(x) + \int \mathrm{d}x \mathrm{d}x' \rho_n(x) V_{\text{dd}}^{\text{intra}}(x - x') \rho_n(x') \quad (4.3a)$$

$$H_{\text{couple}}^{(n)} = - \int \mathrm{d}x J_{\perp} \left(\psi_n^{\dagger}(x) \psi_{n+1}(x) + \psi_{n+1}^{\dagger}(x) \psi_n(x) \right) + \int \mathrm{d}x \mathrm{d}x' \rho_n(x) w V_{\text{dd}}^{\text{inter}}(x - x') \rho_{n+1}(x'), \quad (4.3b)$$

in which $\rho_n(x)$ is the density in the n^{th} stripe, $\psi_n^{\dagger}(x)$ is the creation operator for the n^{th} stripe, and w is some dimensionless constant.

This system is clearly, even after the approximations we have made, a bit cumbersome and complicated, but let's imagine that the coupling term $H_{\text{couple}}^{(n)}$ is so weak that we can neglect it; we can then see what it happens when we bring it in perturbatively.

4.2 Bosonizing a Single Stripe

On its own, each stripe is a one-dimensional system with short(ish) ranged interactions, so we would like to try and bosonize the system. We ought to talk about whether we can actually consider the dipole-dipole interaction to be short ranged – in three dimensions this most certainly isn't the case. Dipole interactions in 3D are a textbook example of long ranged interactions, and are long enough ranged to couple neighbouring stripes. Formally a force is defined to be short ranged if it decreases with distance faster than r^{-d} where d is the dimensionality of the system; this is so that the integral of the interaction up to a shell of radius a will decay algebraically in a . This means that the dipole-dipole interaction is short-ranged in one and two dimensions, so we can attempt to bosonize each stripe.

The contribution to the Hamiltonian from each stripe will take a bosonized form

$$H_{\text{stripe}}^{(n)} = \frac{\hbar v_s}{2\pi} \int dx K (\partial_x \theta)^2 + \frac{1}{K} (\partial_x \varphi)^2 = \frac{\hbar v_s}{2\pi} \int dx K \frac{\pi^2}{\hbar^2} \Pi(x)^2 + \frac{1}{K} (\partial_x \varphi)^2, \quad (4.4)$$

where the sound speed, v_s , and Luttinger parameter, K , now have to encode the physics of the dipole-dipole interaction. We have already seen in Eqn.[2.32] that K and v_s can be related to the compressibility, and hence the ground state energy, of the system via

$$\hbar \frac{v_s}{K} = \hbar v_N = \frac{1}{\pi} \frac{1}{\rho_0^2} \frac{1}{\kappa} = \frac{L}{\pi} \frac{\partial^2 E_0(N_0)}{\partial N_0^2} = \frac{\rho_0^2}{\pi} \frac{\partial^2}{\partial \rho_0^2} \left(\frac{E_0}{L} \right).$$

In the above we have related the density stiffness, v_N , of the bosonized Hamiltonian to physical parameters of the system, particularly the energy per unit length in the ground state: $e(\rho_0) = E_0/L$. Now using the phase stiffness Eqn.[2.26a] we can solve to find that

$$v_s = \sqrt{\frac{1}{m\rho_0} \frac{1}{\kappa}} = \sqrt{\frac{\rho_0^3}{m} e''(\rho_0)} \quad (4.5a)$$

$$K = \sqrt{\frac{\hbar^2 \pi^2 \rho_0^3}{m} \kappa} = \sqrt{\frac{\pi^2 \hbar^2 \rho_0}{m} \frac{1}{e''(\rho_0)}} \quad (4.5b)$$

Invoking the principals of universality with respect to one dimensional systems, we can always write down an effective Luttinger liquid theory (approximately and subject to there being sufficiently short ranged interactions and translational invariance) with phenomenological parameters K and v_s . These parameters can now be estimated if only we can find the ground state energy per unit length of the system for any density.

To apply these concepts to bosonizing a single stripe we have to understand the ground state properties of our one dimensional Bose gas of dipoles. From a first quantized standpoint the Hamiltonian in question is

$$\mathcal{H} = \sum_n -\frac{\hbar^2}{2m} \partial_{x_n}^2 + \sum_{m < n} \frac{C_{\text{dd}}}{4\pi} \sin^2 \alpha \frac{1}{|x_m - x_n|^3}. \quad (4.6)$$

If we remove the dimensions from the system using $z = \rho_0 x$ and introduce an effective Bohr Radius

$$r_0 = \frac{m C_{\text{dd}} \sin^2 \alpha}{2\pi \hbar^2}, \quad (4.7)$$

the Hamiltonian takes the simple form

$$\mathcal{H} = \frac{\hbar^2}{2mr_0^2} (\rho_0 r_0)^2 \left(\sum_n -\partial_{z_n}^2 + (r_0 \rho_0) \sum_{m < n} \frac{1}{|z_m - z_n|^3} \right). \quad (4.8)$$

This is not (yet, and likely never will be) an exactly soluble model, but it has some limits we can understand. As $r_0 \rho_0 \rightarrow 0$ the particles never notice each other until they are right on top of one another and can feel their singularities; hence in this limit the gas behaves like a contact interacting gas with infinite repulsion. This is the Tonks gas (or, depending on your outlook, a free Fermi gas), so in this limit $K \rightarrow 1$. In the other limit as $r_0 \rho_0 \rightarrow \infty$, the kinetic part of the Hamiltonian is totally swamped by the interaction part and we are pushed into a classical crystalline state

$$\mathcal{H} = \frac{\hbar^2}{2mr_0^2} (\rho_0 r_0)^3 \sum_{m < n} \frac{1}{|z_m - z_n|^3}.$$

Since $z \propto 1/\rho_0$, the energy can be approximated by

$$E = \frac{\hbar^2}{2mr_0^2} (\rho_0 r_0)^3 N \sum_n \frac{1}{n^3} = \frac{\hbar^2}{2m} r_0 \rho_0^4 \zeta(3) L,$$

where $\zeta(s)$ is the Riemann Zeta function $\zeta(s) = \sum_n n^{-s}$. This gives us $e''(\rho_0) = 3 \frac{C_{\text{dd}}}{\pi} \sin^2 \alpha \zeta(3) \rho_0^2$, so that $K \sim \rho_0^{-1/2}$. In particular, as the density increases, the Luttinger parameter approaches zero.

This is a little surprising because we have bosons here, so if the interactions were contact (delta functions for example), we would see the Luttinger parameter start out as infinity, so that $\langle \theta(r)\theta(0) \rangle$ is constant and the system is perfectly phase-correlated, and diminish down to unity (algebraic correlations) as the interaction strength is ramped up. In this case the interaction itself is driving the correlation, but it is a density correlation not a phase correlation so $\langle \varphi(r)\varphi(0) \rangle$ becomes constant in the limit, and thus $K \rightarrow 0$.

This is a crucial point which is worth repeating: bosons with a dipole-dipole interaction – even in this heuristic approach which we will shortly improve upon – have a Luttinger parameter that looks like that of a Fermi system. For this reason dipolar bosons supply us with a bosonic system, which as we discuss in the introduction is highly controllable, that simulates the low energy physics of fermions.

We can reasonably expect the Luttinger parameter for a single stripe of dipoles to smoothly interpolate between unity at small $\rho_0 r_0$ to $\sim \rho_0^{-1/2}$ as $\rho_0 r_0 \rightarrow \infty$, as illustrated in Fig.[4.5].

Given that the system does possess an analytic solution, in order to see how it interpolates between these limits we would have, as Anderson put it, “resort to the indignity of numerical simulations”. Fortunately Citro *et al* [78] have performed Reptation Quantum Monte Carlo

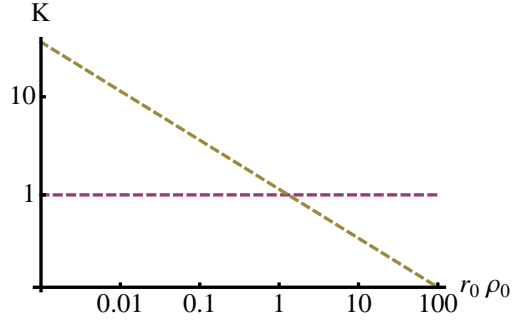


Figure 4.5: Solvable limits of the Luttinger parameter for Bosons with dipole-dipole interactions: at low densities we can expect the system to behave like a Tonks gas and as the interaction strength is ramped up a crystalline order emerges.

simulations on this system in order to find the Luttinger parameter and we can appropriate their results.

As expected, their numerically obtained Luttinger parameter smoothly interpolates our expected limits as $\rho_0 r_0$ is increased. Their RQMC calculations give them a ground state energy density that is well fitted by the functional form

$$e = \frac{\hbar^2}{2mr_0^2} \left\{ \frac{\rho_0 r_0}{\rho_0 r_0 + 1} (\zeta(3)(\rho_0 r_0)^4 + c_1(\rho_0 r_0)^{p_1} + c_2(\rho_0 r_0)^{p_2} + c_3(\rho_0 r_0)^{2+p_2}) + \frac{\pi^2}{3} \frac{(\rho_0 r_0)^2}{1 + c_4(\rho_0 r_0)^{p_3}} \right\} \quad (4.9)$$

which is constructed so as to smoothly interpolate between the known limits. The fitting parameters found by Citro *et alare* tabulated in Tab.[4.1].

c_1	c_2	c_3	c_4	p_1	p_2	p_3
3.1	3.2	4.3	1.7	3.503	3.05	0.34

Table 4.1: Fitting constants for the Luttinger parameter in a gas of dipoles for functional form calculated by Citro *et al* [78].

Employing Citro *et al*'s numerically obtained Luttinger parameter, we can see how the system moves from algebraic decay in correlations to a perfectly correlated crystal as the interaction strength is increased. We have seen that the effective Bohr radius of the dipoles looks like $\sin^2 \alpha$, where α is the angle made by the dipole moments to the stripe, so we can

calculate K in terms of α . To illustrate the variation in K we plot it versus $\rho_0 r_0(\alpha)$ and also show a contour plot of K versus $\rho_0 r_0(\pi/2)$ and α (Fig.[4.6] and Fig.[4.7] respectively).

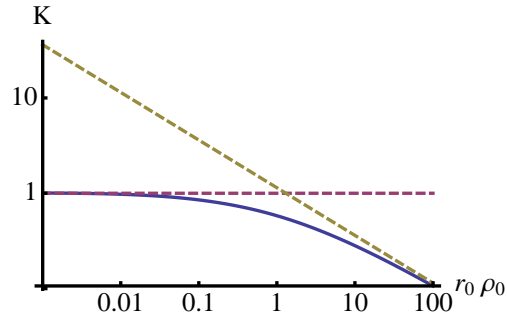


Figure 4.6: Numerical evaluation of the Luttinger parameter for Bosons with dipole-dipole interactions: as anticipated, the numerical results of Citro *et al* smoothly interpolate between the two known limits.

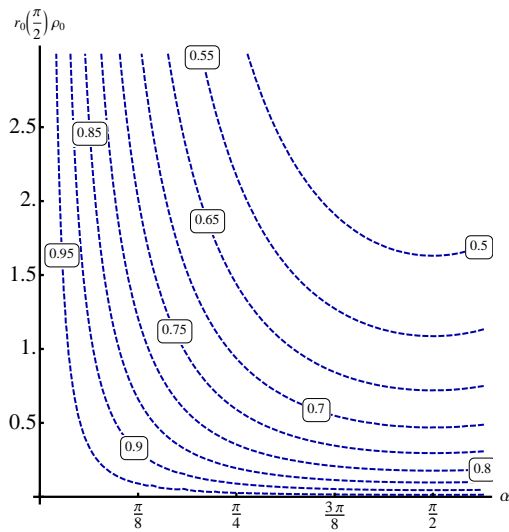


Figure 4.7: Plots of constant Luttinger parameter in the density-angle plane: the most important contour for our future considerations will be the $K = 1/2$ contour.

4.3 Weakly Coupling the Stripes

The previous results tell us how to set up the bosonized Hamiltonian for our model if the stripes are totally decoupled from one another. We are now going to weakly couple in the other stripes. Technically speaking we are breaking the rules set down when we first set out the procedure behind bosonization as the system is no longer one-dimensional. However, so long as the coupling is truly weak we can treat the effect of neighbouring stripes as a perturbation upon the, now solved, decoupled stripe system. Later on we will look at the system more appropriately as a two dimensional model.

For now, the contribution to the Hamiltonian due to a single stripe $H_{\text{stripe}}^{(n)}$ will take the form Eqn.[4.4], as discussed, but we need to look at the bosonized form of the coupling part of the Hamiltonian $H_{\text{couple}}^{(n)}$.

First consider the hopping term,

$$- \int dx J_{\perp} \left(\psi_n^{\dagger}(x) \psi_{n+1}(x) + \psi_{n+1}^{\dagger}(x) \psi_n(x) \right);$$

writing $\psi_n^{\dagger}(x) = \sqrt{\rho_0} e^{-i\theta_n(x)}$, this term becomes recognisable as a Josephson coupling

$$- \int dx J_{\perp} 2\rho_0 \cos(\theta_n(x) - \theta_{n+1}(x)).$$

Next consider the interaction term,

$$\int dx dx' \rho_n(x) w V_{\text{dd}}^{\text{inter}}(x - x') \rho_{n+1}(x');$$

if we were to use $\rho_n(x) = \rho_0 - \partial_x \varphi_n(x)/\pi$, then the non-constant contribution to the Hamiltonian would be

$$\int dx dx' \partial_x \varphi_n(x) w V_{\text{dd}}^{\text{inter}}(x - x') \partial_{x'} \varphi_{n+1}(x').$$

At first glance this forward scattering term ought to be neglected because the shift in n along

with the derivative in x makes this term at a higher harmonic than anything else present in the Hamiltonian so far. However, if we extend the density approximation to include one more harmonic, $\rho_n(x) = \rho_0 - \partial_x \varphi_n(x)/\pi + 2\rho_0 \cos[2\pi\rho_0 x - 2\varphi_n(x)]$, then no more terms appear in our considerations thus far but we do obtain the new non-negligible term,

$$\int dx dx' w V_{\text{dd}}^{\text{inter}}(x-x') 2\rho_0^2 \cos(2\varphi_n(x) - 2\varphi_{n+1}(x')).$$

If a denotes some appropriate ultraviolet cutoff length scale, then we can introduce dimensionless coupling parameters representing the strength of the interaction and hopping perturbations, g_{int} and g_{hop} , via

$$\frac{\hbar v_s}{2\pi} \frac{g_{\text{int}}}{a^2} = \rho_0^2 w \frac{C_{\text{dd}}}{2\pi} \frac{\cos^2 \alpha}{\lambda^3} \quad (4.10a)$$

$$\frac{\hbar v_s}{2\pi} \frac{g_{\text{hop}}}{a^2} = 2J_{\perp} \rho_0. \quad (4.10b)$$

Remember that the stripes are being coupled perturbatively weakly so $g_{\text{int}}, g_{\text{hop}} \ll 1$.

With these definitions in place we now have a neat form for the coupling part of the Hamiltonian

$$H_{\text{couple}}^{(n)} = \frac{\hbar v_s}{2\pi} \int \frac{dx}{a^2} \{g_{\text{int}} \cos 2(\varphi_n - \varphi_{n+1}) - g_{\text{hop}} \cos(\theta_n - \theta_{n+1})\}. \quad (4.11)$$

These terms plus the contribution from single stripes Eqn.[4.4] define the model that we will be working with to explore the physics of this system.

4.4 Equivalence to the Original Stripe System

We have now derived that the appropriate Hamiltonian with which to treat our system is

$$H = H_{\text{intra}} + H_{\text{inter}}$$

$$H_{\text{intra}} = \sum_i \int dx \frac{\hbar v_s}{2\pi} \left\{ K(\partial_x \theta_i)^2 + \frac{1}{K}(\partial_x \varphi_i)^2 \right\} \quad (4.12a)$$

$$H_{\text{inter}} = \sum_{\langle ij \rangle} \int dx \frac{\hbar v_s}{2\pi} \left\{ \frac{g_{\text{int}}}{a^2} \cos[2(\varphi_i - \varphi_j)] - \frac{g_{\text{hop}}}{a^2} \cos[(\theta_i - \theta_j)] \right\}. \quad (4.12b)$$

Comparing what we have here back to the expressions in Eqn.[1.1] we see that this bosonic cold atom system reproduces the behaviour of a fermionic condensed matter striped system.

It is important to restate here how well controlled the parameters here are, much more so than one could ever hope for from a solid state system.

The Luttinger parameter K can be tuned by turning the dipole moment of the trapped atoms. Independently of this, and of one another, the interaction parameters g_{int} and g_{hop} can be tuned by varying the depth and spacing of the optical lattice.

This freedom then may allow access to regions of parameter space which would be inaccessible to condensed matter realizations of this model, giving the experimentalist the ability to focus on the regions where the most interesting physics is to be found.

As it will turn out, the most interesting physics, and hence the parameter set we would want to tune to, is where $K = 1/2$ and $g_{\text{int}} \approx g_{\text{hop}}$

4.5 Mean Field Model

4.5.1 Mean Field Structure

There are two obvious limiting situations that need investigation, where one of g_{int} and g_{hop} dominates over the other. These interaction and hopping dominated limits correspond to the Hamiltonians

$$H_{\text{int}} = \frac{\hbar v_s}{2\pi} \sum_n \int dx \left\{ K(\partial_x \theta_n)^2 + \frac{1}{K}(\partial_x \varphi_n)^2 + \frac{g_{\text{int}}}{a^2} \cos 2(\varphi_n - \varphi_{n+1}) \right\} \quad (4.13a)$$

$$H_{\text{hop}} = \frac{\hbar v_s}{2\pi} \sum_n \int dx \left\{ K(\partial_x \theta_n)^2 + \frac{1}{K}(\partial_x \varphi_n)^2 + \frac{g_{\text{hop}}}{a^2} \cos(\theta_n - \theta_{n+1}) \right\} \quad (4.13b)$$

These limits look very similar, even more so if we make the (commutator preserving) transformation $\theta_n \rightarrow K^{-1/2}\theta_n, \varphi_n \rightarrow K^{1/2}\varphi_n$. Then setting $d_{\text{int}} = K$ and $d_{\text{hop}} = 1/(4K)$, the two Hamiltonians become

$$H_{\text{int}} = \frac{\hbar v_s}{2\pi} \sum_n \int dx \left\{ (\partial_x \theta_n)^2 + (\partial_x \varphi_n)^2 + \frac{g_{\text{int}}}{a^2} \cos 2d_{\text{int}}^{1/2}(\varphi_n - \varphi_{n+1}) \right\} \quad (4.14a)$$

$$H_{\text{hop}} = \frac{\hbar v_s}{2\pi} \sum_n \int dx \left\{ (\partial_x \theta_n)^2 + (\partial_x \varphi_n)^2 + \frac{g_{\text{hop}}}{a^2} \cos 2d_{\text{hop}}^{1/2}(\theta_n - \theta_{n+1}) \right\} \quad (4.14b)$$

We should notice here the duality transformation between φ and θ takes us between the interaction and hopping dominated limits.

It will turn out that d_{int} and d_{hop} represent the scaling dimension of the interaction and hopping perturbations respectively, which we will discuss shortly.

As a first attempt at studying the physics at play in this system, we now make a mean field approximation. Taking the hopping dominated limit as an example, the nature of our mean field approximation is to pretend that rather than each stripe interacting with its neighbours, it interacts with two thermally averaged *copies of itself*. The interaction can thus be simplified as follows

$$\begin{aligned}
\cos 2d_{\text{hop}}^{1/2}(\theta_n - \theta_{n+1}) &= \cos(2d_{\text{hop}}^{1/2}\theta_n) \cos(2d_{\text{hop}}^{1/2}\theta_{n+1}) + \sin(2d_{\text{hop}}^{1/2}\theta_n) \sin(2d_{\text{hop}}^{1/2}\theta_{n+1}) \\
&\rightarrow \cos(2d_{\text{hop}}^{1/2}\theta) \langle \cos(2d_{\text{hop}}^{1/2}\theta) \rangle + \sin(2d_{\text{hop}}^{1/2}\theta) \langle \sin(2d_{\text{hop}}^{1/2}\theta) \rangle \\
&= \langle \cos(2d_{\text{hop}}^{1/2}\theta) \rangle \cos(2d_{\text{hop}}^{1/2}\theta).
\end{aligned}$$

An analogous approximation may be applied to the interaction dominated limit and the mean field Hamiltonians we acquire are

$$H_{\text{int}}^{\text{mf}} = \frac{\hbar v_s}{2\pi} \int dx \left\{ (\partial_x \theta)^2 + (\partial_x \varphi)^2 + 2 \frac{g_{\text{int}}}{a^2} \langle \cos(2d_{\text{int}}^{1/2} \varphi) \rangle \cos(2d_{\text{int}}^{1/2} \varphi) \right\} \quad (4.15a)$$

$$H_{\text{hop}}^{\text{mf}} = \frac{\hbar v_s}{2\pi} \int dx \left\{ (\partial_x \theta)^2 + (\partial_x \varphi)^2 + 2 \frac{g_{\text{hop}}}{a^2} \langle \cos(2d_{\text{hop}}^{1/2} \theta) \rangle \cos(2d_{\text{hop}}^{1/2} \theta) \right\} \quad (4.15b)$$

In either case, we have the same form of action functional in the mean field, and a self consistency equation

$$S^{\text{mf}} = \frac{\hbar v_s}{2\pi} \int d\tau dx \left\{ \frac{1}{v_s^2} (\partial_\tau \phi)^2 + (\partial_x \phi)^2 + \frac{g^{\text{mf}}}{a^2} \cos 2d^{1/2} \phi \right\} \quad (4.16a)$$

$$g^{\text{mf}} = 2g \langle \cos 2d^{1/2} \phi \rangle, \quad (4.16b)$$

with ϕ being θ in the hopping dominated limit and φ in the interaction dominated limit. These two equations must be solved self consistently.

The action Eqn.[4.16a] is that of a Sine-Gordon model in $1 + 1 \sim 2$ Euclidean dimensions.

4.5.2 Mean Field Solution

Comparing Eqn.[4.16] to the exact form of the correlation function Eqn.[2.47], we see that we have a scaling relation

$$\langle \cos 2d^{1/2} \phi \rangle \sim (g^{\text{mf}})^{\frac{d}{2-d}}. \quad (4.17)$$

Now we can solve the self consistency condition to work out how the mean field coupling scales with the bare coupling. We discover that

$$g^{\text{mf}} \sim 2g^{\frac{1}{2}\left(1+\frac{1}{1-d}\right)} \quad \langle \cos 2d^{1/2}\phi \rangle \sim g^{\frac{1}{2}\frac{d}{1-d}} \quad (4.18)$$

The hopping dominated regime is characterized by a non-zero expectation value of $\cos \theta$ and similarly the interaction dominated regime is characterized by non-zero expectation value of $\cos 2\varphi$. As a physical picture, we can see that, as one might have guessed, the interaction dominated regime possesses a density wave order reminiscent of the dipole crystal we saw in the decoupled stripes. This agrees with the analysis of Kollath, Meyer and Giamarchi[76] into the system of dipole-dipole interacting stripes in the absence of hopping. More surprisingly perhaps, the hopping dominated regime possess *phase* correlation, a feature not present at all in the decoupled stripes, meaning that in this limit the system takes on *superfluid* characteristics.

In either case we are interested chiefly in the situation where $d < 1$. We ought to recall that $d_{\text{int}} = K$ and $d_{\text{hop}} = 1/(4K)$. This suggests to us that the self-dual point $K = 1/2$ might be interesting because here the density wave and superfluid phases (for non-zero $g_{\text{int}}, g_{\text{hop}}$) are maximally competing. This is a point we must return to later.

The analysis so far has been at zero temperature, now we would like to estimate the transition temperature of these phases. This in turn will let us decide which phase is dominant when both couplings are non-zero.

Carr and Tsvelik [29] have estimated the transition temperature for this kind of model by looking susceptibility of the relevant phase.

The susceptibility $\chi = -\partial_h^2 F|_{h=0} \sim G(k)$ will be divergent at a second order phase transition by definition. To find divergences in the susceptibility of either phase Carr and Tsvelik treated neighbouring stripes as a perturbation upon a single stripe.

To the level of the random phase approximation they found that the susceptibilities took

the form

$$\chi = \frac{\chi_0}{1 - \frac{g v_s}{a^2} \chi_0}.$$

The single stripe susceptibility is calculated, for example, in the appendix of Giamarchi's book[53] and has the form

$$\chi_0 \sim \frac{1}{2} \frac{a^2}{v_s} \left(\frac{\pi a}{\beta \hbar v_s} \right)^{2d-2},$$

so that the critical temperature is estimated as

$$k_B T_c \sim \frac{\hbar v_s}{\pi a} \left(\frac{g}{2} \right)^{\frac{1}{2-2d}}.$$

Combining this with the definition of $K(\rho_0 r_0)$, d_{int} , d_{hop} and g_{int} and recalling that all of these are functions of the angle α of the dipole moments, we find an angular dependence (in the mean field approximation) for the critical temperatures for the density wave and superfluid phases

$$k_B T_c^{\text{DW}}(\alpha) \sim \frac{\hbar v_s}{\pi a} \left(\frac{1}{2} g_{\text{int}}[0] \cos^2 \alpha \right)^{\frac{1}{2-2K(\rho_0 r_0 [\frac{\pi}{2}] \sin^2 \alpha)}} \quad (4.19a)$$

$$k_B T_c^{\text{SF}}(\alpha) \sim \frac{\hbar v_s}{\pi a} \left(\frac{1}{2} g_{\text{hop}} \right)^{\frac{2K(\rho_0 r_0 [\frac{\pi}{2}] \sin^2 \alpha)}{4K(\rho_0 r_0 [\frac{\pi}{2}] \sin^2 \alpha) - 1}}. \quad (4.19b)$$

These mean field critical temperatures allow us to put forward tentative phase diagrams for when one coupling channel dominates. These are shown in Fig.[4.8] and Fig.[4.9].

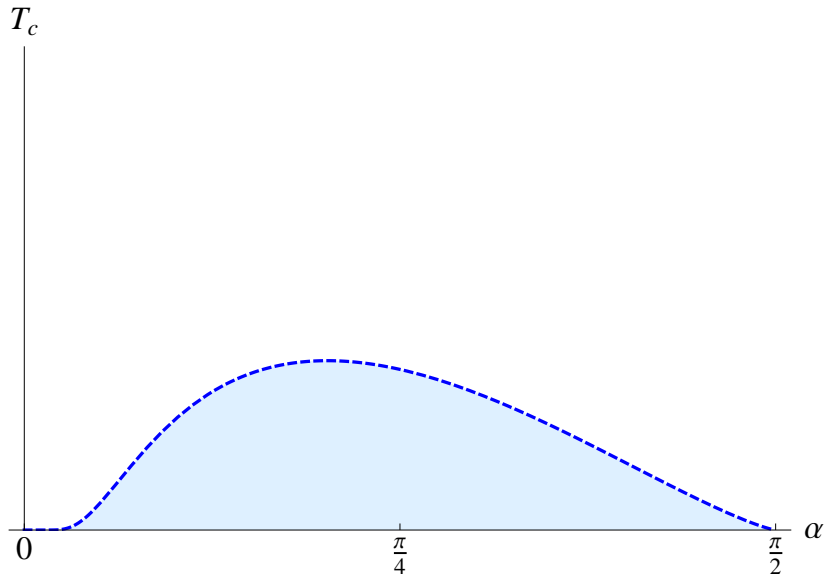


Figure 4.8: Mean field phase diagram of the interaction dominated regime: The blue region contains the density wave phase, the white region is the disordered phase. This plot is generated with $g_{\text{int}} = 0.1$ and $\rho_0 r_0 [\frac{\pi}{2}] = 25$, although the shape is fairly universal for small g_{int} . Based on realistic experimental parameters for the dipole moment taken from [79] and a lattice spacing $\sim 500\text{nm}$, we may estimate the maximum critical temperature of the density wave phase to be of order $T_c^{\text{DW}} \sim 50\text{nK}$

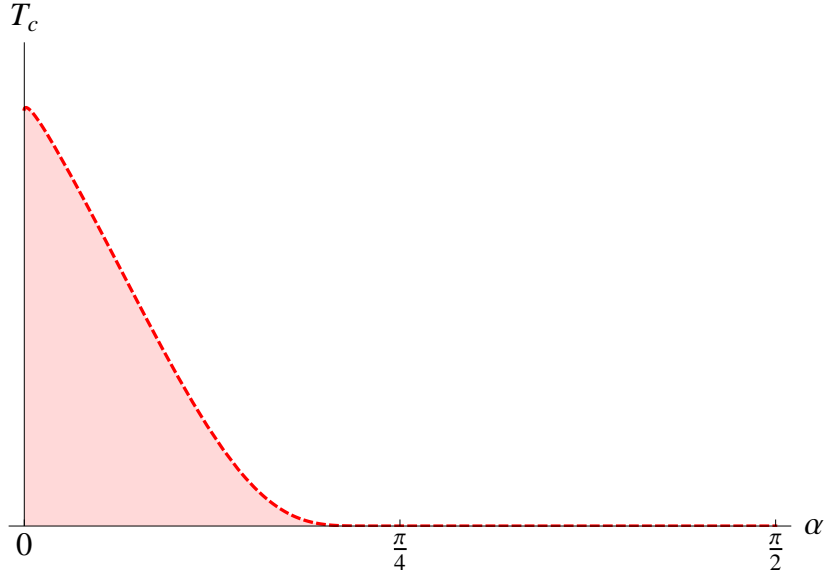


Figure 4.9: Mean field phase diagram of the hopping dominated regime: The pink region contains the superfluid phase, the white region is the disordered phase. This plot is generated with $g_{\text{hop}} = 0.2$ and $\rho_0 r_0[\frac{\pi}{2}] = 25$, although the shape is fairly universal for small g_{hop} . For the sake of comparison, the scale here is the same as that used for the interaction dominated regime. The maximum critical temperature for the superfluid phase is seen to be roughly twice that of the density wave phase, i.e. at its maximum $T_c^{\text{DW}} \sim 100\text{nK}$

These phase diagrams are constructed using the parameters $g_{\text{int}} = 0.1$, $g_{\text{hop}} = 0.2$ and $\rho_0 r_0[\frac{\pi}{2}] = 25$, which were chosen to make the relevant features most obvious. Experimenting with the code used to generate these figures shows that these basic shapes hold for pretty much any choice of parameters as long as the couplings are sufficiently small (which is a good thing because we are treating them as a perturbation!).

As a first stab at treating both couplings simultaneously we might try just superimposing the phase diagrams over one another. This is fair enough when one of $g_{\text{int}}^{\frac{1}{2-2K}}$ or $g_{\text{hop}}^{\frac{2K}{4K-1}}$ is significantly greater than the other, that is to say in the regions $\alpha \sim 0$ and $\alpha > \pi/4$, but it would imply that there might exist a critical angle at which there is a phase transition from superfluid to density wave, as illustrated in Fig.[4.10].

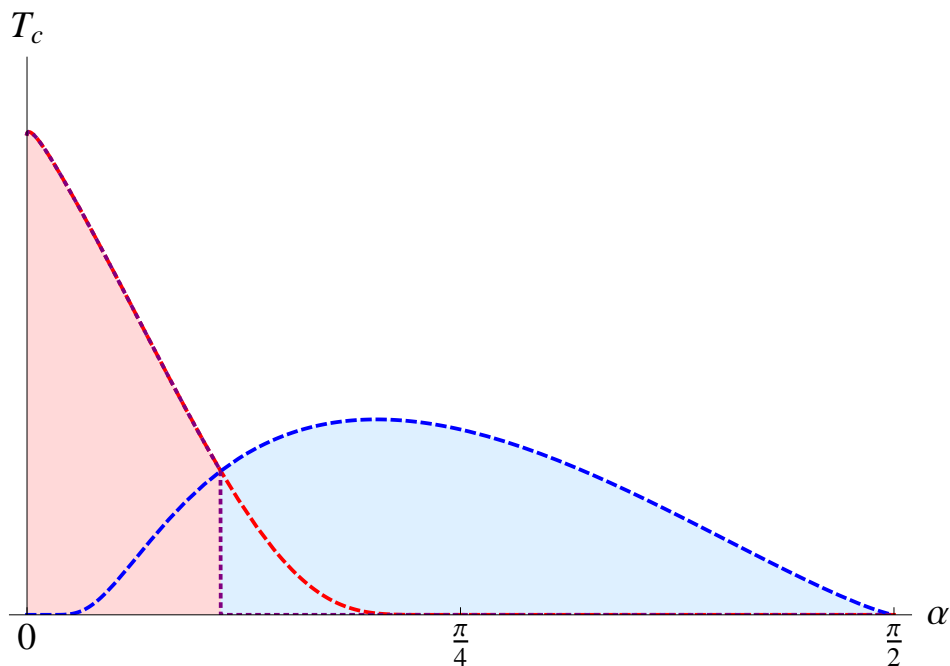


Figure 4.10: Mean field phase diagram including both channels of coupling.

The apparent first order transition between the two BKT orders that we see in this phase diagram is actually forbidden due to the Hohenberg-Mermin-Wagner theorem. This is because at the self dual point there is a symmetry between the two $O(2)$ orders that enhances the total symmetry of the system to $O(4)$, we'll discuss this in detail a little later. Near to the critical point where the two phase transitions meet, the transverse correlation length gets very large and it is no longer appropriate to treat inter-chain coupling. Thus to cope with this critical region we need to treat the system in its full two dimensions.

4.6 Effective Theory at Close Coupling

4.6.1 Coupling the Fields into a Single $SU(2)$ Field

To fix our mean field approach to the stripe model we rewrite the Hamiltonian for this model in a more amenable form. We start from the full Hamiltonian

$$H = \frac{\hbar v_s}{2\pi} \sum_n \int dx \left\{ K(\partial_x \theta_n)^2 + (1/K)(\partial_x \varphi_n)^2 + \frac{g_{\text{int}}}{a^2} \cos 2(\varphi_n - \varphi_{n+1}) + \frac{g_{\text{hop}}}{a^2} \cos(\theta_n - \theta_{n+1}) \right\}. \quad (4.20)$$

We can simplify this expression by introducing the matrix operator

$$\psi_n(x) = \frac{1}{\sqrt{2}} \begin{pmatrix} e^{-2i\varphi_n(x)} & -e^{i\theta_n(x)} \\ e^{-i\theta_n(x)} & e^{2i\varphi_n(x)} \end{pmatrix}. \quad (4.21)$$

We will employ a unitary rescaling of the Pauli matrices (which is equivalent to the quaternionic basis set) as a basis for our 2×2 matrices

$$u_0 = \begin{pmatrix} 1 & 0 \\ 0 & 1 \end{pmatrix} \quad u_1 = \begin{pmatrix} 0 & i \\ i & 0 \end{pmatrix} \quad u_2 = \begin{pmatrix} 0 & -1 \\ 1 & 0 \end{pmatrix} \quad u_3 = \begin{pmatrix} i & 0 \\ 0 & -i \end{pmatrix} \quad (4.22)$$

It is a simple matter to establish that:

$$\begin{aligned} \text{tr} \{ (\partial_x \psi_n^\dagger) (\partial_x \psi_n) \} &= (\partial_x \theta_n)^2 + 4(\partial_x \varphi_n)^2, \\ \text{tr} \{ (\partial_x \psi_n^\dagger) u_3 (\partial_x \psi_n) u_3 \} &= (\partial_x \theta_n)^2 - 4(\partial_x \varphi_n)^2, \\ \text{tr} \{ \psi_{n+1}^\dagger \psi_n \} &= \cos(\theta_n - \theta_{n+1}) + \cos 2(\varphi_n - \varphi_{n+1}), \\ \text{tr} \{ \psi_{n+1}^\dagger u_3 \psi_n u_3 \} &= \cos(\theta_n - \theta_{n+1}) - \cos 2(\varphi_n - \varphi_{n+1}). \end{aligned}$$

Using these results, we see that our Hamiltonian can be rewritten in the form

$$\begin{aligned} H = \frac{\hbar v_s}{4\pi} \sum_n \int dx \text{tr} \left\{ \frac{4K^2 + 1}{4K} (\partial_x \psi_n^\dagger) (\partial_x \psi_n) + \frac{4K^2 - 1}{4K} (\partial_x \psi_n^\dagger) u_3 (\partial_x \psi_n) u_3 \right. \\ \left. + \frac{g_{\text{hop}} + g_{\text{int}}}{a^2} \psi_{n+1}^\dagger \psi_n + \frac{g_{\text{hop}} - g_{\text{int}}}{a^2} \psi_{n+1}^\dagger u_3 \psi_n u_3 \right\}. \end{aligned}$$

In its original form the Hamiltonian had an *antiferromagnetic* signature in the sense that the positive sign of the cosine terms gave both the fields a tendency to anti-align with their counterparts in neighbouring stripes so as to compensate the effective repulsion. We will find it more convenient to map this system onto one with a *ferromagnetic* signature – i.e. one with negative sign on the cosine terms – which we achieve by shifting every other instance of either field along by π . This does not alter the measure in the partition function, the only effect is to add a minus sign to both g_{hop} and g_{int} . How this makes the system easier to deal with will become clear shortly.

Let us now suppose that the inter-stripe spacing λ is small and hence expand the Hamiltonian as a Taylor series. We then have, up to second order in λ ,

$$\begin{aligned}
H = & \frac{\hbar v_s}{4\pi} \sum_n \int dx \text{tr} \left\{ \frac{4K^2 + 1}{4K} \left(\partial_x \psi^\dagger(x, n\lambda) \right) \left(\partial_x \psi(x, n\lambda) \right) + \frac{4K^2 - 1}{4K} \left(\partial_x \psi^\dagger(x, n\lambda) \right) u_3 \left(\partial_x \psi(x, n\lambda) \right) u_3 \right. \\
& - \frac{g_{\text{hop}} + g_{\text{int}}}{a^2} \left(\psi^\dagger(x, n\lambda) \psi(x, n\lambda) + \psi^\dagger(x, n\lambda) \lambda \partial_{(n\lambda)} \psi(x, n\lambda) + \psi^\dagger(x, n\lambda) \frac{\lambda^2}{2} \partial_{(n\lambda)}^2 \psi(x, n\lambda) \right) \\
& \left. - \frac{g_{\text{hop}} - g_{\text{int}}}{a^2} \left(\psi^\dagger(x, n\lambda) u_3 \psi(x, n\lambda) u_3 + \psi^\dagger(x, n\lambda) u_3 \lambda \partial_{(n\lambda)} \psi(x, n\lambda) u_3 + \psi^\dagger(x, n\lambda) u_3 \frac{\lambda^2}{2} \partial_{(n\lambda)}^2 \psi(x, n\lambda) u_3 \right) \right\}.
\end{aligned}$$

Now treating λ as infinitesimal and discarding irrelevant constants, the Hamiltonian can be expressed as

$$\begin{aligned}
H = & \frac{\hbar v_s}{4\pi} \int dx dy \text{tr} \left\{ \frac{4K^2 + 1}{4\lambda K} \left(\partial_x \psi^\dagger(x, y) \right) \left(\partial_x \psi(x, y) \right) + \frac{\lambda}{2} \frac{g_{\text{hop}} + g_{\text{int}}}{a^2} \left(\partial_y \psi^\dagger(x, y) \right) \left(\partial_y \psi(x, y) \right) \right. \\
& + \frac{4K^2 - 1}{4\lambda K} \left(\partial_x \psi^\dagger(x, y) \right) u_3 \left(\partial_x \psi(x, y) \right) u_3 + \frac{\lambda}{2} \frac{g_{\text{hop}} - g_{\text{int}}}{a^2} \left(\partial_y \psi^\dagger(x, y) \right) u_3 \left(\partial_y \psi(x, y) \right) u_3 \\
& \left. + \frac{\lambda}{2} \frac{g_{\text{int}} - g_{\text{hop}}}{a^2} \psi^\dagger(x, y) u_3 \psi(x, y) u_3 \right\}.
\end{aligned}$$

If we de-dimensionalize distances according to

$$\begin{aligned}
x &= ar_1 \sqrt{\frac{4K^2 + 1}{4K}} \\
y &= \lambda r_2 \sqrt{\frac{g_{\text{hop}} + g_{\text{int}}}{2}},
\end{aligned}$$

then the Hamiltonian is

$$H = \frac{\hbar v_s}{4\pi a} \sqrt{\left(\frac{4K^2 + 1}{4K}\right) \left(\frac{g_{\text{hop}} + g_{\text{int}}}{2}\right)} \int \mathrm{d}^2 r \operatorname{tr} \left\{ |\nabla \psi(r)|^2 + \frac{g_{\text{int}} - g_{\text{hop}}}{g_{\text{hop}} + g_{\text{int}}} \psi^\dagger(r) u_3 \psi(r) u_3 \right. \\ \left. + \frac{4K^2 - 1}{4K^2 + 1} \partial_1 \psi^\dagger(r) u_3 \partial_1 \psi(r) u_3 + \frac{g_{\text{hop}} - g_{\text{int}}}{g_{\text{hop}} + g_{\text{int}}} \partial_2 \psi^\dagger(r) u_3 \partial_2 \psi(r) u_3 \right\}.$$

The region of parameter space which is of particularly interesting to us is where the superfluid and density wave orders are in maximal competition. We have already seen that in the mean field approximation the critical temperature for the two competing phases look like $T^{\text{DW}} \propto (g_{\text{int}}/2)^{\frac{1}{2-2K}}$ and $T^{\text{SF}} \propto (g_{\text{hop}}/2)^{\frac{2K}{4K-1}}$. To this end we focus our attention on the region in parameter space in which $g_{\text{int}} \approx g_{\text{hop}}$ and $K \approx 1/2$. The Hamiltonian now looks like

$$H = \frac{\hbar v_s \sqrt{g}}{4\pi a} \int \mathrm{d}^2 r \operatorname{tr} \left\{ |\nabla \psi(r)|^2 + \frac{g_{\text{int}} - g_{\text{hop}}}{g_{\text{int}} + g_{\text{hop}}} \psi^\dagger(r) u_3 \psi(r) u_3 + \frac{4K^2 - 1}{2} \partial_1 \psi^\dagger(r) u_3 \partial_1 \psi(r) u_3 \right. \\ \left. + \frac{g_{\text{int}} - g_{\text{hop}}}{g_{\text{int}} + g_{\text{hop}}} \partial_2 \psi^\dagger(r) u_3 \partial_2 \psi(r) u_3 \right\} \\ \approx \frac{\hbar v_s \sqrt{g}}{4\pi a} \int \mathrm{d}^2 r \operatorname{tr} \left\{ |\nabla \psi(r)|^2 + h \psi^\dagger(r) u_3 \psi(r) u_3 + \tilde{h} \nabla \psi^\dagger(r) u_3 \nabla \psi(r) u_3 \right\},$$

with $h = (g_{\text{int}} - g_{\text{hop}})/(g_{\text{int}} + g_{\text{hop}})$ and $\tilde{h} = \max\{h, (4K^2 - 1)/(4K^2 + 1)\}$.

We define $J = (\hbar v_s \sqrt{g})/(2\pi a)$ and hence arrive at an effective Hamiltonian description of the region of maximal competition

$$H = \frac{J}{2} \int \mathrm{d}^2 r \operatorname{tr} \left\{ |\nabla \psi(r)|^2 + h \psi^\dagger(r) u_3 \psi(r) u_3 + \tilde{h} \nabla \psi^\dagger(r) u_3 \nabla \psi(r) u_3 \right\} \quad (4.23)$$

Looking back to the definition of the matrix field ψ , we notice that $\psi^\dagger \psi = 1$ and that ψ has unit determinant so clearly $\psi(r) \in SU(2)$. In the absence of the coupling terms the Hamiltonian is invariant under left and right multiplication by a constant $SU(2)$ field. This means there is an $SU(2) \times SU(2)$ symmetry to the system. With the anisotropies in place, the

symmetry is reduced as the full Hamiltonian is invariant under pre- and post-multiplication by matrices that are linear combinations of u_0 and u_3 , hence the reduced symmetry group is $U(1) \times U(1)$.

We will find it most convenient to deal with this system in terms of the coefficients in the expansion $\psi(x) = \Psi_0(x)u_0 + \Psi_1(x)u_1 + \Psi_2(x)u_2 + \Psi_3(x)u_3$ with $\Psi_i \in \mathbb{R}$. In terms of the vector of expansion coefficients $\Psi = (\Psi_0, \Psi_1, \Psi_2, \Psi_3) \in \mathbb{R}^4$ the Hamiltonian takes the form

$$H = \frac{J}{2} \int d^2r \nabla \Psi(r) \cdot \nabla \Psi(r) + h \Psi(r) \cdot M \Psi(r) + \tilde{h} \nabla \Psi(r) \cdot M \nabla \Psi(r), \quad (4.24a)$$

where the matrix M has the form

$$M = \begin{pmatrix} -1 & 0 & 0 & 0 \\ 0 & 1 & 0 & 0 \\ 0 & 0 & 1 & 0 \\ 0 & 0 & 0 & -1 \end{pmatrix} \quad (4.24b)$$

We notice that in the absence of anisotropy terms the Hamiltonian is invariant under multiplication of Ψ by $O(4)$ matrices and that the anisotropies reduce the symmetry to multiplication by block $O(2) \times O(2)$ matrices. We further notice that, in order for ψ to be in $SU(2)$ requires that $\Psi_0^2 + \Psi_1^2 + \Psi_2^2 + \Psi_3^2 = 1$. As such Ψ takes its values from the surface of the three-sphere S_3 .

We can now see, as per our prior discussions, that the relevant model with which to study the system in the region of maximal competition is an $O(4)$ nonlinear sigma model with anisotropy terms that break the symmetry down to $O(2) \times O(2)$.

As always we would prefer to work in the action formalism and so we consider the partition function

$$\mathcal{Z} = \int \mathcal{D}[\Psi \in \mathbb{R}^4] \delta(\Psi^2 - 1) e^{-S[\Psi]} \quad (4.25)$$

$$S[\Psi] = \frac{J}{2} \int_0^\beta d\tau \int d^2r \left\{ \frac{1}{v^2} [\partial_\tau \Psi]^2 + [\nabla \Psi]^2 + h \Psi M \Psi + \tilde{h} \nabla \Psi M \nabla \Psi \right\}.$$

In converting into the action formalism it is possible that we would generate an additional topological term to the action

$$S_{\text{top}}[\Psi] = \frac{i q}{12\pi} \int d^{2+1}r \varepsilon_{\mu\nu\lambda} \varepsilon_{\alpha\beta\gamma\delta} \Psi_\alpha \partial_\mu \Psi_\beta \partial_\nu \Psi_\gamma \partial_\lambda \Psi_\delta \quad (4.26)$$

Jaefari *et al*[30] have argued that this kind of term is irrelevant in the region we are considering, so we will happily neglect its existence.

In the above we have seen that the effective theory of the region of maximal competition can be described in terms of an $O(4)$ order parameter. We have seen that the model in this domain can be described by a nonlinear sigma model on $O(4)$ with anisotropy terms which break the symmetry down to $O(2) \times O(2)$. Now let us explore some of the consequences of this realization as regards our proposed phase diagram.

4.6.2 A Ginzburg-Landau Treatment of the High Symmetry Point

At the high symmetry point, vortices are no longer topologically protected and so the only way that the system could order – through a BKT transition – is not viable. Clearly then the system may not have (even quasi-) long-ranged order at this point. However far from this point the model quite clearly decouples into two disjoint $O(2)$ sectors, each of which is allowed to order through a BKT transition, giving credence to our mean field results. In advance of any calculation we can safely say that the (BKT) critical temperature of either phase must somehow drop to zero at high symmetry and hence we can make a schematic adaptation to the phase diagram as illustrated in Fig.[4.11]

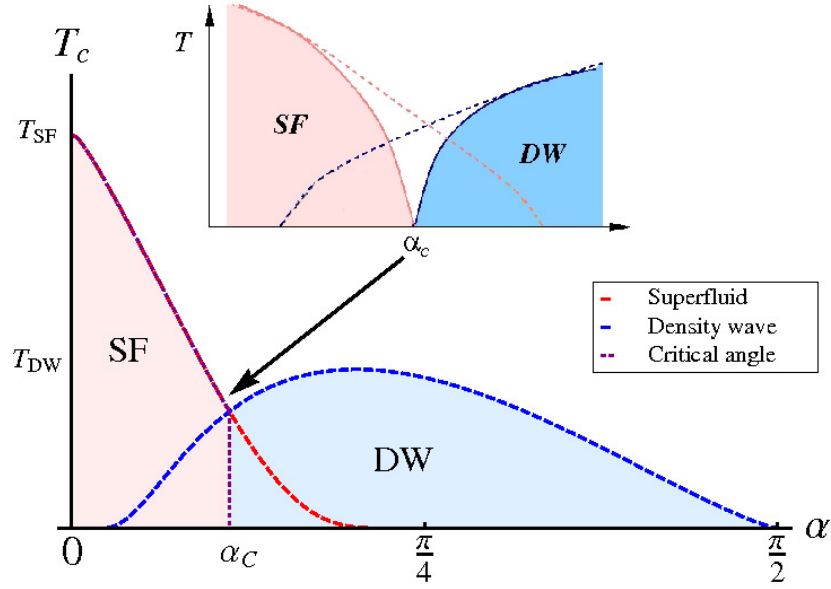


Figure 4.11: Correction to the mean field phase diagram due to the enhanced symmetry at the critical angle. The symmetry enhancement forces both BKT critical temperatures down to zero.

To probe further into this region we attempt an analysis via the renormalization group.

Just by counting powers we can see straight off that the term proportional to \tilde{h} will be irrelevant under renormalization as compared to the term proportional to h and so we will drop it.

We also take into account that, because $\Psi \cdot \Psi = 1$, we can add as much of $\Psi \cdot \Psi$ as we like to the Lagrangian so as to simplify proceedings. Doing this we may redefine the anisotropy matrix as

$$M = \begin{pmatrix} 0 & 0 & 0 & 0 \\ 0 & 1 & 0 & 0 \\ 0 & 0 & 1 & 0 \\ 0 & 0 & 0 & 0 \end{pmatrix}, \quad (4.27)$$

and be left with the partition function

$$\begin{aligned} \mathcal{Z} &= \int \mathcal{D}[\Psi \in \mathbb{R}^4] \delta(\Psi^2 - 1) e^{-S[\Psi]} \\ S[\Psi] &= \frac{J}{2} \int_0^\beta d\tau \int d^2r \left\{ \frac{1}{v^2} [\partial_\tau \Psi(\tau, r)]^2 + [\nabla \Psi(\tau, r)]^2 + h\Psi(\tau, r)M\Psi(\tau, r) \right\}. \end{aligned} \quad (4.28)$$

where M now gives an effective mass to the Ψ_1 and Ψ_2 sectors.

Near to zero temperature, we have a three dimensional nonlinear sigma model with anisotropy which could be treated within a $4 - \epsilon$ expansion. Near to $4D$, the nonlinear constraint can be approximated by a quartic interaction. Hence let us consider the Lagrangian

$$\mathcal{L}[\Psi] = \frac{J}{2} (\partial_\mu \Psi_\varphi)^2 + \frac{J}{2} (\partial_\mu \Psi_\theta)^2 + \frac{Jh}{2} \Psi_\theta^2 + v (\Psi_\varphi^2 + \Psi_\theta^2)^2.$$

Where we have defined $\Psi_\varphi = (\Psi_0, \Psi_3)$ and $\Psi_\theta = (\Psi_1, \Psi_2)$.

This Lagrangian must renormalize to something of the form

$$\mathcal{L}[\Psi] = \frac{J_\varphi}{2} (\partial_\mu \Psi_\varphi)^2 + \frac{J_\theta}{2} (\partial_\mu \Psi_\theta)^2 + m_\theta \Psi_\theta^2 + m_\varphi \Psi_\varphi^2 + v_\varphi \Psi_\varphi^4 + v_\theta \Psi_\theta^4 + 2w \Psi_\theta^2 \Psi_\varphi^2,$$

which we now investigate to get a feel for the critical properties.

Evidently if w renormalizes toward zero the two sectors completely decouple and can be treated separately. We will investigate slowly varying solutions so that we can ignore the gradient terms. We now may as well rescale Ψ_θ and Ψ_φ with respect to v_θ and v_φ respectively, as we have the freedom to do so and it simplifies the proceeding, and then we may minimize the renormalized Lagrangian with respect to Ψ_θ and Ψ_φ . First we note that

$$\begin{aligned} \frac{\delta \mathcal{L}[\Psi]}{\delta \Psi_\theta} &= 2\Psi_\theta (m_\theta + 2\Psi_\theta^2 + 2w\Psi_\varphi^2) \\ \frac{\delta \mathcal{L}[\Psi]}{\delta \Psi_\varphi} &= 2\Psi_\varphi (m_\varphi + 2\Psi_\varphi^2 + 2w\Psi_\theta^2), \end{aligned}$$

hence we may tabulate the extrema

Ψ_θ^2	Ψ_φ^2	$\mathcal{L}[\Psi]$
0	0	0
$-m_\theta/2$	0	$-m_\theta^2/4$
0	$-m_\varphi/2$	$-m_\varphi^2/4$
$(wm_\varphi - m_\theta)/2(1 - w^2)$	$(wm_\theta - m_\varphi)/2(1 - w^2)$	$-(m_\varphi - m_\theta)^2/4(1 - w^2) - m_\varphi m_\theta/2(1 + w)$

The second and third minima indicate phase transitions in the θ and φ sectors respectively. Following the standard Ginzburg-Landau theory we say $m_{\theta/\varphi} \sim (T - T_{\theta/\varphi}^c)/T_{\theta/\varphi}^c$ and hence see that these cases constitute phase transitions in a single sector with the other locked into disorder.

The final minimum is strongly dependent upon the renormalized anisotropy parameter w . When $w > 1$ the two phases cannot simultaneously order as Ψ_θ^2 and Ψ_φ^2 will of opposite sign to one another *unless* $m_\varphi = m_\theta$, and even then this does not constitute a global minimum of the Lagrangian at overly high temperatures. As such, for $w > 1$ there is a (first order) flop line separating the two ordered phases at low temperature which bifurcates forming a *bicritical* point. On the other hand if $w < 1$, Ψ_θ and Ψ_φ can share the same sign for a window of width $\sim (1/w - 1)$ around the line $m_\theta = m_\varphi$, within which the two phases may coexist. The scenario for $w < 1$ is that at low temperatures the two singularly ordered regimes are separated by a domain of dual order, the transition lines for which converge to a point and come out again as the transition lines from the singularly ordered phases into the disordered state. The critical point in this scenario is *tetracritical*. When w is exactly one the critical point only exists at zero temperature.

This very basic Ginzburg-Landau analysis serves to tell us what we should be looking for. If w renormalizes upwards we expect to see a first order phase transition between the two

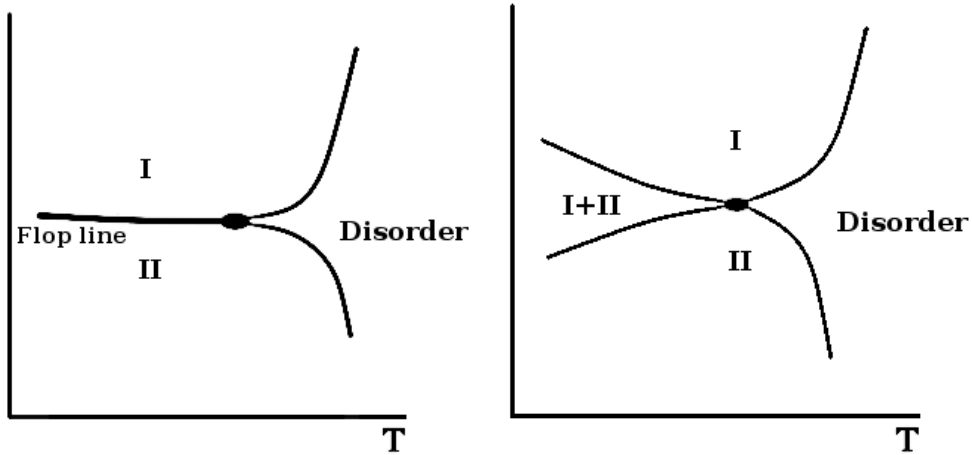


Figure 4.12: Bicritical (left) and tetracritical (right) points.

kinds of order whereas if it renormalizes downward we should expect a region of coexistence of the ordered phases. Although the Ginzburg-Landau treatment distinguishes between possible scenarios we need to do the renormalization separately to see what scenario is actually taken.

Unfortunately w does not renormalize in either direction within one loop, however Calabrese *et al* [80] have performed the renormalization up to five loops (by numerical methods) and find that the correct multicritical behaviour is the tetracritical scenario. Taking Calabrese *et al*'s results into account for our model, we realize that at low temperatures in the vicinity of the high symmetry point there will be a coexistence of the superfluid and density wave phases.

Given that this analysis says the ground state has double order in the vicinity of the self-dual point we expect there to be a finite BKT transition temperature for both sectors above this region, hence a double quasi-long ranged order. This region containing both superfluid and crystalline order could be called a *supersolid*. We will discuss the background of this proposed phase in the next section. Then having seen schematically how the phase diagram should look in the region of maximally competing orders we will go on to study how the enhanced symmetry effects the BKT transition temperatures in much more detail.

4.6.3 The supersolid state

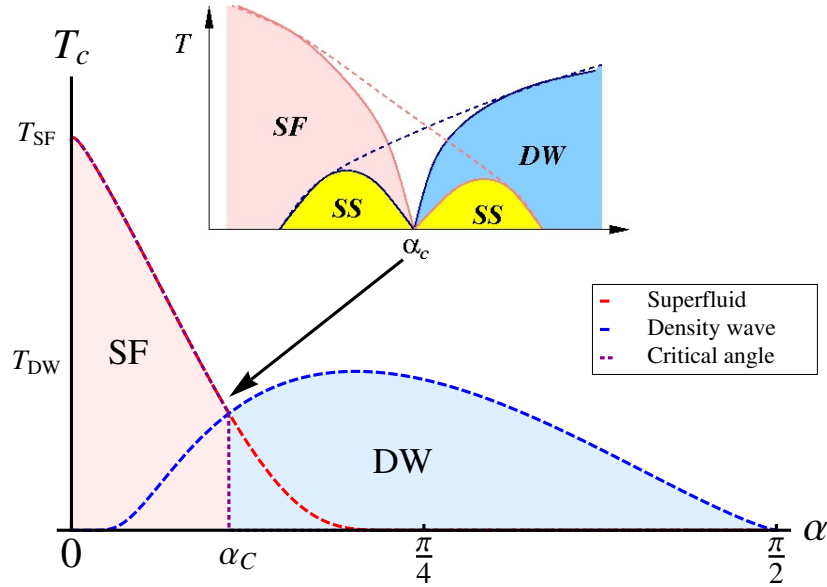


Figure 4.13: Adaptation to the mean field phase diagram due to the enhanced symmetry at the critical angle. The yellow region contains what could be described as a *supersolid* as we will discuss in this section.

Given that the phase in which both $O(2)$ sectors are supported possesses both crystalline and superfluid properties, we are tempted to refer to this state as a *supersolid*. This term is however rather loaded because the possibility of a supersolid state of matter has quite a long and spotted history.

We will refer to the coexistence phase as a supersolid – if only for the want of a better term – but we should pause now to look into some of the history of supersolidity and how the coexistence of phase coherence and density wave ordering ties into this.

The earliest reference to what would now be generally referred to as supersolidity comes

in the seminal 1956 work of Penrose and Onsager [81]. This paper introduces the Penrose-Onsager criterion, which shows that Bose-Einstein condensation is dependent on off-diagonal long-ranged order in the reduced density matrix. It is also shown in this paper that Bose-Einstein condensation is forbidden in a solid. This should be the end of the discussion then.

The problem with their proof of this statement, as pointed out by Chester nearly fifteen years later in 1970[82], is that when Penrose and Onsager proved that Bose-Einstein condensation cannot occur in a system with crystalline order they assumed that a crystal must have every site occupied. If we relax that restriction and allow vacancies into the crystal then condensation becomes a real possibility.

Chester proposed then that the solid phase of ^4He could indeed become a supersolid – as in a solid with Bose-condensed excitations – so long as the zero temperature phase of ^4He has sufficient disorder.

This possibility was also recognised by Andreev and Lifschitz in 1971[83] in their quantum theory of defects in crystals. Andreev and Lifschitz noted that at low temperatures a localised defect can move freely through a crystal giving rise to a fluid of defects. As bosonic excitations, these fluids could give rise to a superfluid.

Over the years there have been numerous experimental reports of evidence of supersolidity in ^4He [84] but a more promising route to the supersolid phase came with the advent of optical lattice experiments[85] as there have been proposals to use such systems to simulate the extended Bose-Hubbard model, in which supersolidity is expected to occur[86].

In the model we propose, the state we would like to call a supersolid is not a Bose condensed fluid of defects as discussed above, but rather a direct coexistence of quasi-long ranged superfluid and crystalline orders. Whether supersolid is the correct term to use is possibly debatable but as no better term springs to mind, this is what we will go with.

CHAPTER 5

THE $O(N)$ NONLINEAR SIGMA MODEL

5.1 Background

Consider a very general action of the form

$$S[\phi] = \int \mathrm{d}^d r \{ |\nabla\phi|^2 + V(\phi) \} \quad (5.1)$$

where ϕ is an N -component field which could be real or complex. Let's now imagine that $V(\phi)$ is invariant under some continuous (unitary or orthogonal) transformation Σ . Then we should look at what happens when we set $\phi \rightarrow \Sigma\phi$. If we make this transformation the action becomes

$$S = \int \mathrm{d}^d r (|\nabla\phi|^2 + |\phi|^2 \mathrm{tr}\{\nabla\Sigma^\dagger \cdot \nabla\Sigma\} + \mathrm{tr}\{j \cdot A\} + V(\phi)) \quad (5.2)$$

where $j = \mathrm{i}(\phi^*[\nabla\phi] - [\nabla\phi^*]\phi)$ and $A = \Sigma^\dagger \nabla\Sigma$. Now we imagine a situation, like we saw when we first introduced spontaneous symmetry breaking, where a saddle point approximation determines a constant minimum for $V(\phi)$ when $|\phi| = \varphi$. Then the low energy theory only cares about the symmetry factor Σ .

$$S = S_0 + \varphi^2 \int \mathrm{d}^d r \mathrm{tr}\{\nabla\Sigma^\dagger \cdot \nabla\Sigma\} \quad (5.3)$$

This action is called the nonlinear sigma model. It may not seem to be so nonlinear, it looks just like a noninteracting quadratic action. The nonlinearity comes from the fact that Σ takes its values from some compact group \mathcal{G} .

The nonlinear sigma model appears all over condensed matter and particle physics because it is the low energy effective theory for many symmetric models. For example, when studying the electroweak force, a particle physicist might be interested in a nonlinear sigma model where $\mathcal{G} = SU(2) \times U(1)$.

The specific nonlinear sigma model we will specialize to is called the $O(N)$ nonlinear sigma model. This is a silly name as we are actually going to consider a nonlinear sigma model on the group $O(N)/O(N-1)$ but the name is traditional so we will stick with it and put up with the confusion.

The model is specified by the action

$$S[n] = \int d^d r (\nabla n)^2 \quad n \in \mathbb{R}^N \quad n^2 = 1 \quad (5.4)$$

this looks a lot like a free action for an N component field, the nonlinearity comes in through a unit length constraint on n . We have of course seen this kind of action before when discussing the XY-model for which $N = 2$.

In the following we will fill in the appropriate physical scales for this model and go through the momentum-shell renormalization calculation to see how the system flows. We will then include quadratic symmetry breaking terms and repeat the renormalization group calculation.

5.2 The Classical $O(N)$ Nonlinear Sigma Model

We will start our considerations of the $O(N)$ non-linear sigma model in d dimensions by considering the simplest classical case given by the (dimensionless) action functional

$$S[n] = \frac{\beta J a^{2-d}}{2} \int_a \mathrm{d}^d x (\nabla n)^2 \quad (5.5)$$

where $\beta = (k_B T)^{-1}$ is the inverse temperature, J is an appropriate energy scale (typically the stiffness) and a is the UV (lattice) length scale.

The nonlinearity comes in through a length constraint on $n \in \mathbb{R}^N$ that enters the partition function as

$$\mathcal{Z} = \int \mathcal{D}[n \in \mathbb{R}^N] \delta(n^2 - 1) e^{-S[n]}. \quad (5.6)$$

If we write $n = (\pi, \sigma)$ where $\pi \in \mathbb{R}^{N-1}$ then we can integrate over the field σ to get

$$\begin{aligned} \mathcal{Z} &= \int \mathcal{D}[\pi \in \mathbb{R}^{N-1}] \mathcal{D}[\sigma] \delta(\pi^2 + \sigma^2 - 1) e^{-S[(\pi, \sigma)]} \\ &= \int \mathcal{D}[\pi \in \mathbb{R}^{N-1}] \mathcal{D}[\sigma] \left[\prod_x \frac{\delta(\sigma - \sqrt{1 - \pi^2})}{\sqrt{1 - \pi^2}} \right] e^{-S[(\pi, \sigma)]} \\ &= \int \mathcal{D}[\pi \in \mathbb{R}^{N-1}] \left[\prod_x \frac{1}{\sqrt{1 - \pi^2}} \right] e^{-S[(\pi, \sqrt{1 - \pi^2})]}. \end{aligned} \quad (5.7)$$

The residual of the delta function can be cast in the same form of the action first by writing

$$\prod_x \frac{1}{\sqrt{1 - \pi^2}} = e^{-\frac{1}{2} \sum_x \ln(1 - \pi^2)}, \quad (5.8)$$

then by converting the sum into an integral by inserting a UV density ρ

$$\sum_x \ln(1 - \pi^2) = \int_a \mathrm{d}^d x \rho \ln(1 - \pi^2). \quad (5.9)$$

The UV density is given by the volume of reciprocal space

$$\rho = \int^\Lambda \frac{\mathrm{d}^d k}{(2\pi)^d} \quad (5.10)$$

where $\Lambda = 1/a$. Clearly ρ is a large – in fact divergent as $a \rightarrow 0$ – quantity but this serves the purpose of forcing the partition function toward $\pi^2 < 1$ and so we must be forgiving.

Our model has become

$$\mathcal{Z} = \int \mathcal{D}[\pi \in \mathbb{R}^{N-1}] e^{-S_{\text{eff}}[\pi]} \quad (5.11a)$$

$$S_{\text{eff}}[\pi] = \frac{1}{2} \int_a \mathrm{d}^d x \left\{ \beta J a^{2-d} \left[(\nabla \pi)^2 + \frac{(\pi \cdot \nabla \pi)^2}{1 - \pi^2} \right] + \rho \ln(1 - \pi^2) \right\}. \quad (5.11b)$$

The partition function is now in a form we know how to handle, but the action has become rather tricky. We can break this action into free and coupling parts $S_{\text{eff}}[\pi] = S_0[\pi] + S_1[\pi]$, where

$$S_0[\pi] = \frac{1}{2} \int_a \mathrm{d}^d x \beta J a^{2-d} (\nabla \pi)^2 \quad (5.12a)$$

$$S_1[\pi] = \frac{1}{2} \int_a \mathrm{d}^d x \left\{ \beta J a^{2-d} \frac{(\pi \cdot \nabla \pi)^2}{1 - \pi^2} + \rho \ln(1 - \pi^2) \right\}. \quad (5.12b)$$

The free propagator associated with $S_0[\pi]$ is

$$\begin{aligned} G_0(x_1 - x_2) &= \langle \pi(x_1) \pi(x_2) \rangle_0 \\ &= \int^\Lambda \frac{\mathrm{d}^d k}{(2\pi)^d} e^{i(x_1 - x_2)k} \frac{a^{d-2}}{\beta J} \frac{1}{k^2}. \end{aligned} \quad (5.13)$$

To make the coupling action less daunting we expand in powers of π , so that to fourth order

$$S_1[\pi] = \frac{1}{2} \int_a \mathrm{d}^d x \left\{ \beta J a^{2-d} (\pi \cdot \nabla \pi)^2 (1 + \pi^2 + \dots) - \rho \left(\pi^2 + \frac{1}{2} \pi^4 + \dots \right) \right\}. \quad (5.14)$$

We can write the field in terms of its Fourier components

$$\pi(x) = \int^\Lambda \frac{\mathrm{d}^d k}{(2\pi)^d} e^{ikx} \pi(k), \quad (5.15a)$$

which allows us to define fast and slow modes

$$\pi^\lambda(x) = \int^{\Lambda/\lambda} \frac{d^d k}{(2\pi)^d} e^{ikx} \pi(k) \quad (5.15b)$$

$$\pi^+(x) = \int_{\Lambda/\lambda}^{\Lambda} \frac{d^d k}{(2\pi)^d} e^{ikx} \pi(k). \quad (5.15c)$$

Following our now familiar Wilson momentum shell RG procedure, we want to integrate out the fast modes perturbatively leaving behind the slow modes. We then rescale the slow modes until we return to the original form of the model, but with a new set of coupling constants, the form of which tell us how the system flows.

We face a problem due to the sheer number of terms we need to keep track of. As such some diagrammatics are in order.

We define a vertex set:

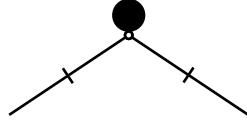
$$\begin{aligned} \beta J a^{2-d} &\Rightarrow \bullet \\ \rho &\Rightarrow \blacksquare \end{aligned}$$

... and an edge set:

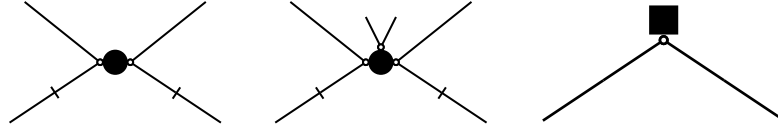
$$\begin{aligned} \pi_i^\lambda &\Rightarrow \text{---} \\ \nabla \pi_i^\lambda &\Rightarrow \text{---} \times \\ \pi_i^+ &\Rightarrow \text{- - -} \\ \nabla \pi_i^+ &\Rightarrow \text{- - -} \times \end{aligned}$$

Now we integrate out fast modes (join up dotted lines) and see what diagrams are generated. We will work to one loop only.

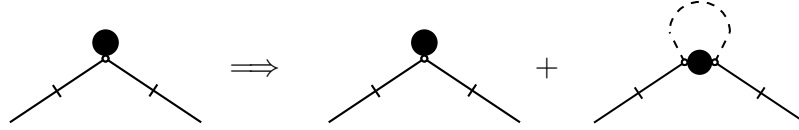
The kinetic energy term in S_0 gives us the diagram



the low order terms in S_1 give us diagrams



The renormalization of the kinetic energy term to one loop comes from the diagrammatic equation



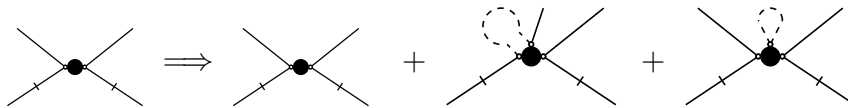
This translates into mathematics as the recursion equation

$$(\beta J a^{2-d})_\lambda = (\beta J a^{2-d}) [1 + G_+(0)] \zeta^2 \lambda^{d-2} \quad (5.16a)$$

where $G_+(0)$ is the free propagator of the fast modes. ζ is a dimensionless quantity brought in to enforce the unit normalization of n , so we get one factor per slow leg. The appearance of λ here comes from the rescaling of distances to recover the domain of the original model. We get d factors from the integral in the action and then 1 per every derivative (dashed leg).

The term Hartree term $G_+(0)$ crops up again so we will give it its own symbol η .

The renormalization of the four legged term comes in from the diagrams



which gives us the recursion equation

$$(\beta J a^{2-d})_\lambda = (\beta J a^{2-d}) [1 + \eta + (N-1)\eta] \zeta^4 \lambda^{d-2} \quad (5.16b)$$

In order for Eqn.[5.16a] and Eqn.[5.16b] to be consistent with one another requires that

$$\zeta^2 = \frac{1 + \eta}{1 + N\eta} \quad (5.17)$$

leaving us with

$$(\beta J)_\lambda = (\beta J) \left[1 + \frac{(1 + \eta)^2}{1 + N\eta} \right] \lambda^{d-2}. \quad (5.18)$$

Let us now take the limit $\lambda \rightarrow 1 + d\Lambda/\Lambda$, then we can calculate η as

$$\begin{aligned} \eta &= \int_{\Lambda-d\Lambda}^{\Lambda} \frac{d^d k}{(2\pi)^d} \frac{a^{d-2}}{\beta J} \frac{1}{k^2} = \int_{\Lambda-d\Lambda}^{\Lambda} \frac{dk}{(2\pi)^d} \cdot \frac{2\pi^{d/2}}{\Gamma(d/2)} k^{d-1} \cdot \frac{a^{d-2}}{\beta J} \frac{1}{k^2} \\ &= \frac{2^{1-d} \pi^{-d/2}}{\Gamma(d/2)} \frac{a^{d-2}}{\beta J} \Lambda^{d-3} d\Lambda = \frac{2^{1-d} \pi^{-d/2}}{\Gamma(d/2)} \frac{1}{\beta J} \frac{d\Lambda}{\Lambda}. \end{aligned}$$

We then define

$$K_d = \frac{2^{1-d} \pi^{-d/2}}{\Gamma(d/2)} \quad (5.19)$$

and see that the recursion equation Eqn.[5.18] becomes

$$(\beta J)_\lambda = (\beta J) \left[1 + \frac{(1 + \frac{K_d d\Lambda}{\beta J \Lambda})^2}{1 + N \frac{K_d d\Lambda}{\beta J \Lambda}} \right] \left(1 + \frac{d\Lambda}{\Lambda} \right)^{d-2} = (\beta J) \left(1 + (2-N) \frac{K_d d\Lambda}{\beta J \Lambda} + (d-2) \frac{d\Lambda}{\Lambda} \right) \quad (5.20)$$

Now writing $(\beta J)_\lambda - (\beta J) = d(\beta J)$ we arrive at the flow equation

$$d \ln(\beta J) = \left[(d-2) + \frac{K_d}{\beta J} (2-N) \right] d \ln \Lambda \quad (5.21)$$

where the dimension dependent coefficients K_d are tabulated as in Tab.[5.2]

d	1	2	3	4
K_d	$1/\pi$	$1/(2\pi)$	$1/(2\pi^2)$	$1/(8\pi^2)$

Table 5.1: Dimension dependent coefficients for the RG flow for the $O(N)$ nonlinear sigma model

The flow form in Eqn.[5.21] gives a beautiful illustration of the Hohenberg-Mermin-Wagner theorem as the trajectories in dimension two or lower flow the system straight toward the high temperature disordered regime whereas in three or higher dimensions we observe a fixed point at

$$k_B T = \frac{d-2}{K_d(N-2)} J \quad (5.22)$$

which separates high and low temperature phases.

The very special case $d = 2$, $N = 2$ is fixed so that no renormalization appears to occur, but we understand that this is the XY model and that vortices, rather than spin waves, control the renormalization.

5.3 The Easy Plane $O(N)$ Nonlinear Sigma Model

We now want to construct a model which again operates with a dimensionless classical field $n(x) \in \mathbb{R}^N$ which satisfies the non-linear constraint $n^2 = 1$, but we now want to discourage n from employing M of its N sectors. (For our model we have $N = 4$ and $M = 2$.)

To this end we will write $n = (\pi, \sigma) = (\pi_S, \pi_H, \sigma)$ with $\sigma \in \mathbb{R}$, $\pi \in \mathbb{R}^{N-1}$, $\pi_H \in \mathbb{R}^M$ and $\pi_S \in \mathbb{R}^{N-M-1}$, where π_S and σ are ‘soft modes’ and π_H are ‘hard modes’ which we gap to discourage occupation.

The (dimensionless) action functional we employ is now

$$S[n] = \frac{\beta J a^{2-d}}{2} \int_a d^d x \left\{ (\nabla n)^2 + \frac{\Delta}{a^2} \pi_H^2 \right\} \quad (5.23)$$

where Δ is a dimensionless anisotropy parameter. We refer to the model as the *easy-plane* (classical) nonlinear sigma model.

The nonlinear constraint is enforced within the partition function Eqn.[5.6].

For the most part the renormalization calculation proceeds in the same vein as in the case we considered before with $\Delta = 0$. The only real source of complications is that we now have two kinds of propagators, one for hard and one for soft modes.

The hard and soft propagators are given by

$$G_0^H(x_1 - x_2) = \int^{\Lambda} \frac{d^d k}{(2\pi)^d} e^{i(x_1 - x_2)k} \frac{a^{d-2}}{\beta J} \frac{1}{k^2 + \frac{\Delta}{a^2}} \quad (5.24a)$$

$$G_0^S(x_1 - x_2) = \int^{\Lambda} \frac{d^d k}{(2\pi)^d} e^{i(x_1 - x_2)k} \frac{a^{d-2}}{\beta J} \frac{1}{k^2}. \quad (5.24b)$$

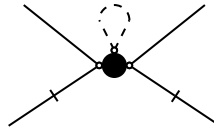
The diagrams that gave rise to the renormalization of kinetic energy Eqn.[5.16a] do not couple hard and soft modes so we can immediately infer

$$(\beta J a^{2-d})_{\lambda} = (\beta J a^{2-d}) [1 + \eta_H] \zeta_H^2 \lambda^{d-2} \quad (5.25a)$$

$$(\beta J a^{2-d})_{\lambda} = (\beta J a^{2-d}) [1 + \eta_S] \zeta_S^2 \lambda^{d-2} \quad (5.25b)$$

where $\eta_H = G_0^H(0)$, $\eta_S = G_0^S(0)$ and ζ_H, ζ_S enforce the normalization of n for the hard and soft sectors.

The renormalization of four legged terms in Eqn.[5.16b] contains one diagram which couples hard and soft modes, namely



because the closed loop is tracing over all $N - 1$ sectors of π . The resulting recursion equation

can be applied to either hard or soft modes and will give the same result, this statement is a corollary of the fact that we need only consider the renormalization of βJ , π and Δ in order to get a consistent theory, a result proven by Amit *et al*[87] when considering models of this form. The arguments they use are much more complex than anything we will attempt, suffice it to say that a very careful reading of their work will produce the flow equations we are about to present.

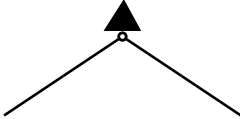
The easy plane analogue of Eqn.[5.16b], which we decide to use to renormalize soft modes, is then seen to be

$$(\beta J a^{2-d})_\lambda = (\beta J a^{2-d}) [1 + \eta_S + (N - M - 1)\eta_S + M\eta_H] \zeta_S^4 \lambda^{d-2} \quad (5.25c)$$

We still need to account for the presence in the action of the mass term $\frac{\Delta}{a^2} \pi_H^2$. To this end we introduce a new member to our vertex set

$$\beta J \Delta a^{-d} \Rightarrow \blacktriangle$$

The contribution to the action is from the diagram



As this diagram is topologically equivalent to that produced by the UV density term they must necessarily be renormalized in tandem, the relevant diagrammatic equation is thus



We need to remember that the triangular vertex is only present when we are renormalizing hard modes. The recursion we arrive at is

$$(\beta J \Delta a^{-d})_\lambda - \rho_\lambda^{(H)} = \left[(\beta J \Delta a^{-d}) - \rho + (\beta J a^{2-d}) \nabla^2 G_+^H(x)|_{x \rightarrow 0} \right] \zeta_H^2 \lambda^d,$$

the superscript on the renormalized UV density is to remind us that this equation renormalizes hard legs only.

The renormalization of the $\rho^{(H)}$ term is trivial:

$$\rho_\lambda^{(H)} = \left[\rho - \int_{\Lambda/\lambda}^\Lambda \frac{d^d k}{(2\pi)^d} \cdot 1 \right] \zeta_H^2 \lambda^d,$$

and we can calculate the derivatives of the hard-fast propagator

$$\nabla^2 G_+^H(x)|_{x \rightarrow 0} = \int_{\Lambda/\lambda}^\Lambda \frac{d^d k}{(2\pi)^d} \frac{a^{d-2}}{\beta J} \frac{k^2}{k^2 + \frac{\Delta}{a^2}} = \frac{1}{\beta J a^{2-d}} \int_{\Lambda/\lambda}^\Lambda \frac{d^d k}{(2\pi)^d} \cdot 1 - \frac{\Delta}{a^2} \eta_H$$

so things cancel out nicely, and what remains is the recursion equation

$$(\beta J \Delta a^{-d})_\lambda = (\beta J \Delta a^{-d}) [1 - \eta_H] \zeta_H^2 \lambda^d \quad (5.25d)$$

The recursion equations we have found in Eqn.[5.25] can then be tidied up a little and brought into the form

$$(\beta J)_\lambda = (\beta J) [1 + \eta_H] \zeta_H^2 \lambda^{d-2} \quad (5.26a)$$

$$(\beta J)_\lambda = (\beta J) [1 + \eta_S] \zeta_S^2 \lambda^{d-2} \quad (5.26b)$$

$$(\beta J)_\lambda = (\beta J) [1 + (N - M)\eta_S + M\eta_H] \zeta_S^4 \lambda^{d-2} \quad (5.26c)$$

$$(\beta J \Delta)_\lambda = (\beta J \Delta) [1 - \eta_H] \zeta_H^2 \lambda^d \quad (5.26d)$$

We can eliminate the field rescaling parameters ζ_H, ζ_S by demanding that the first three of these recursion equations are consistent. Some algebra then tells us that

$$\zeta_S^2 = \frac{(1 + \eta_S)}{(1 + (N - M)\eta_S + M\eta_H)} \quad (5.27a)$$

$$\zeta_H^2 = \frac{(1 + \eta_S)^2}{(1 + \eta_H)(1 + (N - M)\eta_S + M\eta_H)}, \quad (5.27b)$$

so that the system Eqn.[5.26a] reduces to

$$(\beta J)_\lambda = (\beta J)\lambda^{d-2} \frac{(1 + \eta_S)^2}{(1 + (N - M)\eta_S + M\eta_H)} \quad (5.28a)$$

$$(\beta J\Delta)_\lambda = (\beta J\Delta)\lambda^d \frac{(1 - \eta_H)(1 + \eta_S)^2}{(1 + \eta_H)(1 + (N - M)\eta_S + M\eta_H)}. \quad (5.28b)$$

A priori, due to the discussion in the last section, we know that in the limit $\lambda \rightarrow 1 + d\Lambda/\Lambda$ the Hartree terms will be infinitesimals $\eta \sim d\Lambda/\Lambda$ so writing $(\beta J)_\lambda = (\beta J) + d(\beta J)$ and $(\beta J\Delta)_\lambda = (\beta J\Delta) + d(\beta J)$ we see that in this limit Eqn.[5.28] becomes

$$d(\beta J) + (\beta J) = (\beta J) \left(1 + (d - 2) \frac{d\Lambda}{\Lambda} \right) (1 - (N - M - 2)\eta_S - M\eta_H) \quad (5.29a)$$

$$d(\beta J\Delta) + (\beta J\Delta) = (\beta J\Delta) \left(1 + d \frac{d\Lambda}{\Lambda} \right) (1 - (N - M - 2)\eta_S - (M + 2)\eta_H) \quad (5.29b)$$

which we can simplify even further to

$$d \ln(\beta J) = (d - 2)d \ln \Lambda - (N - M - 2)\eta_S - M\eta_H \quad (5.30a)$$

$$d \ln \Delta = 2d \ln \Lambda - 2\eta_H. \quad (5.30b)$$

Finally we get around to evaluating the η_H and η_S :

$$\eta_H = \frac{K_d}{\beta J} \frac{1}{1 + \Delta} \frac{d\Lambda}{\Lambda} \quad (5.31a)$$

$$\eta_S = \frac{K_d}{\beta J} \frac{d\Lambda}{\Lambda}, \quad (5.31b)$$

and arrive at the flow equations

$$d \ln(\beta J) = \left[(d-2) - \left((N-M-2) + \frac{M}{1+\Delta} \right) \frac{K_d}{\beta J} \right] d \ln \Lambda \quad (5.32a)$$

$$d \ln \Delta = 2 \left[1 - \frac{1}{1+\Delta} \frac{K_d}{\beta J} \right] d \ln \Lambda \quad (5.32b)$$

The $N = 3$, $M = 1$ version of this flow form was derived by Nelson and Pelcovitz[88]. I am reliably informed that the general case can be found in Amit *et al*[87], although their style is very different to what is presented here.

We will look into the behaviour of this *RG* flow in the next chapter.

5.4 The Quantum Easy Plane Nonlinear Sigma Model

Just for the sake of completeness we will now consider what happens if we were to include quantum fluctuations within the easy plane nonlinear sigma model.

The appropriate action would then be

$$S[n] = \frac{J a^{2-d}}{2\hbar} \int^{b\hbar} d\tau \int_a d^d r \left\{ \frac{1}{c^2} (\partial_\tau n)^2 + (\nabla n)^2 + \frac{\Delta}{a^2} \pi_H^2 \right\}, \quad (5.33)$$

where c is an appropriate velocity scale (something like the sound speed of phonons).

To simplify notation we will write

$$\frac{1}{c^2} (\partial_\tau n)^2 + (\nabla n)^2 = \partial_\mu n \cdot \partial^\mu n \quad (5.34)$$

with Euclidean signature and Einstein summation convention implied over Greek letters.

The *RG* flow equations can be derived in exactly the same manner as in the classical case with a few substitutions. First of all we need to adapt our edge and vertex sets slightly to account for the new notation,

$$\pi_i^\lambda \Rightarrow \text{---} \nearrow$$

$$\partial_\mu \pi_i^\lambda \Rightarrow \text{---} \nearrow \text{---}$$

$$\pi_i^+ \Rightarrow \text{---} \nearrow$$

$$\partial_\mu \pi_i^+ \Rightarrow \text{---} \nearrow \text{---}$$

$$Ja^{2-d}/\hbar \Rightarrow \bullet$$

$$\rho \Rightarrow \blacksquare$$

$$J\Delta a^{-d}/\hbar \Rightarrow \blacktriangle$$

In terms of Fourier components, the field π and its fast and slow components, π^+ and π^λ , are now given by

$$\pi(\tau, r) = \int^\Lambda \frac{d^d k}{(2\pi)^d} \sum_\omega \frac{e^{i(k \cdot r + \omega \tau)}}{\beta \hbar} \pi(\omega, k) \quad (5.35a)$$

$$\pi^\lambda(\tau, r) = \int^{\Lambda/\lambda} \frac{d^d k}{(2\pi)^d} \sum_\omega \frac{e^{i(k \cdot r + \omega \tau)}}{\beta \hbar} \pi(\omega, k) \quad (5.35b)$$

$$\pi^+(\tau, r) = \int_{\Lambda/\lambda}^\Lambda \frac{d^d k}{(2\pi)^d} \sum_\omega \frac{e^{i(k \cdot r + \omega \tau)}}{\beta \hbar} \pi(\omega, k) \quad (5.35c)$$

where ω are the bosonic Matsubara frequencies, $\omega \in \frac{2\pi}{\beta \hbar} \mathbb{Z}$.

The hard and soft propagators are now

$$G_0^H(\tau, r) = \int^{\Lambda} \frac{d^d k}{(2\pi)^d} \sum_{\omega} \frac{e^{i(k \cdot r + \omega \tau)}}{\beta \hbar} \frac{\hbar}{J a^{2-d}} \frac{1}{k^2 + \omega^2/c^2 + \Delta/a^2} \quad (5.36a)$$

$$G_0^S(\tau, r) = \int^{\Lambda} \frac{d^d k}{(2\pi)^d} \sum_{\omega} \frac{e^{i(k \cdot r + \omega \tau)}}{\beta \hbar} \frac{\hbar}{J a^{2-d}} \frac{1}{k^2 + \omega^2/c^2} \quad (5.36b)$$

Other than these redefinitions, the diagrammatic expressions above remain valid so we can just translate the recursion equations given in Eqn.[5.28], so we have

$$J_{\lambda} = J \lambda^{d-2} \frac{(1 + \eta_S)^2}{(1 + (N - M)\eta_S + M\eta_H)} \quad (5.37a)$$

$$(J\Delta)_{\lambda} = (J\Delta) \lambda^d \frac{(1 - \eta_H)(1 + \eta_S)^2}{(1 + \eta_H)(1 + (N - M)\eta_S + M\eta_H)}, \quad (5.37b)$$

but now the Hartree terms have different meanings.

We'll calculate the hard η and infer the soft version from that. By definition, in the limit $\lambda \rightarrow 1 - d \ln \Lambda$, we have

$$\begin{aligned} \eta_H &= \int_{\Lambda - d\Lambda}^{\Lambda} \frac{d^d k}{(2\pi)^d} \sum_{\omega} \frac{1}{\beta \hbar} \frac{\hbar}{J a^{2-d}} \frac{1}{k^2 + \omega^2/c^2 + \Delta/a^2} \\ &= \int_{\Lambda - d\Lambda}^{\Lambda} \frac{d^d k}{(2\pi)^d} \sum_{n=-\infty}^{\infty} \frac{a^{d-2}}{k^2 + \Delta/a^2 + \left(\frac{2\pi}{\beta \hbar c}\right)^2 n^2}. \end{aligned}$$

We make use of the identity

$$\sum_{n=-\infty}^{\infty} \frac{1}{a + bn^2} \frac{\pi}{\sqrt{ab}} \coth\left(\pi \sqrt{\frac{a}{b}}\right),$$

and the fact that the surface area of a $(d - 1)$ -dimensional ball of radius k is

$$2 \frac{\pi^{d/2}}{\Gamma(d/2)} k^{d-1} = (2\pi)^d k^{d-1} K_d, \quad (5.38)$$

so that we can write

$$\begin{aligned}
\eta_H &= \frac{1}{\beta J} \int_{\Lambda/\lambda}^{\Lambda} \frac{dk}{(2\pi)^d} \frac{2\pi^{d/2} k^{d-1}}{\Gamma(d/2)} \frac{a^{d-2}\pi}{\sqrt{\left(\frac{2\pi}{\beta\hbar c}\right)^2 \left(k^2 + \frac{\Delta}{a^2}\right)}} \coth \left(\pi \sqrt{\frac{\left(k^2 + \frac{\Delta}{a^2}\right)}{\left(\frac{2\pi}{\beta\hbar c}\right)^2}} \right) \\
&= \frac{\hbar c}{J} \frac{2^{-d}\pi^{-d/2}}{\Gamma(d/2)} \frac{a^{d-2}\Lambda^{d-1}}{\sqrt{\Lambda^2 + \frac{\Delta}{a^2}}} \coth \left(\frac{1}{2}\beta\hbar c\sqrt{\Lambda^2 + \frac{\Delta}{a^2}} \right) d\Lambda
\end{aligned}$$

Since $a = 1/\Lambda$, if we define the dimensionless quantity

$$u = \frac{1}{2}\beta\hbar\frac{c}{a}, \quad (5.39)$$

this becomes

$$\eta_H = \frac{K_d}{\beta J} \frac{u}{\sqrt{1+\Delta}} \coth(u\sqrt{1+\Delta}) \frac{d\Lambda}{\Lambda} \quad (5.40a)$$

$$\eta_S = \frac{K_d}{\beta J} u \coth(u) \frac{d\Lambda}{\Lambda} \quad (5.40b)$$

Finally we have the flow equations

$$d \ln J = \left[(d-2) - (N-M-2) \frac{K_d}{\beta J} u \coth(u) - M \frac{K_d}{\beta J} \frac{u}{\sqrt{1+\Delta}} \coth(u\sqrt{1+\Delta}) \right] d \ln \Lambda \quad (5.41a)$$

$$d \ln \Delta = \left[2 - 2 \frac{K_d}{\beta J} \frac{u}{\sqrt{1+\Delta}} \coth(u\sqrt{1+\Delta}) \right] d \ln \Lambda \quad (5.41b)$$

None of β , \hbar or c have an explicit renormalization to one loop so we can see that u renormalizes trivially

$$d \ln u = d \ln \Lambda. \quad (5.42)$$

Following tradition let us now call $d \ln \Lambda = d\ell$. Now we can write

$$d \ln J = \left[(d-2) - \frac{K_d u}{\beta J} \left((N-M-2) \coth u + M \frac{\coth(u\sqrt{1+\Delta})}{\sqrt{1+\Delta}} \right) \right] d\ell \quad (5.43a)$$

$$d \ln \Delta = 2 \left[1 - \frac{K_d u \coth(u\sqrt{1+\Delta})}{\beta J \sqrt{1+\Delta}} \right] d\ell \quad (5.43b)$$

$$d \ln u = d\ell \quad (5.43c)$$

The dimensionless quantities which jump out at us are

$$t = \frac{1}{\beta J} \quad (5.44a)$$

$$q = \frac{u}{\beta J} = \frac{\hbar c/a}{2J}. \quad (5.44b)$$

t plays the role of the temperature or, equivalently, the inverse stiffness in the high temperature classical limit. q plays a similar role in the low temperature quantum limit.

In terms of these new quantities we have the flow equations

$$\frac{d \ln t}{d\ell} = (2-d) + K_d q \left[(N-M-2) \coth(q/t) + M \frac{\coth(q/t\sqrt{1+\Delta})}{\sqrt{1+\Delta}} \right] \quad (5.45a)$$

$$\frac{d \ln q}{d\ell} = (1-d) + K_d q \left[(N-M-2) \coth(q/t) + M \frac{\coth(q/t\sqrt{1+\Delta})}{\sqrt{1+\Delta}} \right] \quad (5.45b)$$

$$\frac{d \ln \Delta}{d\ell} = 2 - 2K_d q \frac{\coth(q/t\sqrt{1+\Delta})}{\sqrt{1+\Delta}} \quad (5.45c)$$

Using our knowledge that for small x

$$\coth x = \frac{1}{x} + \frac{x}{3} - \frac{x^3}{45} + \dots \quad (5.46)$$

we can see that in the limit $q/t = u \rightarrow 0$, which we call the classical limit, we find

$$\frac{d \ln t}{d \ell} = (2 - d) + K_{dt} \left[N - M - 2 + \frac{M}{1 + \Delta} \right] \quad (5.47a)$$

$$\frac{d \ln \Delta}{d \ell} = 2 - \frac{2K_{dt}}{1 + \Delta} \quad (5.47b)$$

The renormalization of the quantum stiffness parameter q is interesting, since from

$$\frac{d \ln q}{d \ell} = (1 - d) + K_{dt} \left[N - M - 2 + \frac{M}{1 + \Delta} \right] \quad (5.47c)$$

we see that for $d = 1$ the flow of q is always toward infinity. This is an aside however, the point is that we have regained the flow equations for the classical easy plane nonlinear sigma model Eqn.[5.32] with t taking the place of $1/(\beta J)$

If we remove the anisotropy in Eqn.[5.45] we get to the the RG flow of the quantum nonlinear sigma model with no anisotropies as calculated by Chakravarty, Halperin and Nelson [89].

CHAPTER 6

DEPLETION OF ORDER DUE TO ENHANCED SYMMETRY

6.1 Motivation

The key feature of our stripe model was the existence of a high symmetry point at which quasi-long-ranged order ceases to be possible.

The mathematical origin of this effect is very clear: The Berezinskii-Kosterlitz-Thouless transition relies upon the propagation of topological excitations in an $O(2)$ symmetric field. In the limit where the two $O(2)$ symmetric fields become a single $O(4)$ symmetric field such topological excitations cease to be possible. Therefore at this point spin wave physics reasserts itself and the phase transition is no longer possible, and as such the transition temperature must be driven to zero.

The mathematical truth of this is beyond doubt, however questions still remain as to what is physically going on here.

1. It would be nice to know the mechanism by which spin wave physics takes over from vortex physics. Presumably the vortices themselves get turned into spin wave excitations.
2. If the vortices are becoming like spin waves, is this something that could be probed experimentally?

3. What measurable effect is happening to the vortices and impact has this upon the Berezinskii-Kosterlitz-Thouless temperature?

The action we are faced with for the model at hand is an easy plane nonlinear sigma model in $2 + 1$ dimensions with symmetry breaking $O(4) \rightarrow O(2) \times O(2)$ but we could just as easily consider the more general symmetry breaking $O(M + 2) \rightarrow O(M) \times O(2)$. This extension is not only interesting from a purely mathematical point of view. For $M = 1$ this is the continuum limit of the easy-plane Heisenberg spin system

$$H = -J \sum_{\langle ij \rangle} s_i s_j + J \frac{\Delta}{2} \sum_i (S_i^z)^2 \quad (6.1)$$

and could also be seen in $SO(5)$ theories. In all cases there is an important topological aspect that we shall now attempt to address.

6.2 Modified Berezinskii-Kosterlitz-Thouless Analysis

6.2.1 A Variational Ansatz

To answer the question of how vortices can become spin waves, we consider a single vortex configuration within the action

$$S[n] = \frac{\beta J}{2} \int_a \mathbb{d}^d r \left\{ (\nabla n)^2 + \frac{\Delta}{a^2} n \cdot \begin{pmatrix} 0 & 0 & 0 \\ 0 & 1_{M \times M} & 0 \\ 0 & 0 & 0 \end{pmatrix} n \right\}. \quad (6.2)$$

For large Δ the system would clearly prefer to avoid the hard modes and so XY-type physics ought to be dominant.

A vortex with unit topological charge in this system would look like

$$n = (\cos \theta, 0_M, \sin \theta). \quad (6.3)$$

The contribution to the action of such a vortex would be

$$S_{\odot} = \pi\beta J \ln(R/a) + S_{\text{core}}. \quad (6.4)$$

Let us now consider a new configuration, which I attempt to illustrate in Fig.[6.2.1], which looks like a normal vortex at length scales greater than some core radius ξ_0 but below this radius points into the hard plane. One would expect such a configuration to have a smaller contribution to the action because it can avoid producing a singularity at the centre of the vortex core.

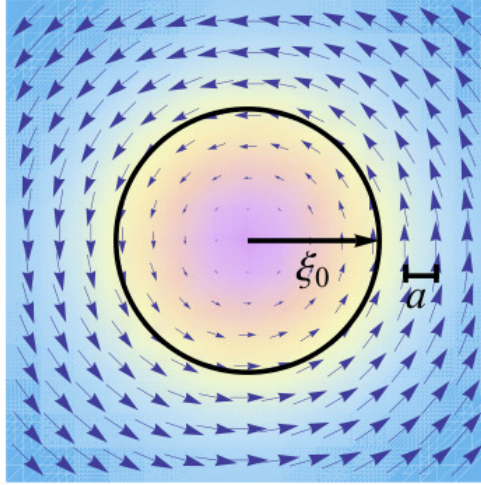


Figure 6.1: Softened vortex near a high symmetry point

The contribution to the action due to such a *softened* vortex is easily seen to be approximately

$$\tilde{S}_{\odot} = \pi\beta J \ln(R/\xi_0) + \beta J \frac{\Delta}{2a^2} \pi \xi_0^2. \quad (6.5)$$

Of course this is a slight oversimplification because we are neglecting edge effects; the field won't just switch from in plane to out-of-plane but should do so gradually. However the

contribution of these edge effects would be negligible so we'll pretend they aren't happening.

Minimizing the action contribution we find the optimal core size gives

$$\pi\beta J \left(-\frac{1}{\xi_0} + \frac{\Delta}{a^2}\xi_0 \right) = 0 \quad \Rightarrow \quad \xi_0 = \frac{a}{\sqrt{\Delta}} \quad (6.6)$$

We therefore predict that the core size diverges as $1/\sqrt{\Delta}$ as the high symmetry point is approached.

In order to see how the BKT temperature is affected we need to adapt the standard treatment to allow for core sizes that are not simply the lattice scale. Before doing this let us take another look at the BKT argument.

6.2.2 Another Look at the BKT Argument

We wish to adapt our vortex argument from our discussion of The Vortex Plasma to account for larger vortex cores. Although it would not be too hard to go back and adapt our previous arguments¹ we will take the opportunity to get a fresh perspective on the vortex unbinding transition and remind ourselves of what is going on.

Once again, our system is described by a Hamiltonian

$$H = \frac{J}{2} \int d^2x [\nabla \mathbf{n}(x)]^2 \quad (6.7a)$$

$$= \frac{J}{2} \int d^2x [\nabla \phi(x)]^2 \quad (6.7b)$$

and again a generic vortex configuration is one in which

$$\phi(r, \theta) = \phi(r, 0) + k\theta$$

so that the winding number k is such that $\phi(r, 2\pi) - \phi(r, 0) = 2\pi k$.

¹You can try this if you like, it is fairly easy once you know the answer, the way we about to see is just neater.

Earlier we were loosely following the arguments given by Kosterlitz and Thouless, we now follow instead the argument given in the excellent book of Chaikin and Lubensky[90].

We are interested in stationary configurations ($\nabla^2\phi = 0$) with winding number k ($\oint d\phi = 2\pi k$). If we introduce the velocity field of the vortex \mathbf{u}_v we see that

$$\mathbf{u}_v = \frac{k}{r}\mathbf{e}_\theta. \quad (6.8)$$

The energy due to a single vortex comes in two flavours, a contribution from the core of the vortex E_{core} which can be estimated as some condensation energy density multiplied by the area of the vortex core, $E_{\text{core}} = f_{\text{cond}}\pi a^2$, where a is the vortex radius, and an elastic contribution E_{el} which we can calculate directly

$$E_{\text{el}} = \frac{J}{2} \int d^2x \left[\frac{k}{r}\mathbf{e}_\theta \right]^2 = \pi k^2 \ln(R/a) \quad (6.9)$$

Similarly, the elastic energy of a system containing two vortices separated by a distance r is found to be

$$E_{\text{el2}}^{(2)} = \pi J(k_1 + k_2)^2 \ln(R/a) + 2\pi Jk_1k_2 \ln(a/r) \quad (6.10)$$

The important point here is that terms which would be divergent in the thermodynamic limit cancel if the vortices have opposite topological charge.

Perhaps unsurprisingly, calculations regarding vortices become simpler if instead of talking about velocity fields we consider vorticity fields. Thinking back to elementary fluid mechanics, we define the vorticity

$$\boldsymbol{\omega} = \nabla \times \mathbf{u}_v = 2\pi\mathbf{e}_z \sum_i k_i \delta(\mathbf{x} - \mathbf{x}_i) = 2\pi\mathbf{e}_z \rho_v \quad (6.11)$$

where ρ_v is the density of the vortices which are situated at x_i .

Taking the curl of the vorticity gives $\nabla \times \boldsymbol{\omega} = -\nabla^2 \mathbf{u}_v$, so if the Green's function of a two dimensional Laplacian is called $G(\mathbf{x})$ we have

$$\mathbf{u}_v(\mathbf{x}) = \nabla_{\mathbf{x}} \times \int d^2y G(\mathbf{x} - \mathbf{y}) \boldsymbol{\omega}(\mathbf{y}). \quad (6.12)$$

Moving now into momentum space, we have

$$\mathbf{u}_v(\mathbf{p}) = \frac{1}{p^2} i\mathbf{p} \times \boldsymbol{\omega}(\mathbf{p}) \quad (6.13)$$

We can, quite generally, split the overall velocity field, $\mathbf{u} = \nabla\phi$, into an incompressible part \mathbf{u}_v ($\nabla \cdot \mathbf{u}_v = 0$), due to vortices and an irrotational part \mathbf{u}_{sw} ($\nabla \times \mathbf{u}_{sw} = 0$) coming from spin waves.

The Hamiltonian, remembering to add in core contributions by hand, can then be written

$$H = \frac{J}{2} \int d^2x u^2(\mathbf{x}) = \frac{J}{2} \int d^2x u_{sw}^2(\mathbf{x}) + \frac{J}{2} \int \frac{d^2p}{(2\pi)^2} \mathbf{u}_v(\mathbf{p}) \cdot \mathbf{u}_v(-\mathbf{p}) + E_{core} \sum_i k_i^2 \quad (6.14a)$$

$$= \frac{J}{2} \int d^2x u_{sw}^2(\mathbf{x}) - \frac{J}{2} \int \frac{d^2p}{(2\pi)^2} \frac{1}{p^2} \boldsymbol{\omega}(p) \cdot \boldsymbol{\omega}(-p) + E_{core} \sum_i k_i^2 \quad (6.14b)$$

Assuming that the field vanishes at infinity, the average velocity must be zero. Now if we perform a global velocity boost $\mathbf{u} \rightarrow \mathbf{u} + \mathbf{v}$, the average velocity should be \mathbf{v} .

We can define a macroscopic stiffness \bar{J} by performing a Galilean boost upon the free energy,

$$F(\mathbf{v}) = F(0) + \frac{\bar{J}}{2} R^2 v^2 \quad (6.15)$$

Actually calculating the free energy we have

$$F(\mathbf{z}) = -\frac{1}{\beta} \ln \text{tr} e^{-\beta H(\mathbf{v})} = -\frac{1}{\beta} \ln \text{tr} e^{-\beta \{H(0) + \frac{\bar{J}}{2} R^2 v^2 + \frac{J}{2} \int d^2x \mathbf{u} \cdot \mathbf{v}\}}, \quad (6.16)$$

which we can write as

$$\begin{aligned}
F(\mathbf{z}) &= F(0) + \frac{J}{2} R^2 v^2 - \frac{1}{\beta} \ln \left\langle e^{-\frac{\beta J}{2} \int \mathrm{d}^2 x \mathbf{u} \cdot \mathbf{v}} \right\rangle \\
&\approx F(0) + \frac{J}{2} R^2 v^2 - \frac{\beta J^2}{2} \int \mathrm{d}^2 x \mathrm{d}^2 y v^i v^j \langle u_i(\mathbf{x}) u_j(\mathbf{y}) \rangle \\
&\approx F(0) + \frac{1}{2} R^2 v^2 \left(J - \beta J^2 \int \mathrm{d}^2 x \langle \mathbf{u}_v(\mathbf{x}) \cdot \mathbf{u}_v(0) \rangle \right)
\end{aligned}$$

Hence to leading order the macroscopic stiffness is given by

$$\begin{aligned}
\bar{J} &= J - \beta J^2 \int \mathrm{d}^2 x \langle \mathbf{u}_v(\mathbf{x}) \cdot \mathbf{u}_v(0) \rangle = J - \beta J^2 \lim_{p \rightarrow 0} \frac{1}{R^2} \langle \mathbf{u}_v(\mathbf{p}) \cdot \mathbf{u}_v(-\mathbf{p}) \rangle \\
&= J - \beta J^2 \lim_{p \rightarrow 0} \frac{1}{p^2} \frac{1}{R^2} \langle \boldsymbol{\omega}(\mathbf{p}) \cdot \boldsymbol{\omega}(-\mathbf{p}) \rangle.
\end{aligned}$$

Let us call the coefficient of βJ^2 in the macroscopic stiffness, U . Expanding the Taylor series and taking $p \rightarrow 0$ limit gives us

$$\begin{aligned}
U &= - \lim_{p \rightarrow 0} \frac{1}{p^2} \frac{1}{R^2} \langle \boldsymbol{\omega}(\mathbf{p}) \cdot \boldsymbol{\omega}(-\mathbf{p}) \rangle = \frac{1}{4R^2} \int \mathrm{d}^2 x \mathrm{d}^2 y \langle \boldsymbol{\omega}(\mathbf{x}) \cdot \boldsymbol{\omega}(\mathbf{y}) \rangle (\mathbf{x} - \mathbf{y})^2 \\
&= \frac{\pi^2}{R^2} \sum_{i,j} (\mathbf{x}_i - \mathbf{x}_j) \langle k_i k_j \rangle.
\end{aligned}$$

The average here only contains winding numbers so as far as the macroscopic stiffness is concerned we only need to average with respect to the (quadratic) Hamiltonian of topological charges

$$H(k) = E_{\text{core}} \sum_i k_i^2 - \frac{J}{2} (2\pi)^2 \sum_{ij} k_i k_j \frac{1}{2\pi} \ln(|\mathbf{x}_i - \mathbf{x}_j|/a) \quad (6.17)$$

If we restrict our attention to neutral configurations of unit topological charge, the average becomes trivial and we have simply

$$\begin{aligned}\langle k_i k_j \rangle &= \frac{-2\mathbb{e}^{2E_{\text{core}} - 2\pi J \ln(|\mathbf{x}_i - \mathbf{x}_j|/a)}}{1 + 2\mathbb{e}^{2E_{\text{core}} + 2\pi J \ln(|\mathbf{x}_i - \mathbf{x}_j|/a)}} \\ &\approx -2\mathbb{e}^{-2\beta E_{\text{core}}} \left(\frac{|\mathbf{x}_i - \mathbf{x}_j|}{a} \right)^{-2\pi\beta J}\end{aligned}$$

which determines the constant U to be

$$U = -2\pi^2 \frac{z^2}{R^2} \sum_{i,j} |\mathbf{x}_i - \mathbf{x}_j|^2 \left(\frac{|\mathbf{x}_i - \mathbf{x}_j|}{a} \right)^{-2\pi\beta J}$$

where $z = \mathbb{e}^{-\beta E_{\text{core}}}$ is the fugacity.

We introduce the microscopic lattice constant a_0 that determines statistically distinct vortices, noting that

$$\sum_i a_0^2 = R^2 \tag{6.18}$$

The key point is that we aren't assuming that the lattice constant is equal to the vortex core size, and this will allow us to consider vortices with a larger core size.

We replace sums with integrals via

$$\sum_i \rightarrow \int \frac{\mathrm{d}^2 x}{a_0^2}, \tag{6.19}$$

so that U becomes

$$U = -2\pi^2 z^2 \frac{1}{a_0^4} \int_a^\infty \mathrm{d}^2 x x^2 \left(\frac{x}{a} \right)^{-2\pi\beta J} = -4\pi^3 z^2 \left(\frac{a}{a_0} \right)^4 \int_a^\infty \frac{\mathrm{d}r}{a} \left(\frac{r}{a} \right)^{3-2\pi\beta J}$$

Now we can write the macroscopic value of the stiffness as

$$\bar{J} = J - \beta J^2 4\pi^3 \left(z \frac{a^2}{a_0^2} \right)^2 \int_a^\infty \frac{\mathrm{d}r}{a} \left(\frac{r}{a} \right)^{3-2\pi\beta J}.$$

To perform the renormalization step, we write

$$\begin{aligned}
(\beta\bar{J}) &= (\beta J) - (\beta J)^2 4\pi^3 \left(z \frac{a^2}{a_0^2} \right)^2 \left\{ \int_a^{ae^\ell} \frac{dr}{a} \left(\frac{r}{a} \right)^{3-2\pi\beta J} - \int_{ae^\ell}^\infty \frac{dr}{a} \left(\frac{r}{a} \right)^{3-2\pi\beta J} \right\} \\
&= (\beta J)_\ell - (\beta J)^2 4\pi^3 \left(z \frac{a^2}{a_0^2} \right)^2 \int_{ae^\ell}^\infty \frac{dr}{a} \left(\frac{r}{a} \right)^{3-2\pi\beta J} \\
&= (\beta J)_\ell - (\beta J)^2 4\pi^3 \left(z \frac{a^2}{a_0^2} \right)^2 e^{(4-2\pi\beta J)\ell} \int_a^\infty \frac{dr}{a} \left(\frac{r}{a} \right)^{3-2\pi\beta J},
\end{aligned}$$

so we immediately get the recursion equations

$$z_\ell = z e^{(2-\pi\beta J)\ell} \quad (6.20a)$$

$$(\beta J)_\ell = (\beta J) - (\beta J)^2 4\pi^3 \left(z \frac{a^2}{a_0^2} \right)^2 \int_1^{e^\ell} dr r^{3-2\pi\beta J}, \quad (6.20b)$$

which in the limit of infinitesimal ℓ become

$$dz = (2 - \pi\beta J) d\ell \quad (6.21a)$$

$$d(\beta J) = -(\beta J)^2 4\pi^3 \left(z \frac{a^2}{a_0^2} \right)^2 d\ell. \quad (6.21b)$$

We have therefore re-derived the RG flow equations for the vortex plasma to account for a separation of length scales.

From our previous discussion (or just by solving the RG equations again) we can see that the BKT transition temperature is given by

$$\frac{1}{\beta_{\text{BKT}} J} = \frac{\pi}{2 + 4\pi \frac{a^2}{a_0^2} e^{-\pi\beta_{\text{BKT}} J}}. \quad (6.22)$$

Inserting the optimal core size from Eqn.[6.6] and writing $x = \pi\beta_{\text{BKT}} J$ we have

$$\frac{4\pi}{\Delta} = (x - 2)e^x \quad (6.23)$$

In the limit $\Delta \rightarrow 0$, to leading order we thus have $x \sim \ln(1/\Delta)$, this gives the small Δ behaviour of the transition temperature to be

$$k_{\text{B}}T_{\text{BKT}} \sim \frac{J}{\ln(1/\Delta)} \quad (6.24)$$

The argument we present here is very simplistic but makes two clear predictions for the behaviour of the system close to the high symmetry point

1. The vortex core size diverges as $1/\sqrt{\Delta}$
2. The BKT transition temperature vanishes as $1/\ln(1/\Delta)$

The analysis we have seen here has been based entirely on the behaviour of the vortices in the system, based on the ansatz of a softening vortex core.

To supplement this analysis in the next section we will inspect the renormalization group flow equations for this system which come from spin wave considerations and will see (perhaps surprisingly) a good agreement.

6.3 Spin Wave Renormalization Analysis

To complement our previous analysis based on interrogating vortices in the high anisotropy regime with an interrogation of the spin wave in the low anisotropy regime.

From our discussion of The Easy Plane $O(N)$ Nonlinear Sigma Model we know the RG flow equations for the temperature and the anisotropy. We now need to analyse this flow.

The flow equations for an easy plane nonlinear sigma model with 2 soft modes and M hard modes in two dimensions are

$$d \ln(\beta J) = \frac{-1}{2\pi\beta J} \frac{M}{1+\Delta} d\ell \quad (6.25a)$$

$$d \ln \Delta = 2 \left[1 - \frac{1}{2\pi\beta J} \frac{1}{1+\Delta} \right] d\ell \quad (6.25b)$$

Taking $2/M$ of Eqn.[6.25a] away from Eqn.[6.25b] we find a conserved quantity

$$\mathrm{d} \ln [\Delta(\beta J)^{-2/M}] = 2\mathrm{d}\ell \quad \Rightarrow \quad \mathrm{d} [\Delta(\beta J)^{-2/M} e^{-2\ell}] = 0. \quad (6.26)$$

To find a second conserved quantity it is most convenient to make a change of variables

$$\begin{aligned} x &= \pi\beta J & \Rightarrow & \quad \mathrm{d} \ln x = \mathrm{d} \ln(\beta J) \\ y &= \Delta(1 + \Delta) & \Rightarrow & \quad \mathrm{d} \ln y = (1 - y)\mathrm{d} \ln \Delta, \end{aligned}$$

then the flow equations become

$$\begin{aligned} \mathrm{d} \ln x &= -\frac{M}{2} \frac{1-y}{x} \mathrm{d}\ell \\ \mathrm{d} \ln y &= \left(2 - \frac{1-y}{x}\right) (1-y) \mathrm{d}\ell. \end{aligned}$$

Dividing the second equation by the first equation we find that

$$\begin{aligned} \mathrm{d} \ln y &= \frac{2}{M} \left(\frac{1-y}{x} - 2 \right) \mathrm{d}x \\ \mathrm{d}(1/y) &= \left(\frac{4}{M} - \frac{2}{M} \frac{1}{x} \right) (1/y) \mathrm{d}x + \frac{2}{M} \frac{\mathrm{d}x}{x} \\ \mathrm{d} \left(\frac{x^{2/M} e^{-\frac{4x}{M}}}{y} \right) &= \frac{2}{M} x^{\frac{2}{M}-1} e^{-\frac{4x}{M}} \mathrm{d}x. \end{aligned}$$

This expression can be pulled into a single differential by making use of the incomplete gamma function

$$\Gamma(s, x) = \int_x^\infty t^{s-1} e^{-t} \mathrm{d}t \quad (6.27a)$$

$$\frac{\mathrm{d}\Gamma(s, x)}{\mathrm{d}x} = -x^{s-1} e^{-x}, \quad (6.27b)$$

or more concisely by using the exponential integral function

$$\mathbb{E}_s(x) = \int_1^\infty t^s e^{-xt} dt \quad (6.28a)$$

$$\mathbb{E}_s(x) = x^{s-1} \Gamma(1-s, x) \quad (6.28b)$$

$$\mathbb{E}_s(x \rightarrow 0) \sim \Gamma(1-s)x^{s-1} + \frac{1}{s-1} - \frac{x}{s-2} + \frac{x^2}{2(s-3)} - \frac{x^3}{6(s-4)} + \dots \quad (6.28c)$$

$$\mathbb{E}_s(x \rightarrow \infty) \sim e^{-x} \left(\frac{1}{x} - \frac{s}{x^2} + \frac{s(s+1)}{x^3} + \dots \right). \quad (6.28d)$$

Then we see that

$$d \left(\frac{x^{\frac{2}{M}} e^{-\frac{4x}{M}}}{y} \right) = -\frac{1}{2} \left(\frac{4}{M} \right)^{1-\frac{2}{M}} \frac{d\Gamma\left(\frac{2}{M}, \frac{4x}{M}\right)}{d\left(\frac{4x}{M}\right)} d \left(\frac{4x}{M} \right),$$

which we write as

$$d \left[x^{\frac{2}{M}} \left(\frac{e^{-\frac{4x}{M}}}{y} + \frac{2}{M} \mathbb{E}_{1-2/M}(4x/M) \right) \right] = 0,$$

leaving us with a new conserved quantity

$$d \left[e^{\frac{2}{M}(\ln(2\pi\beta J) - 2\pi\beta J)} \left(\frac{1}{\Delta} + 1 + \frac{2}{M} e^{4\pi\beta J/M} \mathbb{E}_{1-2/M}(4\pi\beta J/M) \right) \right] = 0 \quad (6.29)$$

Now it is important to remember that the RG flow equations are only valid when $\Delta \ll 1$. When $\Delta \sim 1$ XY physics takes over and we cannot avoid talking about vortices. It thus makes sense to define a scale ℓ^* where $\Delta(\ell^*) = 1$ at which we need to stop the RG and try something else.

Now if we start with bare coupling constants Δ and T and these renormalize at ℓ^* to 1 and $T(\ell^*)$, then if $k_B T(\ell^*) < \frac{\pi}{2} J$ the system should be BKT ordered and if $k_B T(\ell^*) > \frac{\pi}{2} J$ then the system still resides in the easy plane but is disordered.

The conserved quantity

$$X_M(\beta J, \Delta) = e^{\frac{2}{M}(\ln(2\pi\beta J) - 2\pi\beta J)} \left(\frac{1}{\Delta} + 1 + \frac{2}{M} e^{4\pi\beta J/M} \mathbb{E}_{1-2/M}(4\pi\beta J/M) \right) \quad (6.30)$$

obviously does not renormalize so the curve

$$X_M(\beta J, \Delta) = X_M(2/\pi, 1) = X_M^{BKT} \quad (6.31)$$

defines an effective BKT transition temperature as a function of Δ .

X_M^{BKT} is just a number, which for $M = 2$ is about 0.0000876464 but its value is not particularly important to us. What we want to know is how βJ behaves along the BKT curve when Δ is very small. For small Δ , βJ needs to be very big to keep X_M finite. In the limit we can drop any subdominant terms (constants and powers) and just look at

$$X_M(\beta J \rightarrow \infty, \Delta \rightarrow 0) \sim \frac{e^{-\frac{4\pi\beta J}{M}}}{\Delta}. \quad (6.32)$$

Along the BKT curve we then have

$$\ln\left(\frac{1}{\Delta}\right) \sim \frac{4\pi\beta J}{M} + \ln X_M^{BKT}$$

so that

$$k_B T_{BKT} \sim \frac{J}{\ln(1/\Delta)}. \quad (6.33)$$

This confirms the prediction of our variational argument Eqn.[6.24].

It should come as a bit of a shock that the RG flow equations – which are after all blind to topological excitations – give the same prediction as an analysis of the topological excitations themselves. To understand this better we need only look at the scale at which we stop the RG: $\xi^* = a e^{\ell^*}$. If we call the temperature at ℓ^* T^* then due to the conservation

law Eqn.[6.26], we find that

$$\xi^* = \frac{a}{\sqrt{\Delta}} \left(\frac{T^*}{T} \right)^{1/M} \quad (6.34)$$

this gives a correction to our variational treatment of the optimal core size Eqn.[6.6]. For small T the renormalization is very slow so we regain our initial estimate for the increase in the core size near to the high symmetry point. The size of the vortex cores, relative to the lattice scale, is illustrated in Fig.[6.3].

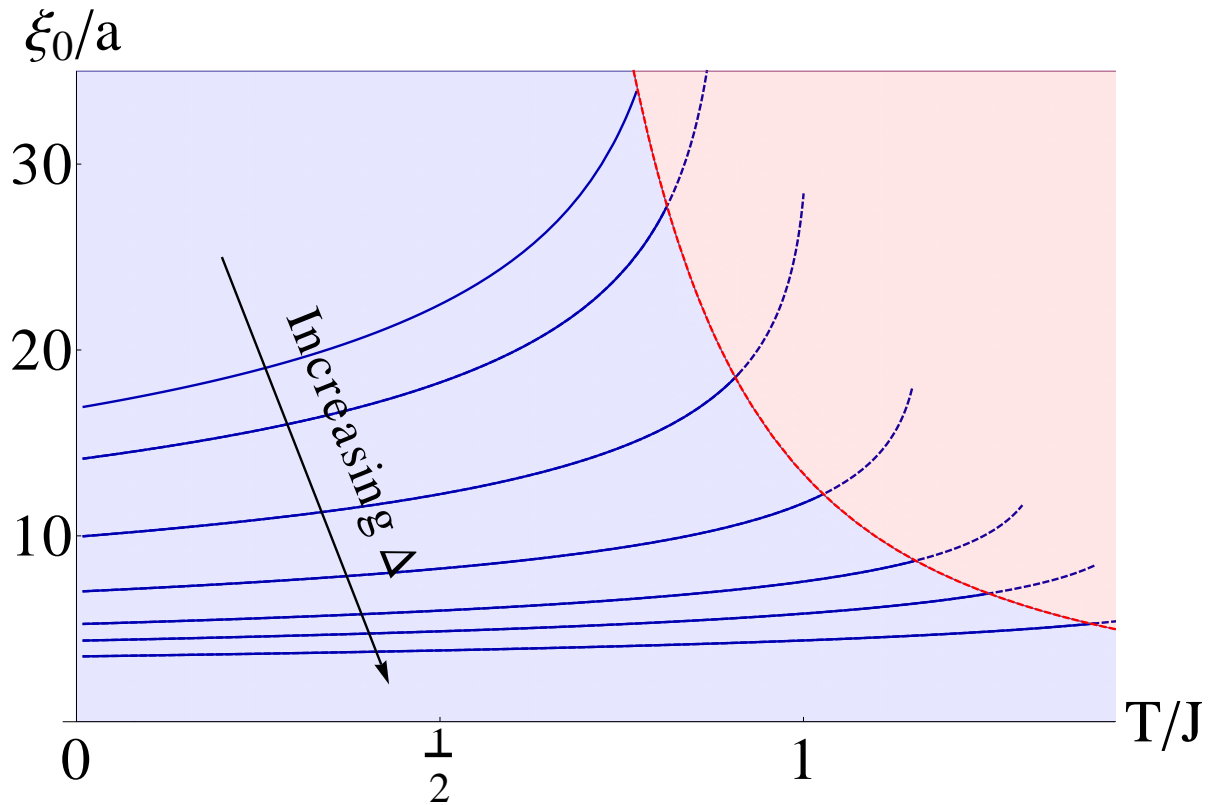


Figure 6.2: Increase in the vortex core size as the high symmetry point is approached. The lines get higher as the anisotropy is decreased. The red line meets the curves at the value of T_{BKT} where $\Delta = 1$ hence giving the size of the vortex cores at BKT vortex unbinding transition.

We are now able to sketch a schematic phase diagram for this kind of system. To do so we simply colour the RG flow according to whether the anisotropy flows to zero or infinity

and if $\Delta \rightarrow \infty$ whether the temperature flows to above or below the bare BKT transition temperature. The result is shown in Fig.[6.3].

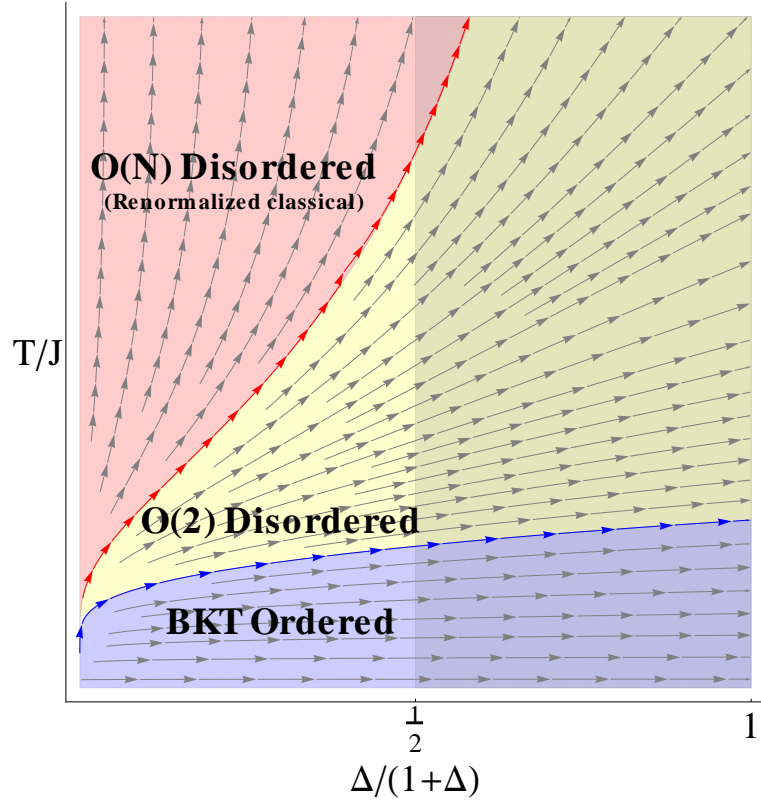


Figure 6.3: Schematic phase diagram in the vicinity of the enhanced symmetry point: The thick blue line indicates the BKT transition temperature varying with the anisotropy. The BKT transition separates the quasi-long range ordered state (blue) from the $O(2)$ disordered state. The red line indicates the crossover temperature between a disordered $O(2)$ state (yellow) which is vortex dominated from a disordered $O(N)$ state (red) which is spin wave dominated.

6.4 Conclusions

In this chapter we have asked what happens to the vortices mediating a BKT transition when the symmetry is enhanced beyond $O(2)$. We have used both spin wave renormalization

group and modified BKT arguments in order to attack both the weak and strong symmetry breaking limits. Somewhat surprisingly, the two approaches have conspired to give the same picture.

At the outset we posed the questions

Q1 By what mechanism does spin wave physics take over from vortex physics?

Q2 Is this something that could be probed experimentally?

Q3 What happens to the BKT transition temperature?

From the analysis we have presented we are now ready to answer these questions.

A1 At the very core of the vortex it is energetically preferable to avoid a divergent cost by exploiting the anisotropy-suppressed sectors, regardless of how great the anisotropy is. For lower symmetry breaking the core-cost versus anisotropy-cost balance encourages the field to exploit the suppressed sector for a wide radius about the core. As the anisotropy vanishes, the core radius diverges as $1/\sqrt{\Delta}$ and the spin-wave character of the full-symmetry field within the core takes over the whole system.

A2 Our physical picture is of enlarged vortex cores supporting an island of suppressed phase. This is actually pre-empted by experimental data on Lanthanum Cuprate – a system with competing antiferromagnetism and superconductivity – which is consistent with finite-size vortices with large spin density wave susceptibilities[91].

A3 The BKT transition temperature vanishes as the anisotropy is decreased. Near to zero anisotropy the BKT transition temperature looks like $T_{\text{BKT}} \sim J/\ln(1/\Delta)$.

CHAPTER 7

CONCLUSIONS

In this thesis we have proposed a setup for an ultracold atom experiment in which dipolar bosons are confined in a highly anisotropic quasi-one dimensional lattice. We have shown that the effective low energy Hamiltonian, which is constructed by bosonizing and weakly coupling a two dimensional array of Luttinger liquids, is identical to that which is used to describe many striped condensed matter systems, including the striped phase of the cuprates and structurally anisotropic materials such as the telephone number compound $\text{Sr}_{14}\text{Cu}_{24}\text{O}_{41}$.

A key feature of our proposed experimental realization of this system is the great degree of control over the parameters of the model. These, we have seen, can be independently tuned by varying the spacing and depth of the confining optical lattice potential and the angle made by the dipoles to the axis of the stripes. By tuning the model parameters to the self dual point where the Luttinger parameter $K = 1/2$ and to where the strength of inter-stripe hopping and interactions are maximally competing, we have seen that we can access a special region of phase space where a superfluid and a longitudinal crystallization phase come into direct competition.

We have then studied the effects of the phase competition upon the phase diagram in the region of the enhanced symmetry point of maximal competition. This is made all the more interesting by the fact that it happens in two dimensions. Where the strengths of the superfluid and crystalline perturbations are equal, the symmetry of the system is enhanced from $O(2) \times O(2)$ to $O(4)$. We have seen that this symmetry enhancement must destroy the Berezinskii-Kosterlitz-Thouless transitions that allow either phase to quasi-long-range order, and reassert the dominance of the Hohenberg-Mermin-Wagner theorem, which forbids long

ranged order in low dimensions. In simple terms this means that at this special point the BKT critical temperature of either phase must vanish to zero.

A simple Ginzburg-Landau treatment of the region around this special high symmetry point suggests the existence of a tetracritical point in the phase diagram such that on either side of the point where both the density wave and superfluid transition temperatures go to zero there are lobes containing *both* phases. We dub the phase with quasi-long range ordering of both density wave and superfluid order a *supersolid* phase for this system.

A more in depth analysis of this system through a nonlinear sigma model with quadratic symmetry breaking gives no indication either way as to the presence of our proposed supersolid phase. This is an avenue for possible future work.

Inspired by this system, we have considered a more general problem of a model in two dimensions with $O(M) \times O(2)$ symmetry that possesses a special point in parameter space where the symmetry is enhanced to $O(M+2)$. Again the transition temperature of the BKT ordered phase in the $O(2)$ sector must vanish at the high symmetry point.

Given that we understand the BKT transition through the unbinding of vortex dipoles, we have tried to understand what happens to the vortices in the $O(2)$ sector of the $O(2) \times O(M)$ model as we approach the enhanced $O(M+2)$ symmetry point.

By modifying the standard Berezinskii-Kosterlitz-Thouless argument we have been able to predict that the size of the vortex cores is divergent as the high symmetry point is approached, with the core size diverging as $1/\sqrt{\Delta}$, where Δ measures the degree of anisotropy. By the same approach we have been able to predict that the BKT transition temperature vanishes as the high symmetry point is approached like $1/\ln(1/\Delta)$.

It is worth pointing out that although the ground state for $\Delta > 0$ is ordered and the ordering temperature is vanishing as $\Delta \rightarrow 0$, $\Delta = 0$ is *not* a quantum critical point. The vanishing of the BKT transition temperature comes about solely due to the sensitivity of the spin wave sector to the high symmetry point through the formation of Goldstone modes.

Further to considering the vortices, we have performed the same calculations but looking at the spin wave sector of the model rather than at the vortices. Surprisingly, we have found perfect agreement in the two methods. This works because both approaches invoke the existence of a length scale separating the physics of the full symmetry of the model from that of the BKT sector.

This patching together of the perturbative spin wave sector and the non-perturbative vortex aspects of the model shows promise as a method for studying other two dimensional models possessing a BKT transition.

LIST OF REFERENCES

- [1] J. M. Fellows, S. T. Carr, C. A. Hooley, and J. Schmalian. Unbinding of giant vortices in states of competing order. *Physical review letters*, 109:155703, Oct 2012.
- [2] J.M. Fellows and S.T. Carr. Superfluid, solid, and supersolid phases of dipolar bosons in a quasi-one-dimensional optical lattice. *Physical Review A*, 84:051602, Nov 2011.
- [3] J.M. Fellows and R.A. Smith. A new two-parameter family of potentials with a tunable ground state. *Journal of Physics A: Mathematical and Theoretical*, 44:335302, 2011.
- [4] J.M. Fellows and R.A. Smith. Factorization solution of a family of quantum nonlinear oscillators. *Journal of Physics A: Mathematical and Theoretical*, 42:335303, 2009.
- [5] P. Bak and V.J. Emery. Theory of the structural phase transformations in tetrathiafulvalene-tetracyanoquinodimethane (TTF-TCNQ). *Physical Review Letters*, 36(16):978–982, 1976.
- [6] P. Bak and S.A. Brazovskiy. Theory of quasi-one-dimensional conductors: Interaction between chains and impurity effects. *Physical Review B*, 17(8):3154, 1978.
- [7] M. Takigawa, N. Motoyama, H. Eisaki, and S. Uchida. Spin and charge dynamics in the hole-doped one-dimensional-chain–ladder composite material $\text{Sr}_{14}\text{Cu}_{24}\text{O}_{41}:\text{Cu}$ NMR/NQR studies. *Physical Review B*, 57(2):1124, 1998.
- [8] S. Carr, J. Quintanilla, and J.J. Betouras. Deconfinement and quantum liquid crystalline states of dipolar fermions in optical lattices. *Condensed Matter Theories*, 24:140, 2009.
- [9] S.T. Carr, J. Quintanilla, and J.J. Betouras. Lifshitz transitions and crystallization of fully-polarised dipolar fermions in an anisotropic 2D lattice. *arXiv preprint arXiv:1004.5276*, 2010.
- [10] J. Quintanilla, S.T. Carr, and J.J. Betouras. Metanematic, smectic, and crystalline phases of dipolar fermions in an optical lattice. *Physical Review A*, 79(3):031601, 2009.

- [11] M.M. Parish, S.K. Baur, E.J. Mueller, and D.A. Huse. Quasi-one-dimensional polarized Fermi superfluids. *Physical review letters*, 99(25):250403, 2007.
- [12] P. Lecheminant and H. Nonne. Exotic quantum criticality in one-dimensional coupled dipolar bosons tubes. *Physical Review B*, 85(19):195121, 2012.
- [13] J.G. Bednorz and K.A. Müller. Possible high t_c superconductivity in the Ba–La–Cu–O system. *Zeitschrift für Physik B Condensed Matter*, 64(2):189–193, 1986.
- [14] J.M. Tranquada, B.J. Sternlieb, J.D. Axe, Y. Nakamura, and S. Uchida. Evidence for stripe correlations of spins and holes in copper oxide superconductors. *Nature*, 375(6532):561–563, 1995.
- [15] J. Orenstein and A.J. Millis. Advances in the physics of high-temperature superconductivity. *Science*, 288(5465):468–474, 2000.
- [16] E. Berg, E. Fradkin, and S.A. Kivelson. Theory of the striped superconductor. *Physical Review B*, 79(6):064515, 2009.
- [17] E. Berg, E. Fradkin, E.A. Kim, S.A. Kivelson, V. Oganesyan, J.M. Tranquada, and S.C. Zhang. Dynamical layer decoupling in a stripe-ordered high- t_c superconductor. *Physical review letters*, 99(12):127003, 2007.
- [18] S.A. Kivelson, I.P. Bindloss, E. Fradkin, V. Oganesyan, J.M. Tranquada, A. Kapitulnik, and C. Howald. How to detect fluctuating stripes in the high-temperature superconductors. *Reviews of Modern Physics*, 75(4):1201, 2003.
- [19] S. Chakravarty, R.B. Laughlin, D.K. Morr, and C. Nayak. Hidden order in the cuprates. *Physical Review B*, 63(9):094503, 2001.
- [20] V.J. Emery, S.A. Kivelson, and O. Zachar. Spin-gap proximity effect mechanism of high-temperature superconductivity. *Physical Review B*, 56(10):6120, 1997.
- [21] M. Vojta. Lattice symmetry breaking in cuprate superconductors: stripes, nematics, and superconductivity. *Advances in Physics*, 58(6):699–820, 2009.

- [22] J. Quintanilla and C. Hooley. The strong-correlations puzzle. *Physics World*, 22(6):32–37, 2009.
- [23] I. Bloch. Ultracold quantum gases in optical lattices. *Nature Physics*, 1(1):23–30, 2005.
- [24] M. Granath, V. Oganesyan, S.A. Kivelson, E. Fradkin, and V.J. Emery. Nodal quasi-particles in stripe ordered superconductors. *Physical review letters*, 87(16):167011, 2001.
- [25] E.W. Carlson, D. Orgad, S.A. Kivelson, and V.J. Emery. Dimensional crossover in quasi-one-dimensional and high- t_c superconductors. *Physical Review B*, 62(5):3422, 2000.
- [26] T. Noda, H. Eisaki, and S. Uchida. Evidence for one-dimensional charge transport in $\text{La}_{2-x-y}\text{Nd}_y\text{Sr}_x\text{CuO}_4$. *Science*, 286(5438):265–268, 1999.
- [27] Y. Nakamura and S. Uchida. Anisotropic transport properties of single-crystal $\text{La}_{2-x}\text{Sr}_x\text{CuO}_4$: Evidence for the dimensional crossover. *Physical Review B*, 47:8369–8372, 1993.
- [28] A. Vishwanath and D. Carpentier. Two-dimensional anisotropic non-Fermi-liquid phase of coupled Luttinger liquids. *Physical Review Letters*, 86(4):676–679, 2001.
- [29] S.T. Carr and A.M. Tsvelik. Superconductivity and charge-density waves in a quasi-one-dimensional spin-gap system. *Physical Review B*, 65(19):195121, 2002.
- [30] A. Jaefari, S. Lal, and E. Fradkin. Charge-density wave and superconductor competition in stripe phases of high-temperature superconductors. *Physical Review B*, 82(14):144531, 2010.
- [31] E. Dagotto and T.M. Rice. Surprises on the way from one-to two-dimensional quantum magnets: the ladder materials. *Science*, 271(5249):618–623, 1996.
- [32] E. Dagotto. Experiments on ladders reveal a complex interplay between a spin-gapped normal state and superconductivity. *Reports on Progress in Physics*, 62(11):1525, 1999.
- [33] R.P. Feynman. Simulating physics with computers. *International journal of theoretical physics*, 21(6):467–488, 1982.

- [34] K.B. Davis, M.O. Mewes, M.R. Andrews, N.J. Van Druten, D.S. Durfee, D.M. Kurn, and W. Ketterle. Bose-Einstein condensation in a gas of sodium atoms. *Physical Review Letters*, 75(22):3969–3973, 1995.
- [35] M.H. Anderson, J.R. Ensher, M.R. Matthews, C.E. Wieman, and E.A. Cornell. Observation of Bose-Einstein condensation in a dilute atomic vapor. *Science*, 269(5221):198–201, 1995.
- [36] D. Jaksch, C. Bruder, J.I. Cirac, C.W. Gardiner, and P. Zoller. Cold bosonic atoms in optical lattices. *Physical Review Letters*, 81(15):3108–3111, 1998.
- [37] I. Bloch. Quantum gases in optical lattices. *Physics World*, 17(4):25–29, 2004.
- [38] M. Greiner, O. Mandel, T. Esslinger, T.W. Hänsch, I. Bloch, et al. Quantum phase transition from a superfluid to a Mott insulator in a gas of ultracold atoms. *Nature*, 415(6867):39–44, 2002.
- [39] L. Sanchez-Palencia and M. Lewenstein. Disordered quantum gases under control. *Nature Physics*, 6(2):87–95, 2010.
- [40] J. Singleton and C. Mielke. Quasi-two-dimensional organic superconductors: a review. *Contemporary Physics*, 43(2):63–96, 2002.
- [41] B.J. Powell and R.H. McKenzie. Strong electronic correlations in superconducting organic charge transfer salts. *Journal of Physics: Condensed Matter*, 18:R827, 2006.
- [42] H. Shishido, T. Shibauchi, K. Yasu, T. Kato, H. Kontani, T. Terashima, and Y. Matsuda. Tuning the dimensionality of the heavy fermion compound CeIn₃. *Science*, 327(5968):980–983, 2010.
- [43] P. Coleman. The lowdown on heavy fermions. *Science*, 327(5968):969–970, 2010.
- [44] S.C. Zhang. A unified theory based on $so(5)$ symmetry of superconductivity and anti-ferromagnetism. *Science*, 275(5303):1089, 1997.

- [45] E. Demler, W. Hanke, and S.C. Zhang. $so(5)$ theory of antiferromagnetism and superconductivity. *Reviews of modern physics*, 76(3):909, 2004.
- [46] S. Tomonaga. Remarks on Bloch’s method of sound waves applied to many-fermion problems. *Progress of Theoretical Physics*, 5:544–569, 1950.
- [47] J.M. Luttinger. An exactly soluble model of a many-fermion system. *Journal of Mathematical Physics*, 4:1154, 1963.
- [48] A. Luther and I. Peschel. Single-particle states, Kohn anomaly, and pairing fluctuations in one dimension. *Physical Review B*, 9(7):2911, 1974.
- [49] D.C. Mattis. New wave-operator identity applied to the study of persistent currents in 1D. *Journal of Mathematical Physics*, 15(5), 1974.
- [50] J. Von Delft and H. Schoeller. Bosonization for beginners—re-fermionization for experts. *Arxiv preprint cond-mat/9805275*, 1998.
- [51] F.D.M. Haldane. Effective harmonic-fluid approach to low-energy properties of one-dimensional quantum fluids. *Physical Review Letters*, 47(25):1840–1843, 1981.
- [52] M.A. Cazalilla. Bosonizing one-dimensional cold atomic gases. *Journal of Physics B: Atomic, Molecular and Optical Physics*, 37:S1, 2004.
- [53] T. Giamarchi. *Quantum physics in one dimension*, volume 121. Oxford University Press, 2004.
- [54] A. Grishin, I.V. Yurkevich, and I.V. Lerner. Functional integral bosonization for an impurity in a Luttinger liquid. *Physical Review B*, 69(16):165108, 2004.
- [55] V.N. Popov. *Functional integrals and collective excitations*. Cambridge Univ Pr, 1991.
- [56] V.N. Popov and J. Niederle. *Functional integrals in quantum field theory and statistical physics*, volume 8. Kluwer Academic Print on Demand, 2001.

- [57] A. Altland and B. Simons. *Condensed matter field theory*. Cambridge Univ Press, 2006.
- [58] H. Kleinert. *Path integrals in quantum mechanics, statistics, polymer physics, and financial markets*. World Scientific Pub Co Inc, 2009.
- [59] A. Barone, W.J. Johnson, and R. Vaglio. Current flow in large Josephson junctions. *Journal of Applied Physics*, 46(8):3628–3632, 1975.
- [60] O.M. Braun and Y.S. Kivshar. Nonlinear dynamics of the Frenkel–Kontorova model. *Physics Reports*, 306(1):1–108, 1998.
- [61] M.J. Ablowitz, D.J. Kaup, A.C. Newell, and H. Segur. Method for solving the sine-Gordon equation. *Physical Review Letters*, 30(25):1262–1264, 1973.
- [62] S. Coleman. Quantum sine-Gordon equation as the massive Thirring model. *Physical Review D*, 11(8):2088, 1975.
- [63] H. Bergknoff and H.B. Thacker. Method for solving the massive Thirring model. *Physical Review Letters*, 42(3):135–138, 1979.
- [64] A.B. Zamolodchikov. Exact two-particle S matrix of quantum solitons of the sine-Gordon model. *JETP Lett*, 25(10), 1977.
- [65] V.E. Korepin. Direct calculation of the S matrix in the massive Thirring model. *Theoretical and Mathematical Physics*, 41(2):953–967, 1979.
- [66] S. Lukyanov and A. Zamolodchikov. Exact expectation values of local fields in the quantum sine-Gordon model. *Nuclear Physics B*, 493(3):571–587, 1997.
- [67] M.N. Barber. An introduction to the fundamentals of the renormalization group in critical phenomena. *Physics Reports*, 29(1):2–84, 1977.
- [68] K.G. Wilson. The renormalization group: Critical phenomena and the Kondo problem. *Reviews of Modern Physics*, 47(4):773, 1975.

- [69] K.G. Wilson and J. Kogut. The renormalization group and the $[\epsilon]$ expansion. *Physics Reports*, 12(2):75–199, 1974.
- [70] H.J. Maris and L.P. Kadanoff. Teaching the renormalization group. *American Journal of Physics*, 46:652, 1978.
- [71] N.D. Mermin and H. Wagner. Absence of ferromagnetism or antiferromagnetism in one- or two-dimensional isotropic Heisenberg models. *Physical Review Letters*, 17(22):1133–1136, 1966.
- [72] V.L. Berezinskii. Destruction of long-range order in one-dimensional and two-dimensional systems having a continuous symmetry group i. classical systems. *Soviet Journal of Experimental and Theoretical Physics*, 32:493, 1971.
- [73] V.L. Berezinskii. Destruction of long-range order in one-dimensional and two-dimensional systems possessing a continuous symmetry group. ii. quantum systems. *Soviet Journal of Experimental and Theoretical Physics*, 34:610, 1972.
- [74] J.M. Kosterlitz and D.J. Thouless. Ordering, metastability and phase transitions in two-dimensional systems. *Journal of Physics C: Solid State Physics*, 6:1181, 1973.
- [75] J.M. Kosterlitz. The critical properties of the two-dimensional XY model. *Journal of Physics C: Solid State Physics*, 7:1046, 1974.
- [76] C. Kollath, J.S. Meyer, and T. Giamarchi. Dipolar bosons in a planar array of one-dimensional tubes. *Physical review letters*, 100(13):130403, 2008.
- [77] A.F. Ho, M.A. Cazalilla, and T. Giamarchi. Deconfinement in a 2D optical lattice of coupled 1D boson systems. *Physical review letters*, 92(13):130405, 2004.
- [78] R. Citro, S. De Palo, E. Orignac, P. Pedri, and M.L. Chiofalo. Luttinger hydrodynamics of confined one-dimensional Bose gases with dipolar interactions. *New Journal of Physics*, 10:045011, 2008.
- [79] T. Lahaye, C. Menotti, L. Santos, M. Lewenstein, and T. Pfau. The physics of dipolar bosonic quantum gases. *Reports on Progress in Physics*, 72(12):126401, 2009.

- [80] P. Calabrese, A. Pelissetto, and E. Vicari. Multicritical phenomena in $o(n_1) \times o(n_2)$ -symmetric theories. *Physical Review B*, 67(054505), 2003.
- [81] O. Penrose and L. Onsager. Bose-Einstein condensation and liquid helium. *Physical Review*, 104(3):576, 1956.
- [82] G.V. Chester. Speculations on Bose-Einstein condensation and quantum crystals. *Physical Review A*, 2:256–258, 1970.
- [83] A.F. Andreev and I.M. Lifshitz. Quantum theory of defects in crystals. *Soviet Physics Uspekhi*, 13:670, 1971.
- [84] E. Kim and M.H.W. Chan. Probable observation of a supersolid helium phase. *Nature*, 427(6971):225–227, 2004.
- [85] D. Jaksch. Solid-state physics: Supersolid simulations. *Nature*, 442(7099):147–149, 2006.
- [86] V.W. Scarola, E. Demler, and S.D. Sarma. Searching for a supersolid in cold-atom optical lattices. *Physical Review A*, 73(5):051601, 2006.
- [87] D.J. Amit, Y.Y. Goldschmidt, and L. Peliti. Cross-over behavior of the nonlinear sigma model with quadratically broken symmetry. *Annals of Physics*, 116(1):1–34, 1978.
- [88] D.R. Nelson and R.A. Pelcovits. Momentum-shell recursion relations, anisotropic spins, and liquid crystals in $2+\epsilon$ dimensions. *Physical Review B*, 16(5):2191–2199, 1977.
- [89] S. Chakravarty, B.I. Halperin, and D.R. Nelson. Two-dimensional quantum Heisenberg antiferromagnet at low temperatures. *Physical Review B*, 39(4):2344, 1989.
- [90] P.M. Chaikin, T.C. Lubensky, and T.A. Witten. *Principles of condensed matter physics*, volume 1. Cambridge Univ Press, 2000.
- [91] B. Lake, G. Aeppli, K.N. Clausen, D.F. McMorrow, K. Lefmann, N.E. Hussey, N. Mangkorntong, M. Nohara, H. Takagi, T.E. Mason, et al. Spins in the vortices of a high-temperature superconductor. *Science*, 291(5509):1759–1762, 2001.